NAVAL POSTGRADUATE SCHOOL
Monterey, California

THESIS

RECURSIVE RAY ACOUSTICS FOR
THREE-DIMENSIONAL
SOUND-SPEED PROFILES

by

F. Wynn Polnicky

September 1991

Thesis Advisor Lawrence J. Ziomek

'nclassified

curity classification of this page

REPORT DOCUMENTATION PAGE

a Report Security Classification Unclassified		1b Restrictive Markings	
:a Security Classification Authority		3 Distribution Availability of Report	
:b Declassification Downgrading Schedule		Approved for public release; distribution is unlimited.	
Performing Organization Report Number(s)		5 Monitoring Organization Report Number(s)	
›a Name of Performing Organization Naval Postgraduate School	6b Office Symbol *(if applicable)* 52	7a Name of Monitoring Organization Naval Postgraduate School	
;c Address *(city, state, and ZIP code)* Monterey, CA 93943-5000		7b Address *(city, state, and ZIP code)* Monterey, CA 93943-5000	
8a Name of Funding Sponsoring Organization	8b Office Symbol *(if applicable)*	9 Procurement Instrument Identification Number	
8c Address *(city, state, and ZIP code)*		10 Source of Funding Numbers	
		Program Element No | Project No | Task No | Work Unit Accession No	

11 Title *(include security classification)* RECURSIVE RAY ACOUSTICS FOR THREE-DIMENSIONAL SOUND-SPEED PROFILES (Unclassified)

12 Personal Author(s) F. Wynn Polnicky

13a Type of Report	13b Time Covered	14 Date of Report *(year, month, day)*	15 Page Count
Master's Thesis	From To	September 1991	112

16 Supplementary Notation The views expressed in this thesis are those of the author and do not reflect the official policy or position of the Department of Defense or the U.S. Government.

17 Cosati Codes			18 Subject Terms *(continue on reverse if necessary and identify by block number)*
Field	Group	Subgroup	ray acoustics, sound-speed profile, spatial Fourier series

19 Abstract *(continue on reverse if necessary and identify by block number)*

A comparison of a simple recursive ray acoustics algorithm versus a ray acoustics algorithm based on solving a system of first-order ordinary differential equations was conducted. The recursive ray acoustics (RRA) algorithm was found to be accurate and relatively fast. The RRA algorithm is capable of handling sound speed as a function of all three spatial coordinates, and this capability was demonstrated.

Two separate methods of representing a sound-speed profile (SSP) based on data points were examined: Akima cubic spline and spatial Fourier series (SFS). The SFS representation encountered difficulties in accurately modeling SSPs. Various techniques were applied to improve the SFS sound-speed representation. While accurate sound-speed fits were eventually achieved, difficulties remained in the SFS modeling of first and second-order derivatives of the sound-speed data.

The RRA algorithm was tested using the SFS sound-speed representation and found to be significantly inaccurate.

A demonstration was conducted of the ability of the SFS sound-speed representation to incorporate randomness in the SSP.

20 Distribution Availability of Abstract	21 Abstract Security Classification	
☒ unclassified unlimited ☐ same as report ☐ DTIC users	Unclassified	
22a Name of Responsible Individual Lawrence J. Ziomek	22b Telephone *(include Area code)* (408) 646-3206	22c Office Symbol 72Zm

DD FORM 1473,84 MAR 83 APR edition may be used until exhausted
All other editions are obsolete

security classification of this page

Unclassified

Approved for public release; distribution is unlimited.

Recursive Ray Acoustics for Three-Dimensional
Sound-Speed Profiles

by

F. Wynn Polnicky
Lieutenant, Canadian Navy
B.Math, University of Waterloo, Canada, 1976

Submitted in partial fulfillment of the
requirements for the degrees of

MASTER OF SCIENCE IN APPLIED SCIENCE
and
MASTER OF SCIENCE IN ENGINEERING ACOUSTICS

from the

NAVAL POSTGRADUATE SCHOOL
September 1991

Author: F. Wynn Polnicky

Approved by: Lawrence J. Ziomek, Thesis Advisor

Hung-Mou Lee, Second Reader

J. N. Eagle, Chairman,
Anti-Submarine Warfare Academic Group

Anthony A. Atchley, Chairman,
Engineering Acoustics Academic Committee

ABSTRACT

A comparison of a simple recursive ray acoustics algorithm versus a ray acoustics algorithm based on solving a system of first-order ordinary differential equations was conducted. The recursive ray acoustics (RRA) algorithm was found to be accurate and relatively fast. The RRA algorithm is capable of handling sound speed as a function of all three spatial coordinates, and this capability was demonstrated.

Two separate methods of representing a sound-speed profile (SSP) based on data points were examined: Akima cubic spline and spatial Fourier series (SFS). The SFS representation encountered difficulties in accurately modeling SSPs. Various techniques were applied to improve the SFS sound-speed representation. While accurate sound-speed fits were eventually achieved, difficulties remained in the SFS modeling of first and second-order derivatives of the sound-speed data.

The RRA algorithm was tested using the SFS sound-speed representation and found to be significantly inaccurate.

A demonstration was conducted of the ability of the SFS sound-speed representation to incorporate randomness in the SSP.

TABLE OF CONTENTS

LIST OF TABLES

LIST OF FIGURES

I. INTRODUCTION

The primary focus of this thesis was to test the accuracy and capabilities of a recursive ray acoustics (RRA) algorithm that can be used to calculate the position, angles of propagation, travel time, and path length along a ray path and to generate ray trace plots for speeds of sound that are functions of all three spatial coordinates. The RRA algorithm is an extension and slight modification of an algorithm briefly discussed by Klein [Ref. 1: pp. 29-31]. The algorithm discussed by Klein [Ref. 1: pp. 29-31] was expressed in terms of an index of refraction while herein, the RRA algorithm is expressed directly in terms of the speed of sound. No computer simulation results were presented by Klein [Ref. 1: pp. 29-31].

The accuracy of the RRA algorithm was tested by comparing its computer simulation results with those obtained from a previously developed ray acoustics algorithm based on solving a system of first-order ordinary differential equations (ODE) [Ref. 2]. The ODE algorithm as applied to ray acoustics was discussed in detail by Lim [Ref. 3]. Both the ODE algorithm and the RRA algorithm used the IMSL Version 10 double precision computer program DCSAKM to obtain an Akima cubic spline fit to one-dimensional, depth-dependent, sound-speed data for testing and comparison purposes. The computer simulation results are presented in Chapter III, Section A. An Akima cubic spline was chosen since it is designed to produce a curve that matches the shape of the data while minimizing oscillations. In addition, the RRA algorithm was tested and shown to be capable of handling a sound-speed profile (SSP) that is a function of all three spatial coordinates. This capability was demonstrated by first separating the ocean into zones along the z axis. In each zone, the SSP is a different function, in general, of both cross-range x and depth y. A SSP with a gradient in the cross-range direction will cause a sound ray to leave its initial plane of propagation. Chapter III, Section B, includes demonstrations of the special three-dimensional capabilities of the RRA algorithm.

A secondary objective of this thesis was to examine the use of a spatial Fourier series (SFS) to fit sound-speed data and to assess its utility relative to an Akima cubic spline fit. The appeal of the SFS lay in its representation of spectral content in terms of spatial frequencies, as well as its ability to represent derivatives. The precision of the two sound-speed fits, as well as that of the first and second-order derivatives of the sound-

speed data were compared since the first-order derivative as well as the sound-speed fit itself are utilized in the ray trace algorithms mentioned above. Chapter IV, Section A, contains the results of this comparison as generated by computer simulation. The SFS representation of a SSP was then employed within the RRA algorithm and tested by using the same SSPs that were used to compare the ODE and RRA algorithms. Chapter IV, Section B, discusses the accuracy of the RRA algorithm incorporating the SFS representation of the various SSPs.

Additionally, random fluctuations in the SSP were modeled using the inherent suitability of a SFS representation for the inclusion of components at particular harmonics. This random element was intended to simulate fluctuations generated by such processes as internal waves or by inaccurate collection of sound-speed data.

II. THEORETICAL ANALYSIS

A. THE RRA ALGORITHM

If a sound source is located at $\underline{r}_0 = (x_0, y_0, z_0)$ and if a ray is launched with initial angles of propagation β_0 and ϕ_0 (see Figure 1), then an estimate of the position of subsequent points along the ray path is given by (see Figure 2)

$$\underline{r}_i = \underline{r}_{i-1} + \Delta\underline{r}_{i-1}, \quad i = 1,2,3, \ldots \tag{2.1}$$

where

$$\Delta\underline{r}_i = \Delta s_i \, \hat{n}_i , \tag{2.2}$$

Δs_i is an increment of arc length, the magnitude of which is at the user's discretion,

$$\hat{n}_i = u_i \, \hat{x} + v_i \, \hat{y} + w_i \, \hat{z} \tag{2.3}$$

is the unit vector along the ray path where

$$u_i = \sin \beta_i \cos \phi_i , \tag{2.4}$$

$$v_i = \cos \beta_i , \tag{2.5}$$

and

$$w_i = \sin \beta_i \sin \phi_i \tag{2.6}$$

are the dimensionless direction cosines with respect to the x, y and z axes, respectively, and β_i and ϕ_i are the angles of propagation.

Since, in general, $\hat{n}_{i-1}$ is not identical with $\hat{n}_i$, from Klein [Ref. 1: pp. 29-31] we see that, as amplified and applied to the ocean acoustics environment in Ziomek [Ref. 4: pp. 225 and 230],

$$\frac{d(n(\underline{r})\hat{n}(\underline{r}))}{ds} = \nabla n(\underline{r}), \tag{2.7}$$

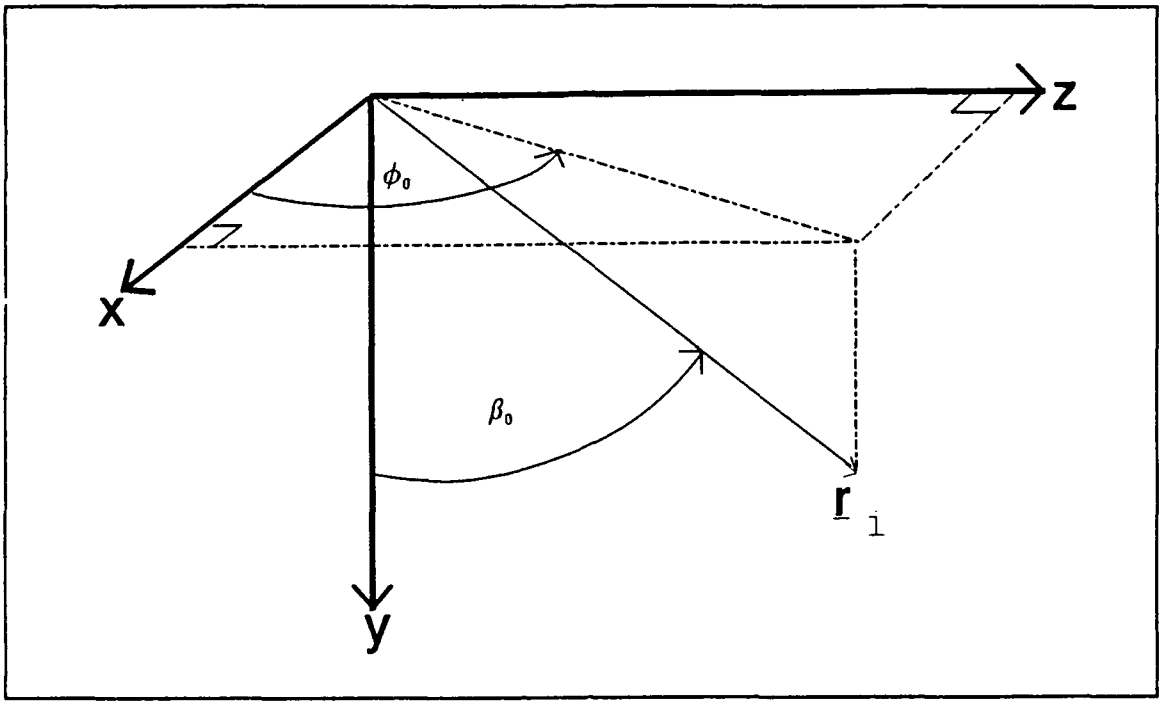

Figure 1. Initial Angles of Propagation β_0 and ϕ_0.

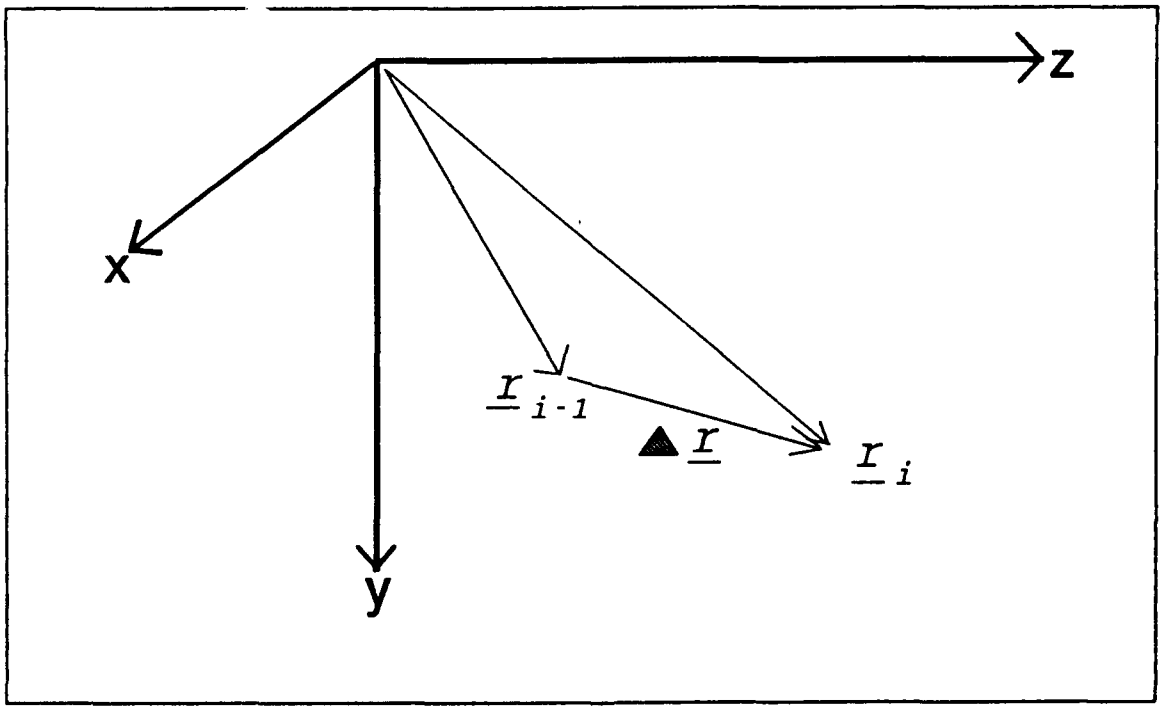

Figure 2. Ray Geometry.

or, approximately,

$$\Delta(n(\underline{r}_i)\hat{n}_i) = \nabla n(\underline{r}_i)\Delta s_i \tag{2.8}$$

where $\hat{n}(\underline{r}_i) \equiv \hat{n}_i$,

$$n(\underline{r}_i) = \frac{c(\underline{r}_0)}{c(\underline{r}_i)} \tag{2.9}$$

is the dimensionless index of refraction, $c(\underline{r}_0)$ is the three-dimensional speed of sound at

$$\underline{r}_0 = x_0\,\hat{x} + y_0\,\hat{y} + z_0\,\hat{z}\ , \tag{2.10}$$

and, $c(\underline{r}_i)$ is the three-dimensional speed of sound at

$$\underline{r}_i = x_i\,\hat{x} + y_i\,\hat{y} + z_i\,\hat{z}\ , \tag{2.11}$$

which is the position vector to a point on the ray path after the ith iteration.

It follows from Equation (2.8) that

$$n(\underline{r}_i)\,\hat{n}_i \;-\; n(\underline{r}_{i-1})\,\hat{n}_{i-1} \;=\; \nabla n(\underline{r}_i)\,\Delta s_i \tag{2.12}$$

and, as a result,

$$\hat{n}_i = \frac{n(\underline{r}_{i-1})\hat{n}_{i-1}}{n(\underline{r}_i)} + \frac{\Delta s_i}{n(\underline{r}_i)}\,\nabla n(\underline{r}^{*}_{i-1})\ , \tag{2.13}$$

where, for better accuracy in the evaluation of the gradient,

$$\underline{r}^{*}_{i-1} = \underline{r}_{i-1} + \frac{\Delta s_{i-1}}{2}\,\hat{n}_{i-1}\ , \tag{2.14}$$

which is the three-dimensional spatial location half-way along the arc length between $\underline{r}_{i-1}$ and $\underline{r}_i$, and

$$\nabla = \frac{\partial}{\partial x}\,\hat{x} + \frac{\partial}{\partial y}\,\hat{y} + \frac{\partial}{\partial z}\,\hat{z} \tag{2.15}$$

is the gradient expressed in rectangular coordinates. It should be noted that although

Δs_i has been shown as a function of iteration number, it will be constant, in general, except when it needs to be adjusted to properly handle surface and bottom reflections and maximum down range limits.

In terms of the direction cosines u, v, and w,

$$u_i = \frac{n(\underline{r}_{i-1})u_{i-1}}{n(\underline{r}_i)} + \frac{\Delta s}{n(\underline{r}_i)} \frac{\partial n(\underline{r}^*_{i-1})}{\partial x}, \tag{2.16}$$

$$v_i = \frac{n(\underline{r}_{i-1})v_{i-1}}{n(\underline{r}_i)} + \frac{\Delta s}{n(\underline{r}_i)} \frac{\partial n(\underline{r}^*_{i-1})}{\partial y}, \tag{2.17}$$

and

$$w_i = \frac{n(\underline{r}_{i-1})w_{i-1}}{n(\underline{r}_i)} + \frac{\Delta s}{n(\underline{r}_i)} \frac{\partial n(\underline{r}^*_{i-1})}{\partial z}. \tag{2.18}$$

If $c(\underline{r}_i) = c(x_i, y_i, z_i)$ is the three-dimensional speed of sound, and if $c_0 = c(\underline{r}_0)$ is the speed of sound at the source location, then it follows that

$$\frac{n(\underline{r}_{i-1})}{n(\underline{r}_i)} = \frac{c_0}{c(\underline{r}_{i-1})} \frac{c(\underline{r}_i)}{c_0} = \frac{c(\underline{r}_i)}{c(\underline{r}_{i-1})}, \tag{2.19}$$

and

$$\frac{1}{n(\underline{r}_i)} \frac{\partial n(\underline{r})}{\partial x} = -c(\underline{r}_i) \left[\frac{1}{c^2(\underline{r})} \frac{\partial c(\underline{r})}{\partial x} \right]_{\underline{r} = \underline{r}^*_{i-1}}. \tag{2.20}$$

Analogous reasoning applied to the y and z coordinates yields results similar to Equation (2.20), and substitution of these results into Equation (2.13) yields

$$\hat{n}_i = \frac{c(\underline{r}_i)}{c(\underline{r}_{i-1})} \hat{n}_{i-1} - c(\underline{r}_i)\Delta s_i \left[\frac{1}{c^2(\underline{r})} \nabla c(\underline{r}) \right]_{\underline{r} = \underline{r}^*_{i-1}}. \tag{2.21}$$

In addition, although Klein did not discuss travel time τ and path length s calculations, these quantities were computed using the following formulae:

$$\tau = \sum_{i=1} \frac{\Delta s_i}{c(\overset{*}{r}_{i-1})}, \tag{2.22}$$

and

$$s = \sum_{i=1} \Delta s_i . \tag{2.23}$$

Equations (2.1) through (2.23) constitute what is referred to herein as the recursive ray acoustics (RRA) algorithm first mentioned in Chapter 1. Input to this algorithm in the form of mathematical formulae for the sound-speed profile or some particular numerical fit to sound-speed data must be provided to enable the algorithm to function.

B. SPATIAL FOURIER SERIES REPRESENTATION OF SOUND-SPEED DATA

Given an ocean D meters deep with a one-dimensional, depth-dependent sound-speed profile (SSP), the speed of sound $c(y)$ can be represented by the following spatial Fourier series (SFS):

$$c(y) = |c_0| + 2\sum_{s=1}^{S} |c_s| \cos(2\pi f_{y_0} y - \angle c_s), 0 \le y \le D \tag{2.24}$$

where $|c_s|$ and $\angle c_s$ are the magnitude and phase(angle), respectively, of the complex Fourier series coefficient c_s at harmonic s, $|c_0|$ is the magnitude of c_s at harmonic $s = 0$ and is the "DC component" or average value of the sound-speed data,

$$f_{y_0} = \frac{1}{NT_{S_y}} \tag{2.25}$$

is the fundamental spatial frequency in the y direction in cycles per meter where N is the total number of sound-speed data points taken and T_{S_y} is the uniform sampling period in the y direction in meters per sample, and S is the highest harmonic. Derivatives of this Fourier series representation can be directly obtained.

The complex Fourier series coefficients c_s are obtained by taking the spatial discrete Fourier transform (DFT) of the sound-speed data as follows:

$$c_s = \frac{1}{N} \sum_{n=0}^{N-1} c(nT_{S_y}) W_N^{sn}, \quad s = -S,...,0,...,S \tag{2.26}$$

where

$$W_N = \exp(+j2\pi/N) \tag{2.27}$$

and, when sampling at the Nyquist rate,

$$N = 2S + 1. \tag{2.28}$$

An attempt to represent a function by a truncated Fourier series will always result in oscillations about the functions' true value. These oscillations normally have small enough amplitudes that they are of little consequence. However, an attempt to use a SFS representation of a linear SSP with a single constant gradient results in significant discrepancies in amplitude near the ocean surface and bottom, due to the inherent discontinuity in the SSP that exists at these boundaries. This difficulty, known as "Gibbs' phenomenon", does not diminish as more harmonics, that is, sound-speed data points, are added to the Fourier series.

C. Lanczos [Ref. 5] suggested that this phenomenon would be ameliorated if the Fourier series could be forced to converge more rapidly by modifying the Fourier series coefficients c_s by a correction factor, such that the Lanczos smoothed Fourier series coefficients c_{s_L} are given by

$$c_{s_L} = \frac{\sin(s\pi/S)}{s\pi/S} c_s, \quad s \neq 0, \tag{2.29}$$

where c_s is given by Equation (2.25). Hamming [Ref. 6] states that S in Equation (2.29) is usually replaced with $S + 1$ and, thus, our representation of the correction factor will be

$$c_{s_L} = \frac{\sin(s\pi/(S+1))}{s\pi/(S+1)} c_s, \quad s \neq 0. \tag{2.30}$$

C. INCORPORATION OF RANDOMNESS INTO THE SOUND-SPEED PROFILE

The speed of sound as a function of depth, $c(y)$, can be represented as the sum of deterministic and random components as follows:

$$c(y) = c_D(y) + c_R(y), \tag{2.31}$$

with $c_D(y)$ being the deterministic and $c_R(y)$ the random speeds of sound as functions of depth y.

The autocorrelation function of $c_R(y)$ is , for any particular y and y' ,

$$R_{c_R}(y, y') = E\{c_R(y)c_R^*(y')\}, \tag{2.32}$$

where $c_R^*(y')$ is the complex conjugate of c_R at depth y', $0 \le y' \le D$.

If

$$c_R(y) = \sum_{n=-N}^{N} c_n \exp(-j2\pi n f_{y_0} y), \tag{2.33}$$

for some set of Fourier series coefficients c_n, and

$$f_{y_0} = 1/D \tag{2.34}$$

for D the ocean depth in meters, then

$$c_n = \frac{1}{D}\int_0^D c_r(y) \exp(+j2\pi n f_{y_0} y)dy. \tag{2.35}$$

If $c_R(y)$ is a random function of depth, then c_n will be a random variable.

Since

$$E\{c_n(c_{n'})^*\} = \frac{1}{D^2}\int_0^D\int_0^D E\{c_R(y)c_R^*(y')\} \exp(+j2\pi f_{y_0}(ny - n'y'))dydy', \tag{2.36}$$

where

$$E\{c_R(y)c_R^*(y')\} = R_{c_R}(y, y'), \tag{2.37}$$

and $(c_{n'})^*$ is the complex conjugate of $c_{n'}$, and if it is assumed that $c_R(y)$ is a wide-sense stationary (i.e., statistically homogeneous) random process, then

$$R_{c_R}(y, y') = R_{c_R}(\Delta y), \tag{2.38}$$

where $\Delta y = y - y'$. If R_{c_R} is represented by a finite Fourier series

$$R_{c_R}(\Delta y) = \sum_{m=-N}^{N} r_m \exp(-j2\pi m f_{y_0} \Delta y), \tag{2.39}$$

then, as developed in Thomas [Ref. 7: pp. 148-153],

$$r_m = \frac{1}{2N+1} S_{c_R}(m f_{y_0}), \tag{2.40}$$

where S_{c_R} is the power spectral density of $c_R(y)$.

Thomas [Ref. 7: pp 148-153] goes on to show that

$$E\{c_n c_{n'}^*\} = r_n \delta_{nn'}, \tag{2.41}$$

where $\delta_{nn'}$ is the Kronecker delta function. Therefore,

$$E\{|c_n|^2\} = r_n = \frac{1}{2N+1} S_{c_R}(n f_{y_0}). \tag{2.42}$$

Hence, if c_n is a zero mean Gaussian random variable with variance r_n, that is, if

$$c_n = N(0, r_n), \tag{2.43}$$

then $c_R(y)$ will be a zero mean Gaussian random process.

Therefore,

$$R_{c_R}(y, y') = R_{c_R}(\Delta y) = \sum_n r_n \exp(-j2\pi f_{y_0} \Delta y), \tag{2.44}$$

which represents the Inverse Discrete Fourier Transform of the power spectral density.

Thus, knowledge of the power spectral density of $c_R(y)$ enables calculation of r_n via Equation (2.42), which in turn yields c_n via (2.43) and $c_R(y)$ via (2.33).

III. COMPUTER SIMULATION RESULTS

A. RAY ACOUSTICS - COMPARATIVE ANALYSIS OF ODE VERSUS RRA ALGORITHMS

Four distinct sound-speed profiles (SSPs) were examined for purposes of comparative analysis. For all cases, a sound source spatial location of $x_0 = 0$ m and $z_0 = 0$ m was used. The source depth y_0 was established at a point half-way between the ocean surface and bottom, 100 m in most cases. A constant ocean depth of 200 m was modeled, unless otherwise noted, and for all cases three separate rays were examined. All rays were propagated initially in the direction of the positive z axis, that is, $\phi_0 = 90°$, but β_0 was altered in order to generate unique rays. For SSPs 1 to 3, the launch angle β_0 was set to 45°, 85°, and 135° . SSP 4 was designed to simulate a SOFAR channel. Launch angles were therefore chosen to result in the first two rays propagating down range without reflection, i.e., $\beta_0 = 85°$ and 95°, while the third launch angle was set to $\beta_0 = 135°$ to test reflection as well.

The four SSPs considered are defined as follows:

- SSP 1: Constant speed of sound ($c = 1500$ m/s)
- SSP 2: Linear SSP with a positive gradient ($c(y) = c(0) + g\,y$ m/s where the speed of sound at the surface $c(0) = c(y = 0) = 1500$ m/s and $g = +0.017$ 1/s)
- SSP 3: Linear SSP with a negative gradient ($c(y) = c(0) + g\,y$ m/s where the speed of sound at the surface $c(0) = c(y = 0) = 1500$ m/s and $g = -0.017$ 1/s)
- SSP 4: Parabolic SSP with vertex at y_0 where $c(y_0) = 1490$ m/s and the speed of sound at both the ocean surface and bottom is equal to 1500 m/s ($c(y) = c(y_0) + a(y - y_0)^2$ m/s with $a = 0.001 \frac{1}{\text{m s}}$ for an ocean depth of 200 m).

The above four SSPs generated nine sound-speed data points which were input to the Akima cubic spline routine. The results from the ODE algorithm were used throughout as the benchmark for comparison purposes. The ODE algorithm used the IMSL Version 10 double precision computer program DIVPBS in order to solve the system of first-order ordinary differential equations. A range step size of 2.0 m and an error tolerance of 1×10^{-7} was used in DIVPBS, except for SSP 3, Ray 1 in Table 3, where the tolerance had to be reduced to 1×10^{-6} in order for the ODE algorithm to run. The arc length step size used in the RRA algorithm was 2.0 m unless otherwise noted. The results of the various simulation runs are presented in the following seven tables.

Table 1. RAY ACOUSTICS RESULTS FOR SSP 1, RAYS 1 THROUGH 3

Method	y_0 (m)	β_0 (deg)	r (km)	y (m)	β (deg)	τ (sec)	s (km)
ODE	100.0	45.0	10.0	100.00	45.000	9.428090	14.1421
RRA	100.0	45.0	10.0	99.95	45.000	9.428091	14.1421
ODE	100.0	85.0	10.0	174.89	85.000	6.692132	10.0382
RRA	100.0	85.0	10.0	174.88	85.000	6.692132	10.0382
ODE	100.0	135.0	10.0	100.00	135.000	9.428090	14.1421
RRA	100.0	135.0	10.0	100.05	135.000	9.428091	14.1421

For SSP 1 (constant speed of sound), Table 1 shows that at a horizontal range $r = 10$ km, the differences between the two algorithms are as follows:

- between 0.01 and 0.05 m in depth y and
- 1 μ sec in travel time τ.

Table 2. RAY ACOUSTICS RESULTS FOR SSP 2, RAYS 1 THROUGH 3

Method	y_0 (m)	β_0 (deg)	r (km)	y (m)	β (deg)	τ (sec)	s (km)
ODE	100.0	45.0	10.0	99.99	45.000	9.417413	14.1421
RRA	100.0	45.0	10.0	99.95	45.000	9.417422	14.1421
ODE	100.0	85.0	10.0	162.50	85.487	6.683492	10.0374
RRA	100.0	85.0	10.0	162.57	85.487	6.683496	10.0374
ODE	100.0	135.0	10.0	100.01	135.000	9.417413	14.1421
RRA	100.0	135.0	10.0	100.05	135.000	9.417422	14.1421

For SSP 2 (linear SSP with a positive gradient), Table 2 shows that at a horizontal range $r = 10$ km, the differences between the two algorithms are as follows:

- between 0.04 and 0.07 m in depth y and
- between 4 and 9 μ sec in travel time τ.

Table 3. RAY ACOUSTICS RESULTS FOR SSP 3, RAYS 1 THROUGH 3

Method	y_0 (m)	β_0 (deg)	r (km)	y (m)	β (deg)	τ (sec)	s (km)
ODE	100.0	45.0	10.0	99.99	45.000	9.438784	14.1421
RRA	100.0	45.0	10.0	99.95	45.000	9.438795	14.1421
ODE	100.0	85.0	10.0	168.89	84.512	6.699404	10.0380
RRA	100.0	85.0	10.0	168.96	84.511	6.699409	10.0380
ODE	100.0	135.0	10.0	100.01	135.000	9.438784	14.1421
RRA	100.0	135.0	10.0	100.05	135.000	9.438794	14.1421

For SSP 3 (linear SSP with a negative gradient), Table 3 shows that at a horizontal range $r = 10$ km, the differences between the two algorithms are as follows:

- between 0.04 and 0.07 m in depth y ,
- 0.001 deg in angle of arrival β , and
- between 5 and 11 μ sec in travel time τ.

The data presented in Tables 1 through 3 demonstrate that the two algorithms are in very good agreement. Note that the accuracy of the RRA algorithm can always be improved by reducing the arc length step size. This is demonstrated in Tables 5 and 6.

Table 4. RAY ACOUSTICS RESULTS FOR SSP 4, RAYS 1 THROUGH 3

Method	y_0 (m)	β_0 (deg)	r (km)	y (m)	β (deg)	τ (sec)	s (km)
ODE	100.0	85.0	10.0	37.06	87.244	6.710387	10.0183
RRA	100.0	85.0	10.0	36.63	87.224	6.710335	10.0184
ODE	100.0	95.0	10.0	162.94	92.756	6.710387	10.0183
RRA	100.0	95.0	10.0	163.37	92.776	6.710335	10.0184
ODE	100.0	135.0	10.0	144.97	134.922	9.448852	14.1104
RRA	100.0	135.0	10.0	144.24	134.930	9.449238	14.1110

For SSP 4 (parabolic SSP), Table 4 shows that at a horizontal range $r = 10$ km, with the ocean bottom at 200 m, the differences between the two algorithms are as follows:

- between 0.43 and 0.73 m in depth y ,
- between 0.008 and 0.02 deg in angle of arrival β ,
- between 52 and 386 μ sec in travel time τ , and
- between 0.1 and 0.6 m in path length s.

As is indicated in Table 4, the differences in travel time are relatively large when compared with previous cases. This lower level of accuracy was considered unacceptable since, in general, accuracy in the millisecond region is normally required for travel time. An attempt to improve accuracy was made by reducing the arc length increment used in the RRA algorithm from 2.0 to 1.0 m (see Tables 5 and 6).

The parabolic SSP which produced Table 4 has the most extreme gradient of all the SSPs examined and, thus, the two rays launched at 85° and 95° proceed down range without reflection from the surface or bottom, as illustrated in Figures 3 and 4. This extreme gradient was considered to have been the probable cause of the discrepancies noted above and, therefore, the gradient was reduced and the ocean depth increased to permit an examination of a similar profile with a more typical gradient (see Table 7).

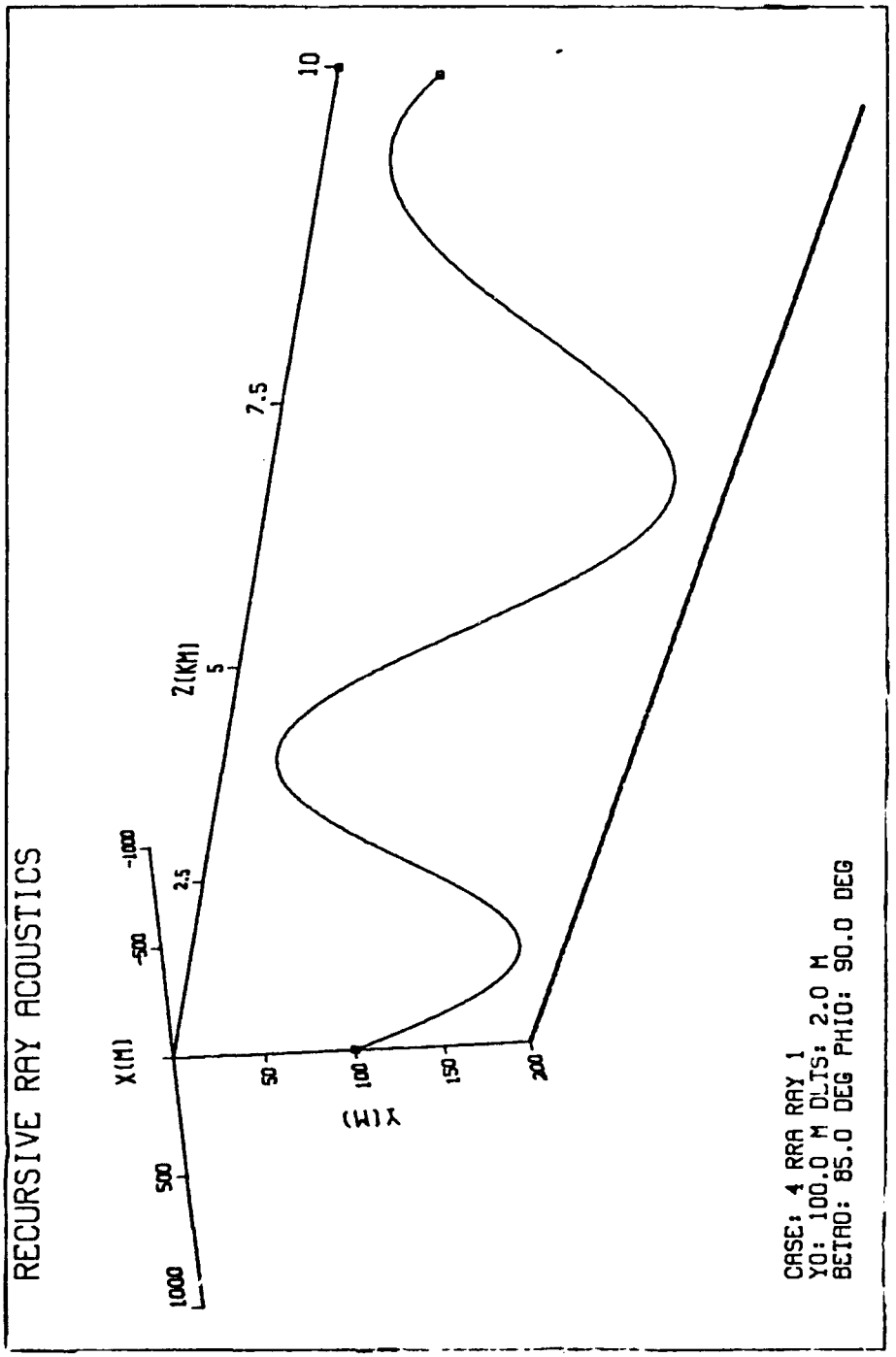

Figure 3. SSP 4 - No Reflections for $\beta_0 = 85°$.

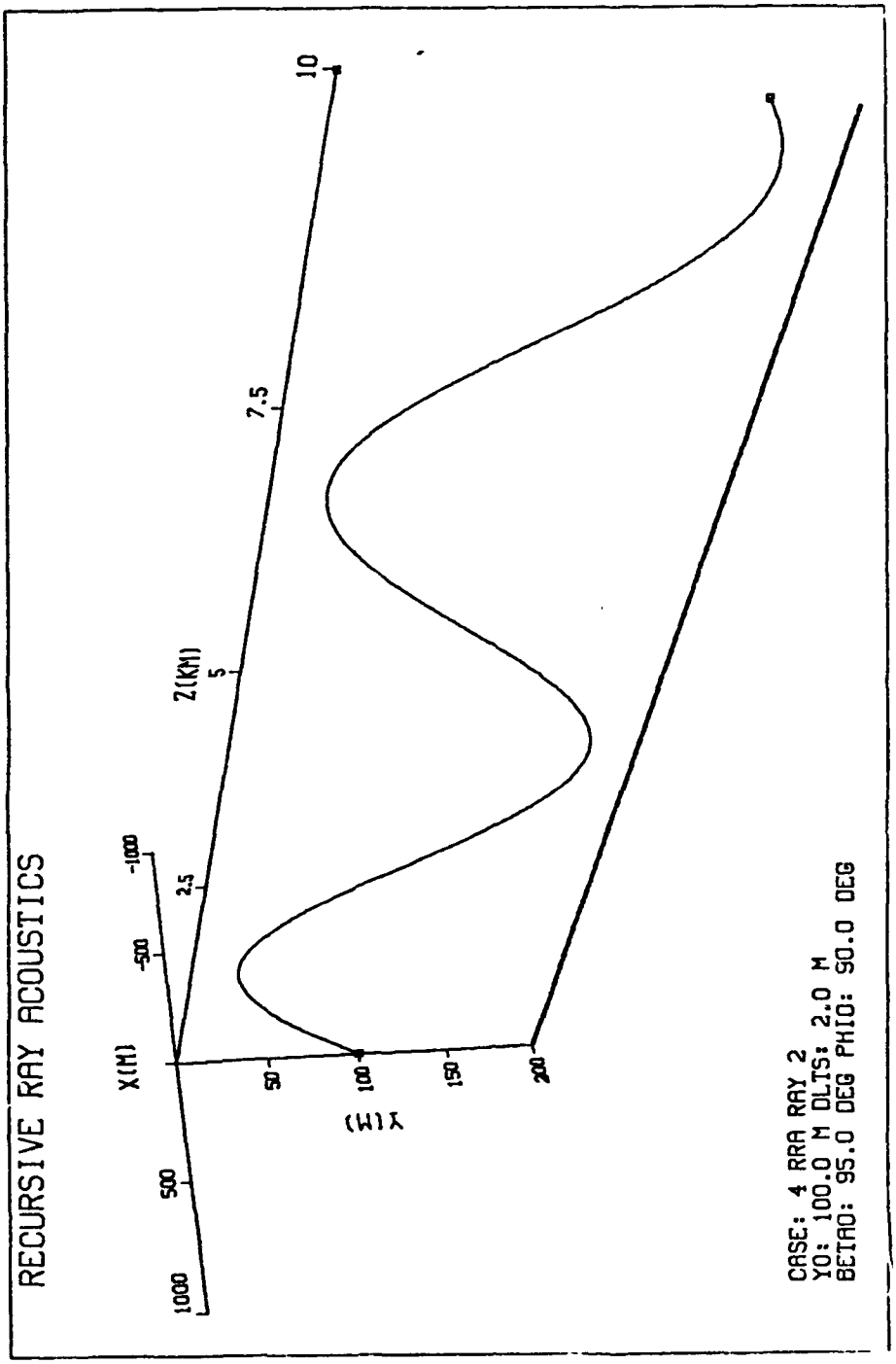

Figure 4. SSP 4 - No Reflections for $\beta_0 = 95°$.

Table 5. RAY ACOUSTICS RESULTS FOR SSP 4, RAYS 1 THROUGH 3, 2.0 M ARC LENGTH STEP SIZE

Method	y_0 (m)	β_0 (deg)	r (km)	y (m)	β (deg)	τ (sec)	s (km)
ODE	100.0	85.0	5.0	64.25	85.597	3 354779	5.0088
RRA	100.0	85.0	5.0	64.13	85.581	3.354757	5.0088
ODE	100.0	95.0	5.0	135.75	94.403	3.354779	5.0088
RRA	100.0	95.0	5.0	135.87	94.419	3.354757	5.0088
ODE	100.0	135.0	5.0	77.50	45.019	4.724411	7.0552
RRA	100.0	135.0	5.0	77.66	45.017	4.724506	7.0553

The data in Table 5 for a horizontal range of 5 km and using an arc length step size of 2.0 m was generated in order to enable a direct comparison with the arc length step size in the RRA algorithm set to 1.0 m, as shown in Table 6. The reduction in final range from 10 to 5 km was necessitated by the structure of the RRA computer code, which required large quantities of computer storage space to be allocated, particularly as arc length step size was decreased. This drawback could be rectified by straightforward modifications to the simulation program.

For SSP 4 (parabolic SSP), Table 5 shows that at a horizontal range of $r = 5$ km, the differences between the two algorithms are as follows:

- between 0.12 and 0.16 m in depth y ,
- between 0.002 and 0.016 deg in angle of arrival β ,
- between 22 and 95 μ sec in travel time τ , and
- 0.1 m in path length s

Table 6. RAY ACOUSTICS RESULTS FOR SSP 4, RAYS 1 THROUGH 3, 1.0 M ARC LENGTH STEP SIZE

Method	y_0 (m)	β_0 (deg)	r (km)	y (m)	β (deg)	τ (sec)	s (km)
ODE	100.0	85.0	5.0	64.25	85.597	3.354779	5.0088
RRA	100.0	85.0	5.0	64.19	85.589	3.354768	5.0088
ODE	100.0	95.0	5.0	135.75	94.403	3.354779	5.0088
RRA	100.0	95.0	5.0	135.81	94.411	3.354768	5.0088
ODE	100.0	135.0	5.0	77.50	45.019	4.724411	7.0552
RRA	100.0	135.0	5.0	77.56	45.018	4.724458	7.0553

For SSP 4 (parabolic SSP), Table 6 shows that at a horizontal range of $r = 5$ km, and with the RRA arc length step size set to 1.0 m, the differences between the two algorithms are as follows:

- 0.06 m in depth y ,
- between 0.001 and 0.008 deg in angle of arrival β ,
- between 11 and 47 μ sec in travel time τ , and
- 0.1 m in path length s.

A significant improvement in the consistency of travel time calculations can be seen by comparing Tables 5 and 6. Cutting the arc length increment in half reduced the travel time discrepancy by approximately one-half. Further reductions in arc length increment, an input parameter to the simulation program, would yield further improvements in travel time accuracy.

Table 7. RAY ACOUSTICS RESULTS FOR SSP 4, RAYS 1 THROUGH 3, 2.0 M ARC LENGTH STEP SIZE, BOTTOM DEPTH 1000 M

Method	y_0 (m)	β_0 (deg)	r (km)	y (m)	β (deg)	τ (sec)	s (km)
ODE	500.0	85.0	10.0	777.41	93.388	6.705898	10.0150
RRA	500.0	85.0	10.0	777.48	93.389	6.705893	10.0150
ODE	500.0	95.0	10.0	222.59	86.612	6.705898	10.0150
RRA	500.0	95.0	10.0	222.52	86.611	6.705893	10.0150
ODE	500.0	135.0	10.0	545.01	134.997	9.448814	14.1104
RRA	500.0	135.0	10.0	545.00	134.997	9.448829	14.1104

For SSP 4 (parabolic SSP) with vertex $c(500) = 1490$ m/s, speed of sound at the ocean surface $c(0) = 1500$ m/s, and speed of sound at the ocean bottom $c(1000) = 1500$ m/s, i.e., an ocean depth of 1000 m; with $c(y) = c(500) + a(y - 500)^2$ where $a = 0.00004$, at a horizontal range $r = 10$ km, the differences between the two algorithms are as follows:

- between 0.01 and 0.07 m in depth y,
- 0.001 deg in angle of arrival β and,
- between 5 and 15 μ sec in travel time τ.

Table 7, when compared with Table 4, both pertaining to an arc length step size of 2.0 m, demonstrates that a more realistic gradient of 0.02 1/sec enables the RRA algorithm to handle propagation in a SOFAR channel to a range of 10 km with a much improved degree of accuracy. Of course, this could be improved still further by reducing the arc length step size.

B. RRA THREE-DIMENSIONAL CAPABILITIES

Figure 5 demonstrates the ability of the RRA algorithm to handle launch angles other than $\phi_0 = 90°$. This figure was produced using the parabolic SSP 4 with

$$c(y) = c(y_0) + a(y - y_0)^2 , \; 0 \leq y \leq 200 \text{ m} , \tag{3.1}$$

where $y_0 = 100$ m, $c(y_0) = 1490.0$ m/s, $a = 0.001 \; \frac{1}{\text{m s}}$, and $\phi_0 = 85°$. Note that the ray stays in the plane created by this angle, as illustrated by the projection of the ray onto the XZ plane as a straight line.

The RRA algorithm also has the capability to divide the ocean into separate zones as a function of z. Each zone can have its own SSP as a function of both cross range x and depth y. For computer simulation purposes, the speed of sound was defined as follows:

$$c(x, y) = c(y_0) + a(y - y_0)^2 + g_x x , \; 0 \leq y \leq 200 \text{ m} , \tag{3.2}$$

where $y_0 = 100$ m, $c(y_0) = 1490.0$ m/s, $a = 0.001 \; \frac{1}{\text{m s}}$ and

$$g_x = \begin{cases} 0.0 \;\; 1/\text{s}, & z \leq 5 \text{ km} \\ -0.05 \;\; 1/\text{s}, & 5 < z \leq 10 \text{ km} \end{cases} \tag{3.3}$$

The particular gradient in the x direction was selected solely for computer simulation purposes to illustrate the capability of the RRA algorithm to accommodate sound speed as a function of both x and y. Figure 6 illustrates the ray trace provided by the RRA algorithm for the SSP given by Equations 3.2 and 3.3, showing the ray staying in the YZ plane until reaching 5 km, where the gradient in the x direction comes into effect, resulting in out-of-plane propagation.

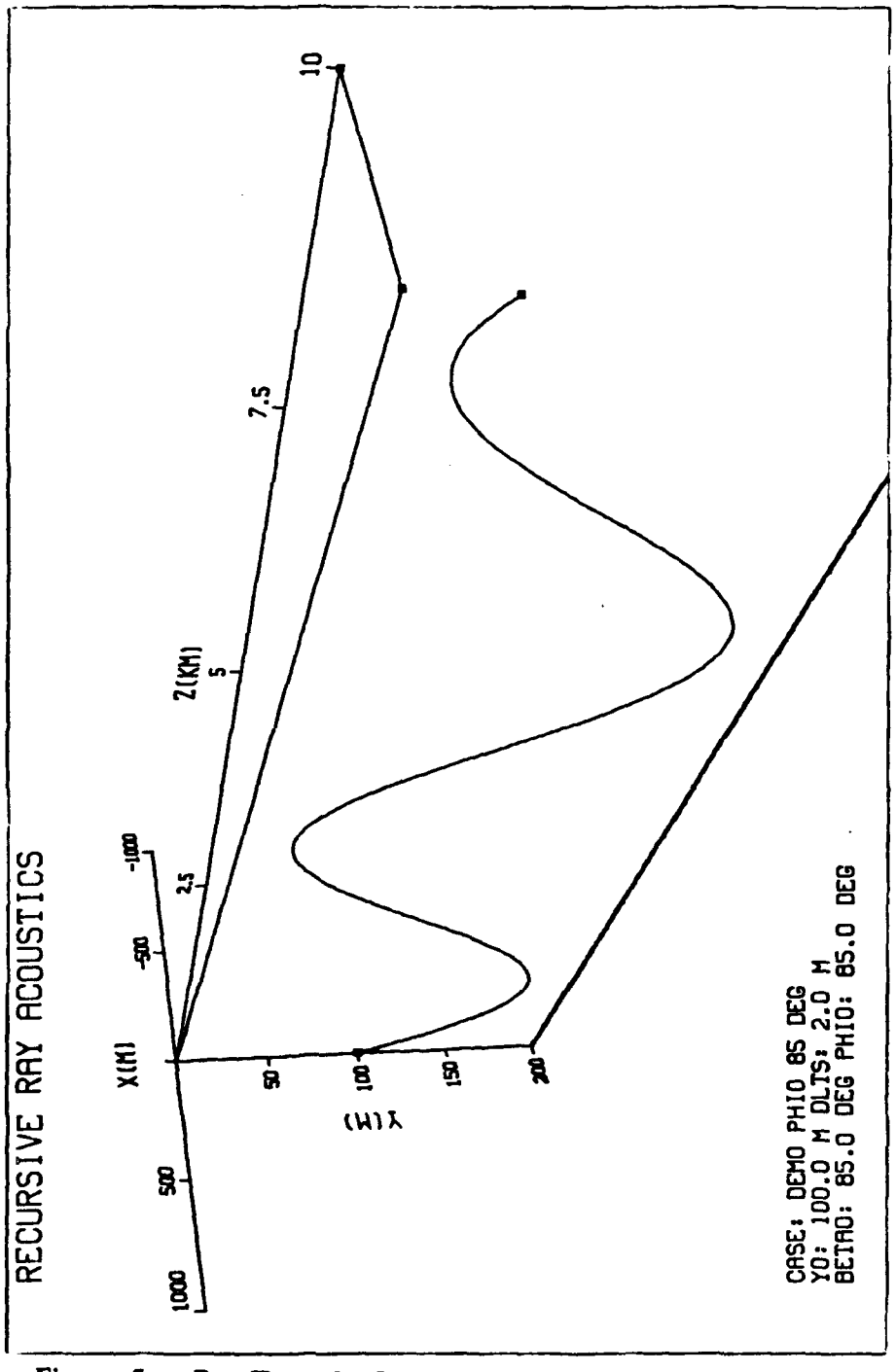

Figure 5. Ray Trace for Launch Angles $\beta_0 = 85°$ and $\phi_0 = 85°$.

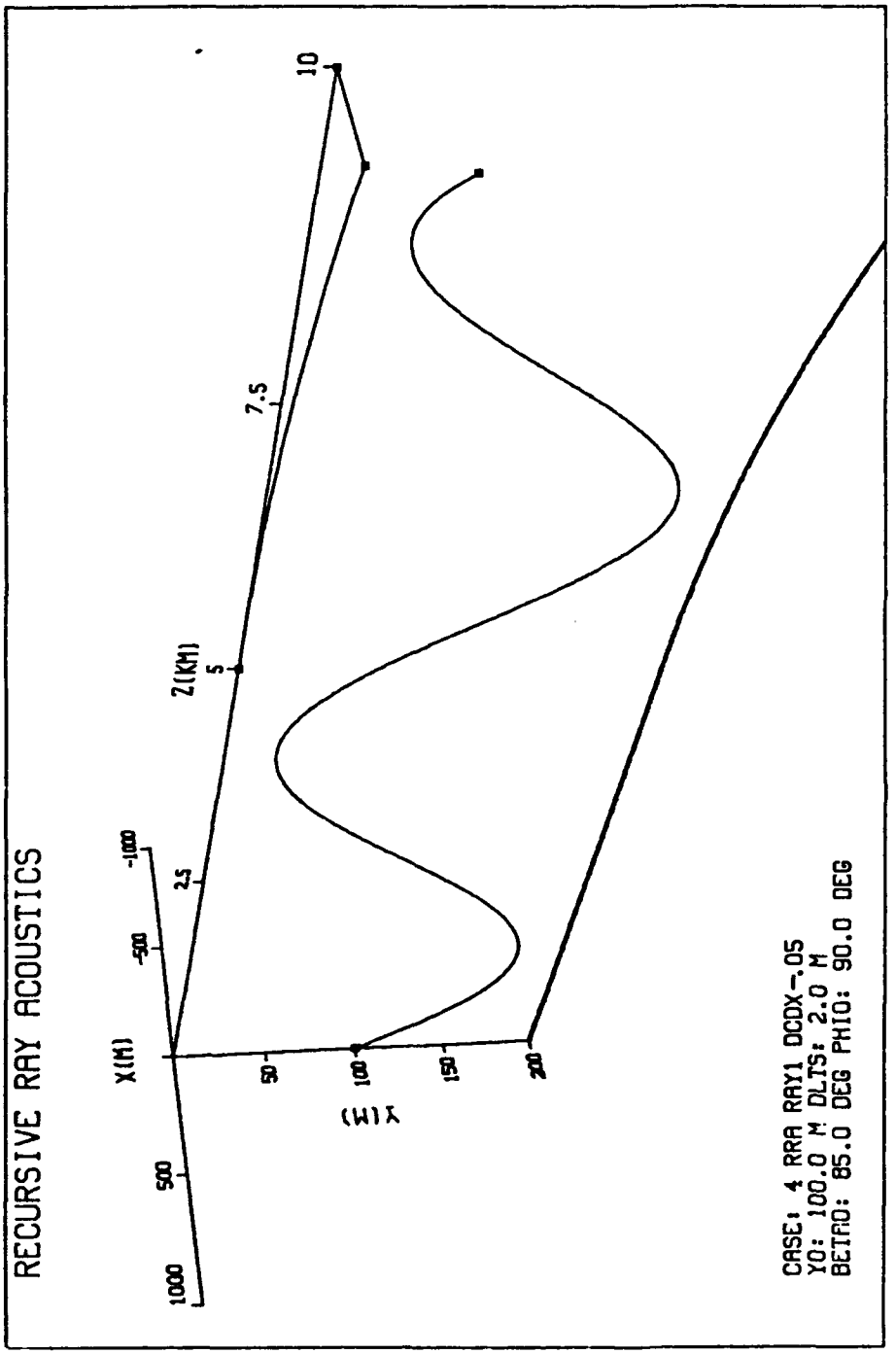

Figure 6. Ray Trace Based on a SSP as a Function of x, y and z .

IV. REPRESENTATION OF SOUND-SPEED DATA

A. COMPARATIVE ANALYSIS - SPATIAL FOURIER SERIES VERSUS AKIMA CUBIC SPLINE REPRESENTATIONS OF SOUND-SPEED DATA

Five different exact mathematical functions were used to generate 11 sound-speed data points evenly spaced in depth in a 200 m deep ocean. Akima cubic spline and spatial Fourier series representations of the SSPs were produced from these data points. Percent error calculations of their sound-speed fits as well as their first and second-order derivative fits were performed with respect to the known exact values. If the error between the exact and modeled values was less than 10^{-6}, percent error was set to zero.

The exact functions examined were as follows:

- Constant speed of sound ($c = 1500$ m/s)
- Linear SSP with a positive gradient ($c(y) = 1500.0 + 0.017y$ m/s)
- Linear SSP with a negative gradient ($c(y) = 1500.0 - 0.017y$ m/s)
- Half-period sine wave SSP ($c(y) = 1500.0 - 25.0 \sin(\frac{\pi y}{200})$ m/s)
- Parabolic SSP ($c(y) = 1450.0 + 0.005(y - 100.0)^2$ m/s)

Tables 8 and 9 with Figures 7, 8 and 9 illustrate the difficulties that the Fourier representation encounters in dealing with data derived from an exact constant speed of sound. No noticeable difference in the sound-speed fit itself is observed for either the Akima cubic spline or the Fourier series representation, but the latter generates some small errors in both the first and second-order derivatives.

Tables 10 and 11 along with Figures 10, 11 and 12 compare the Akima cubic spline and Fourier series representations of sound-speed data generated from a linear SSP with a positive gradient. In Figure 10 and Table 11 it can be seen that the Fourier representation does not precisely match the sound-speed function, although Figure 10 and Table 10 show that the Akima cubic spline does. Problems similar to those noted for a constant speed of sound can be observed by examining Figures 11 and 12 and Table 11. Discrepancies in the derivatives are now much larger.

Tables 12 and 13 along with Figures 13, 14 and 15 show analogous results for a linear SSP with a negative gradient. Once again, neither the sound-speed fit nor the derivatives are precisely modeled by the Fourier series representation.

Table 8. AKIMA CUBIC SPLINE RESULTS - CONSTANT SPEED OF SOUND

CONSTANT SPEED OF SOUND

NUMBER OF ORIGINAL DATA POINTS = 11

TECHNIQUE: AKIMA CUBIC SPLINE FIT

DEPTH (M)	C(EXACT) (M/S)	C(FIT) (M/S)	% ERROR	CDOT(EXACT) (1/S)	CDOT(FIT) (1/S)	% ERROR	CDOT2(EXACT) (1/M-S)	CDOT2(FIT) (1/M-S)	% ERROR
0.00	1500.0	1500.0	0.000	0.0000E+00	0.0000E+00	0.000	0.0000E+00	0.0000E+00	0.000
10.00	1500.0	1500.0	0.000	0.0000E+00	0.0000E+00	0.000	0.0000E+00	0.0000E+00	0.000
20.00	1500.0	1500.0	0.000	0.0000E+00	0.0000E+00	0.000	0.0000E+00	0.0000E+00	0.000
30.00	1500.0	1500.0	0.000	0.0000E+00	0.0000E+00	0.000	0.0000E+00	0.0000E+00	0.000
40.00	1500.0	1500.0	0.000	0.0000E+00	0.0000E+00	0.000	0.0000E+00	0.0000E+00	0.000
50.00	1500.0	1500.0	0.000	0.0000E+00	0.0000E+00	0.000	0.0000E+00	0.0000E+00	0.000
60.00	1500.0	1500.0	0.000	0.0000E+00	0.0000E+00	0.000	0.0000E+00	0.0000E+00	0.000
70.00	1500.0	1500.0	0.000	0.0000E+00	0.0000E+00	0.000	0.0000E+00	0.0000E+00	0.000
80.00	1500.0	1500.0	0.000	0.0000E+00	0.0000E+00	0.000	0.0000E+00	0.0000E+00	0.000
90.00	1500.0	1500.0	0.000	0.0000E+00	0.0000E+00	0.000	0.0000E+00	0.0000E+00	0.000
100.00	1500.0	1500.0	0.000	0.0000E+00	0.0000E+00	0.000	0.0000E+00	0.0000E+00	0.000
110.00	1500.0	1500.0	0.000	0.0000E+00	0.0000E+00	0.000	0.0000E+00	0.0000E+00	0.000
120.00	1500.0	1500.0	0.000	0.0000E+00	0.0000E+00	0.000	0.0000E+00	0.0000E+00	0.000
130.00	1500.0	1500.0	0.000	0.0000E+00	0.0000E+00	0.000	0.0000E+00	0.0000E+00	0.000
140.00	1500.0	1500.0	0.000	0.0000E+00	0.0000E+00	0.000	0.0000E+00	0.0000E+00	0.000
150.00	1500.0	1500.0	0.000	0.0000E+00	0.0000E+00	0.000	0.0000E+00	0.0000E+00	0.000
160.00	1500.0	1500.0	0.000	0.0000E+00	0.0000E+00	0.000	0.0000E+00	0.0000E+00	0.000
170.00	1500.0	1500.0	0.000	0.0000E+00	0.0000E+00	0.000	0.0000E+00	0.0000E+00	0.000
180.00	1500.0	1500.0	0.000	0.0000E+00	0.0000E+00	0.000	0.0000E+00	0.0000E+00	0.000
90.00	1500.0	1500.0	0.000	0.0000E+00	0.0000E+00	0.000	0.0000E+00	0.0000E+00	0.000
0.00	1500.0	1500.0	0.000	0.0000E+00	0.0000E+00	0.000	0.0000E+00	0.0000E+00	0.000

Table 9. FOURIER SERIES RESULTS - CONSTANT SPEED OF SOUND

CONSTANT SPEED OF SOUND

NUMBER OF ORIGINAL DATA POINTS = 11
TECHNIQUE: SPATIAL FOURIER SERIES FIT

DEPTH (M)	C(EXACT) (M/S)	C(FIT) (M/S)	% ERROR	CDOT(EXACT) (1/S)	CDOT(FIT) (1/S)	% ERROR	CDOT2(EXACT) (1/M-S)	CDOT2(FIT) (1/M-S)	% ERROR
0.00	1500.0	1500.0	0.000	0.0000E+00	0.6346E-13	0.000	0.0000E+00	-0.2551E-14	0.000
10.00	1500.0	1500.0	0.000	0.0000E+00	0.7595E-14	0.000	0.0000E+00	-0.6958E-14	0.000
20.00	1500.0	1500.0	0.000	0.0000E+00	-0.4149E-13	0.000	0.0000E+00	-0.1700E-14	0.000
30.00	1500.0	1500.0	0.000	0.0000E+00	-0.2451E-13	0.000	0.0000E+00	0.4171E-14	0.000
40.00	1500.0	1500.0	0.000	0.0000E+00	0.1456E-13	0.000	0.0000E+00	0.2382E-14	0.000
50.00	1500.0	1500.0	0.000	0.0000E+00	0.1289E-13	0.000	0.0000E+00	-0.2342E-14	0.000
60.00	1500.0	1500.0	0.000	0.0000E+00	-0.1322E-13	0.000	0.0000E+00	-0.1790E-14	0.000
70.00	1500.0	1500.0	0.000	0.0000E+00	-0.1103E-13	0.000	0.0000E+00	0.2101E-14	0.000
80.00	1500.0	1500.0	0.000	0.0000E+00	0.1442E-13	0.000	0.0000E+00	0.2022E-14	0.000
90.00	1500.0	1500.0	0.000	0.0000E+00	0.1696E-13	0.000	0.0000E+00	-0.1525E-14	0.000
100.00	1500.0	1500.0	0.000	0.0000E+00	-0.4398E-14	0.000	0.0000E+00	-0.1843E-14	0.000
110.00	1500.0	1500.0	0.000	0.0000E+00	-0.6789E-14	0.000	0.0000E+00	0.1472E-14	0.000
120.00	1500.0	1500.0	0.000	0.0000E+00	0.1480E-13	0.000	0.0000E+00	0.1943E-14	0.000
130.00	1500.0	1500.0	0.000	0.0000E+00	0.1744E-13	0.000	0.0000E+00	-0.1629E-14	0.000
140.00	1500.0	1500.0	0.000	0.0000E+00	-0.8355E-14	0.000	0.0000E+00	-0.2557E-14	0.000
150.00	1500.0	1500.0	0.000	0.0000E+00	-0.1584E-13	0.000	0.0000E+00	0.1459E-14	0.000
160.00	1500.0	1500.0	0.000	0.0000E+00	0.1273E-13	0.000	0.0000E+00	0.3161E-14	0.000
170.00	1500.0	1500.0	0.000	0.0000E+00	0.2342E-13	0.000	0.0000E+00	-0.1817E-14	0.000
180.00	1500.0	1500.0	0.000	0.0000E+00	-0.2076E-13	0.000	0.0000E+00	-0.5912E-14	0.000
190.00	1500.0	1500.0	0.000	0.0000E+00	-0.6329E-13	0.000	0.0000E+00	-0.1123E-14	0.000
200.00	1500.0	1500.0	0.000	0.0000E+00	-0.3175E-13	0.000	0.0000E+00	0.6845E-14	0.000

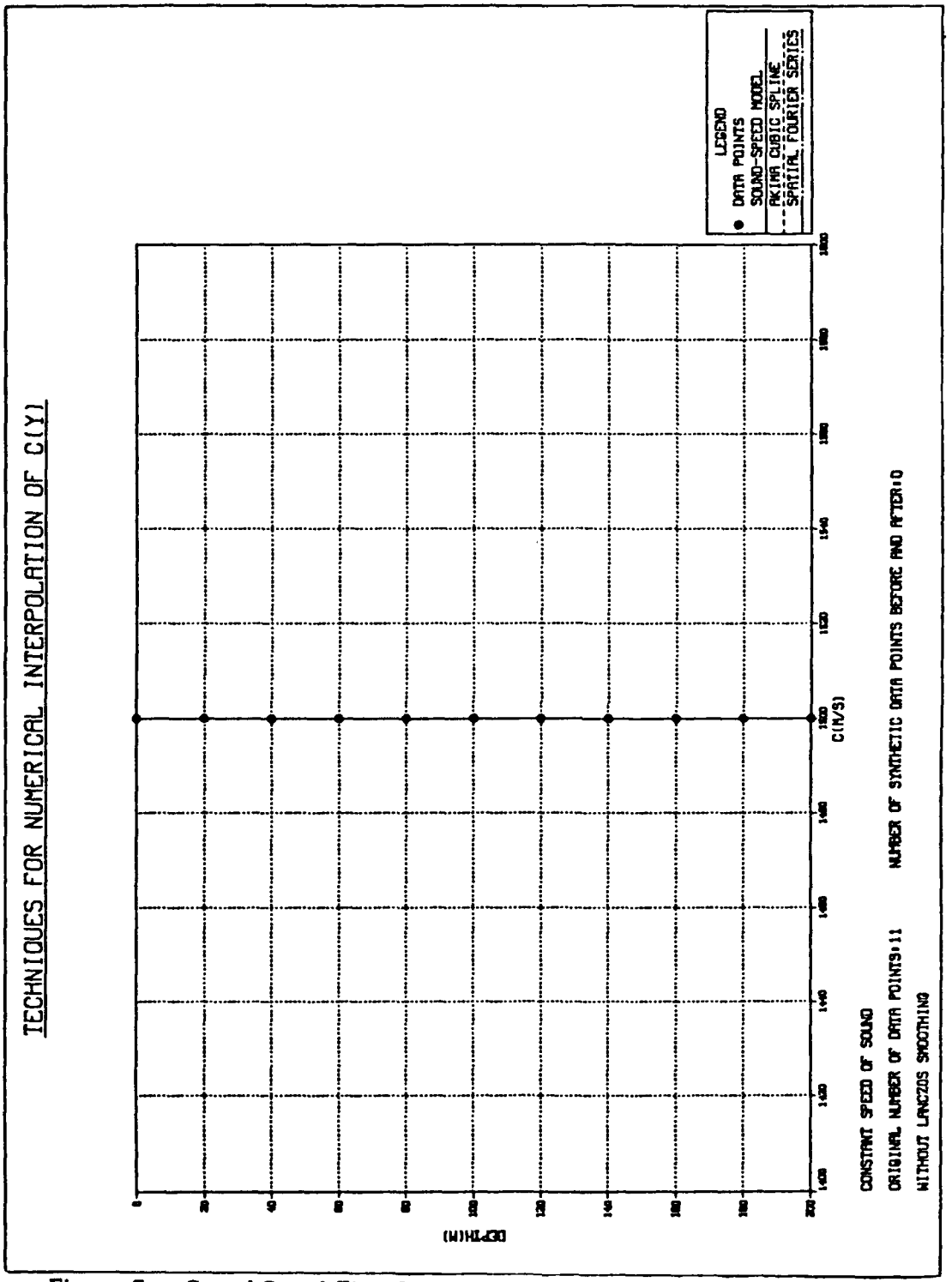

Figure 7. Sound Speed Fit - Constant Speed of Sound.

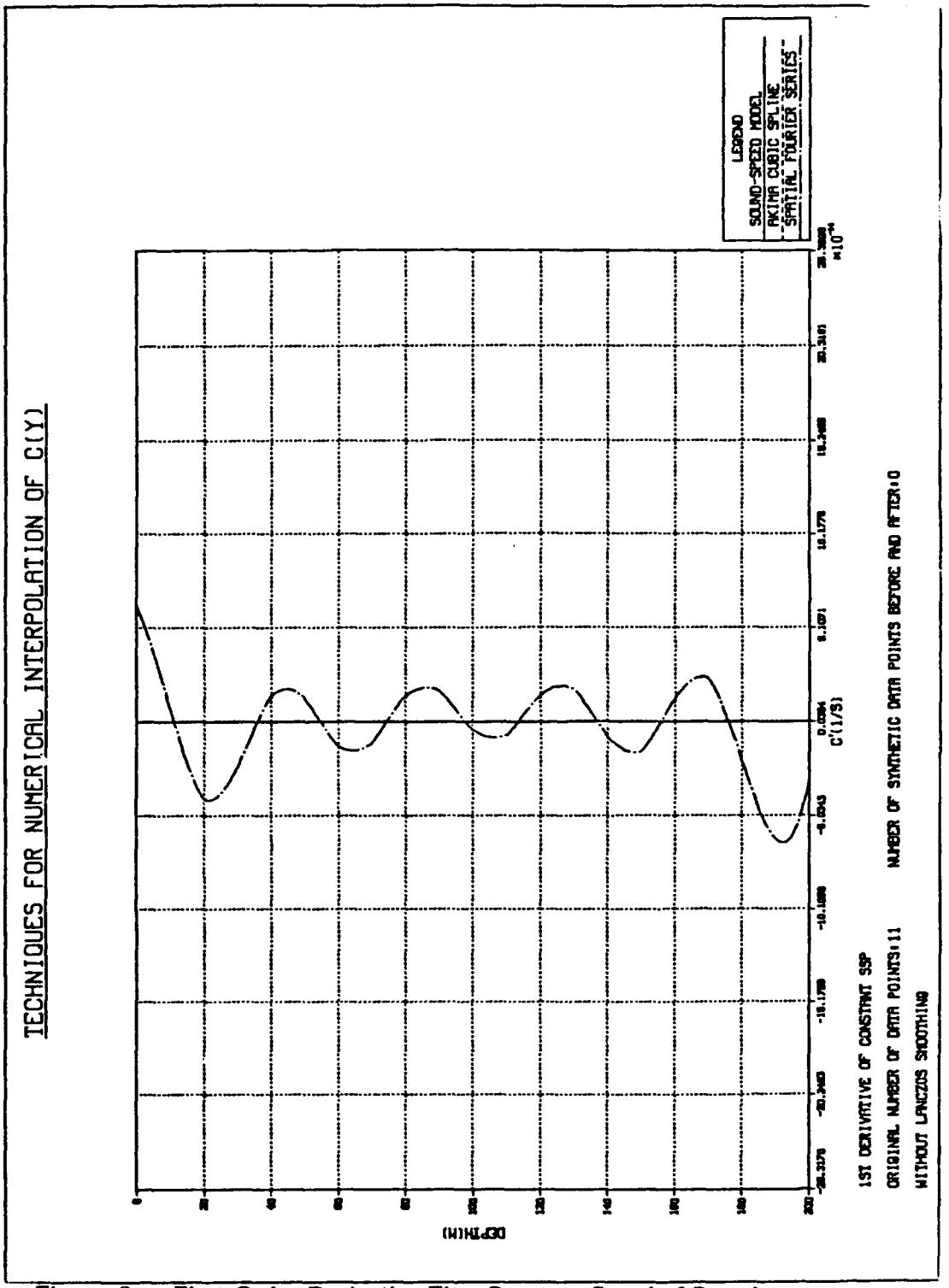

Figure 8. First-Order Derivative Fit - Constant Speed of Sound.

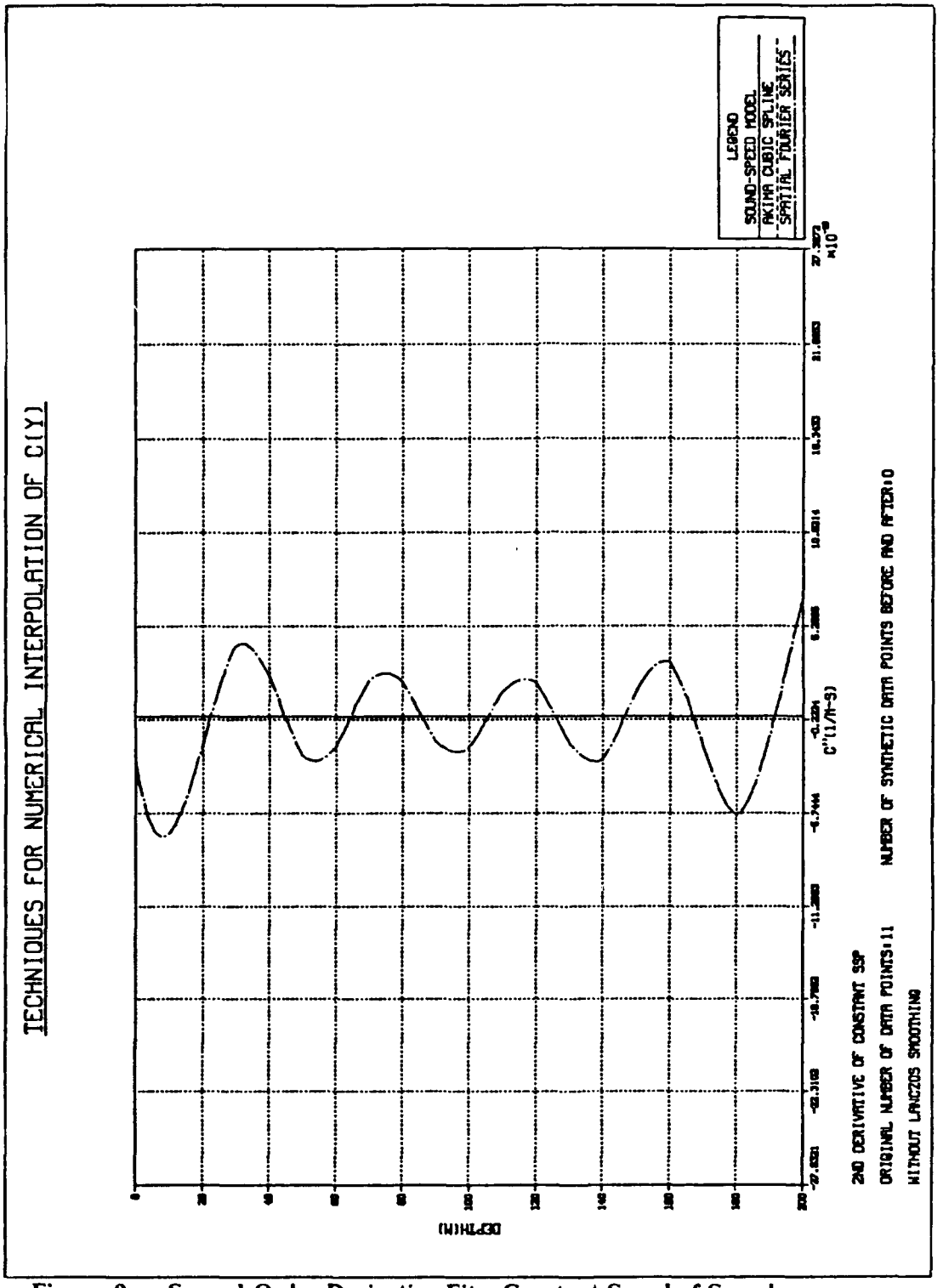

Figure 9. Second-Order Derivative Fit - Constant Speed of Sound.

Table 10. AKIMA CUBIC SPLINE RESULTS - LINEAR SSP WITH A POSITIVE GRADIENT

LINEAR SOUND-SPEED PROFILE WITH A POSITIVE GRADIENT

NUMBER OF ORIGINAL DATA POINTS = 11

TECHNIQUE: AKIMA CUBIC SPLINE FIT

DEPTH (M)	C(EXACT) (M/S)	C(FIT) (M/S)	% ERROR	CDOT(EXACT) (1/S)	CDOT(FIT) (1/S)	% ERROR	CDOT2(EXACT) (1/M-S)	CDOT2(FIT) (1/M-S)	% ERROR
0.00	1500.0	1500.0	0.000	0.1700E-01	0.1700E-01	0.000	0.0000E+00	0.1735E-18	0.000
10.00	1500.2	1500.2	0.000	0.1700E-01	0.1700E-01	0.000	0.0000E+00	-0.8674E-19	0.000
20.00	1500.3	1500.3	0.000	0.1700E-01	0.1700E-01	0.000	0.0000E+00	0.5204E-18	0.000
30.00	1500.5	1500.5	0.000	0.1700E-01	0.1700E-01	0.000	0.0000E+00	0.1204E-34	0.000
40.00	1500.7	1500.7	0.000	0.1700E-01	0.1700E-01	0.000	0.0000E+00	0.7111E-15	0.000
50.00	1500.8	1500.8	0.000	0.1700E-01	0.1700E-01	0.000	0.0000E+00	0.7108E-16	0.000
60.00	1501.0	1501.0	0.000	0.1700E-01	0.1700E-01	0.000	0.0000E+00	-0.4260E-15	0.000
70.00	1501.2	1501.2	0.000	0.1700E-01	0.1700E-01	0.000	0.0000E+00	-0.4930E-31	0.000
80.00	1501.4	1501.4	0.000	0.1700E-01	0.1700E-01	0.000	0.0000E+00	0.4267E-15	0.000
90.00	1501.5	1501.5	0.000	0.1700E-01	0.1700E-01	0.000	0.0000E+00	0.0000E+00	0.000
100.00	1501.7	1501.7	0.000	0.1700E-01	0.1700E-01	0.000	0.0000E+00	-0.4260E-15	0.000
110.00	1501.9	1501.9	0.000	0.1700E-01	0.1700E-01	0.000	0.0000E+00	-0.4930E-31	0.000
120.00	1502.0	1502.0	0.000	0.1700E-01	0.1700E-01	0.000	0.0000E+00	0.5689E-15	0.000
130.00	1502.2	1502.2	0.000	0.1700E-01	0.1700E-01	0.000	0.0000E+00	-0.7108E-16	0.000
140.00	1502.4	1502.4	0.000	0.1700E-01	0.1700E-01	0.000	0.0000E+00	0.5204E-18	0.000
150.00	1502.5	1502.5	0.000	0.1700E-01	0.1700E-01	0.000	0.0000E+00	0.1204E-34	0.000
160.00	1502.7	1502.7	0.000	0.1700E-01	0.1700E-01	0.000	0.0000E+00	0.5204E-18	0.000
170.00	1502.9	1502.9	0.000	0.1700E-01	0.1700E-01	0.000	0.0000E+00	0.1204E-34	0.000
180.00	1503.1	1503.1	0.000	0.1700E-01	0.1700E-01	0.000	0.0000E+00	0.4268E-15	0.000
190.00	1503.2	1503.2	0.000	0.1700E-01	0.1700E-01	0.000	0.0000E+00	0.2132E-15	0.000
200.00	1503.4	1503.4	0.000	0.1700E-01	0.1700E-01	0.000	0.0000E+00	-0.4337E-18	0.000

Table 11. FOURIER SERIES RESULTS - LINEAR SSP WITH A POSITIVE GRADIENT

LINEAR SOUND-SPEED PROFILE WITH A POSITIVE GRADIENT

NUMBER OF ORIGINAL DATA POINTS = 11
TECHNIQUE: SPATIAL FOURIER SERIES FIT

DEPTH (M)	C(EXACT) (M/S)	C(FIT) (M/S)	% ERROR	CDOT(EXACT) (1/S)	CDOT(FIT) (1/S)	% ERROR	CDOT2(EXACT) (1/M-S)	CDOT2(FIT) (1/M-S)	% ERROR
0.00	1500.0	1500.0	0.000	0.1700E-01	-0.1133E+00	-766.225	0.0000E+00	0.1525E-01	********
10.00	1500.2	1499.7	-0.035	0.1700E-01	0.3658E-01	115.206	0.0000E+00	0.1133E-01	********
20.00	1500.3	1500.3	0.000	0.1700E-01	0.7632E-01	348.914	0.0000E+00	-0.3184E-02	********
30.00	1500.5	1500.8	0.020	0.1700E-01	0.1101E-01	-35.237	0.0000E+00	-0.7100E-02	********
40.00	1500.7	1500.7	0.000	0.1700E-01	-0.2247E-01	-232.172	0.0000E+00	0.1203E-02	********
50.00	1500.8	1500.6	-0.015	0.1700E-01	0.1955E-01	14.995	0.0000E+00	0.5322E-02	********
60.00	1501.0	1501.0	0.000	0.1700E-01	0.4819E-01	183.475	0.0000E+00	-0.5432E-03	********
70.00	1501.2	1501.4	0.012	0.1700E-01	0.1586E-01	-6.732	0.0000E+00	-0.4497E-02	********
80.00	1501.4	1501.4	0.000	0.1700E-01	-0.1050E-01	-161.776	0.0000E+00	0.2215E-03	********
90.00	1501.5	1501.4	-0.011	0.1700E-01	0.1734E-01	2.006	0.0000E+00	0.4159E-02	********
100.00	1501.7	1501.7	0.000	0.1700E-01	0.4344E-01	155.502	0.0000E+00	-0.8671E-06	0.000
110.00	1501.9	1502.0	0.011	0.1700E-01	0.1733E-01	1.920	0.0000E+00	-0.4160E-02	********
120.00	1502.0	1502.0	0.000	0.1700E-01	-0.1052E-01	-161.866	0.0000E+00	-0.2207E-03	********
130.00	1502.2	1502.0	-0.012	0.1700E-01	0.1586E-01	-6.733	0.0000E+00	0.4499E-02	********
140.00	1502.4	1502.4	0.000	0.1700E-01	0.4821E-01	183.570	0.0000E+00	0.5442E-03	********
150.00	1502.5	1502.8	0.015	0.1700E-01	0.1956E-01	15.084	0.0000E+00	-0.5324E-02	********
160.00	1502.7	1502.7	0.000	0.1700E-01	-0.2247E-01	-232.189	0.0000E+00	-0.1205E-02	********
170.00	1502.9	1502.6	-0.020	0.1700E-01	0.1099E-01	-35.333	0.0000E+00	0.7099E-02	********
180.00	1503.1	1503.1	0.000	0.1700E-01	0.7631E-01	348.876	0.0000E+00	0.3186E-02	********
190.00	1503.2	1503.7	0.035	0.1700E-01	0.3660E-01	115.295	0.0000E+00	-0.1133E-01	********
200.00	1503.4	1503.4	0.000	0.1700E-01	-0.1132E+00	-766.108	0.0000E+00	-0.1525E-01	********

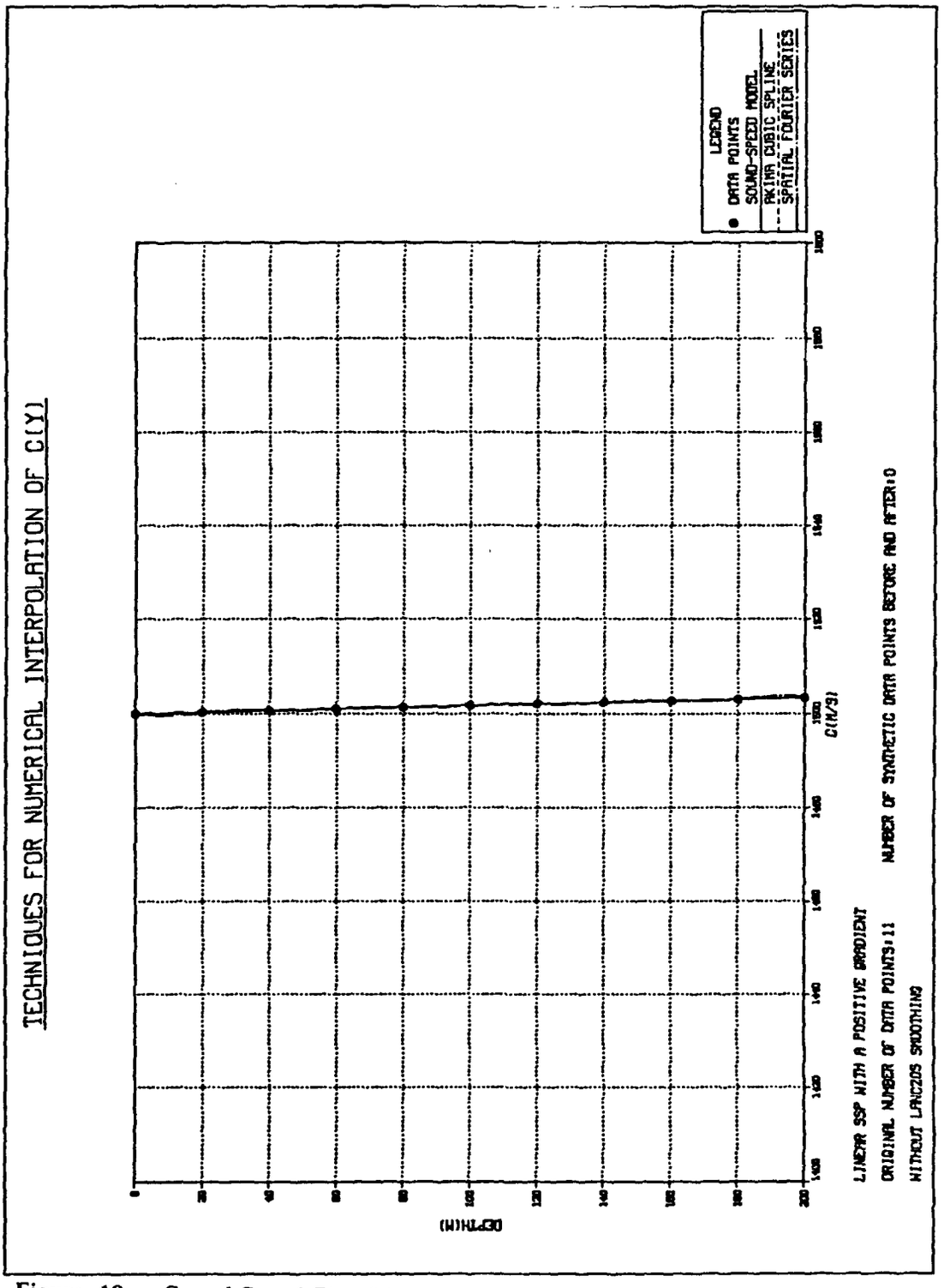

Figure 10. Sound Speed Fit - Linear SSP with a Positive Gradient.

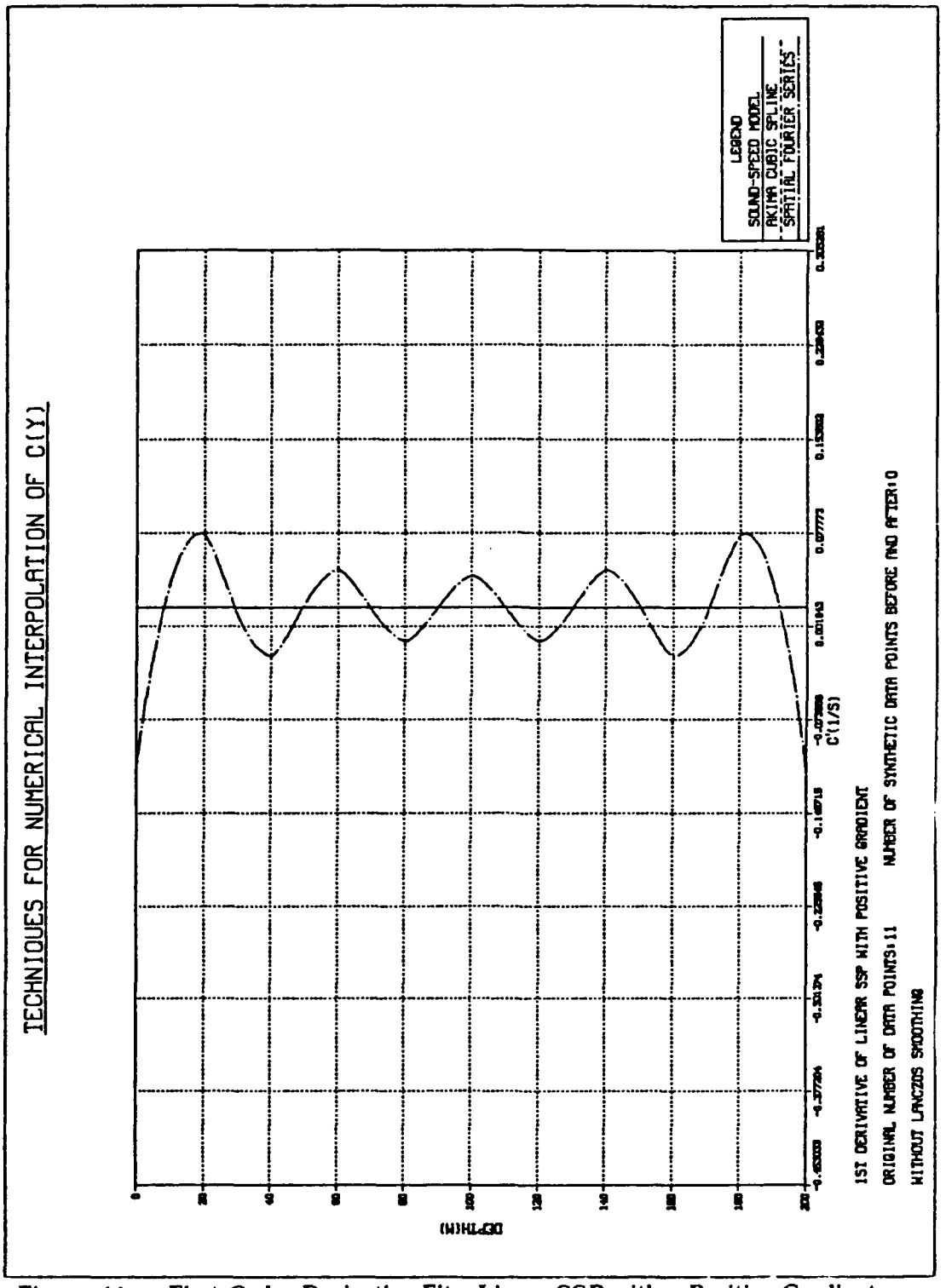

Figure 11. First-Order Derivative Fit - Linear SSP with a Positive Gradient.

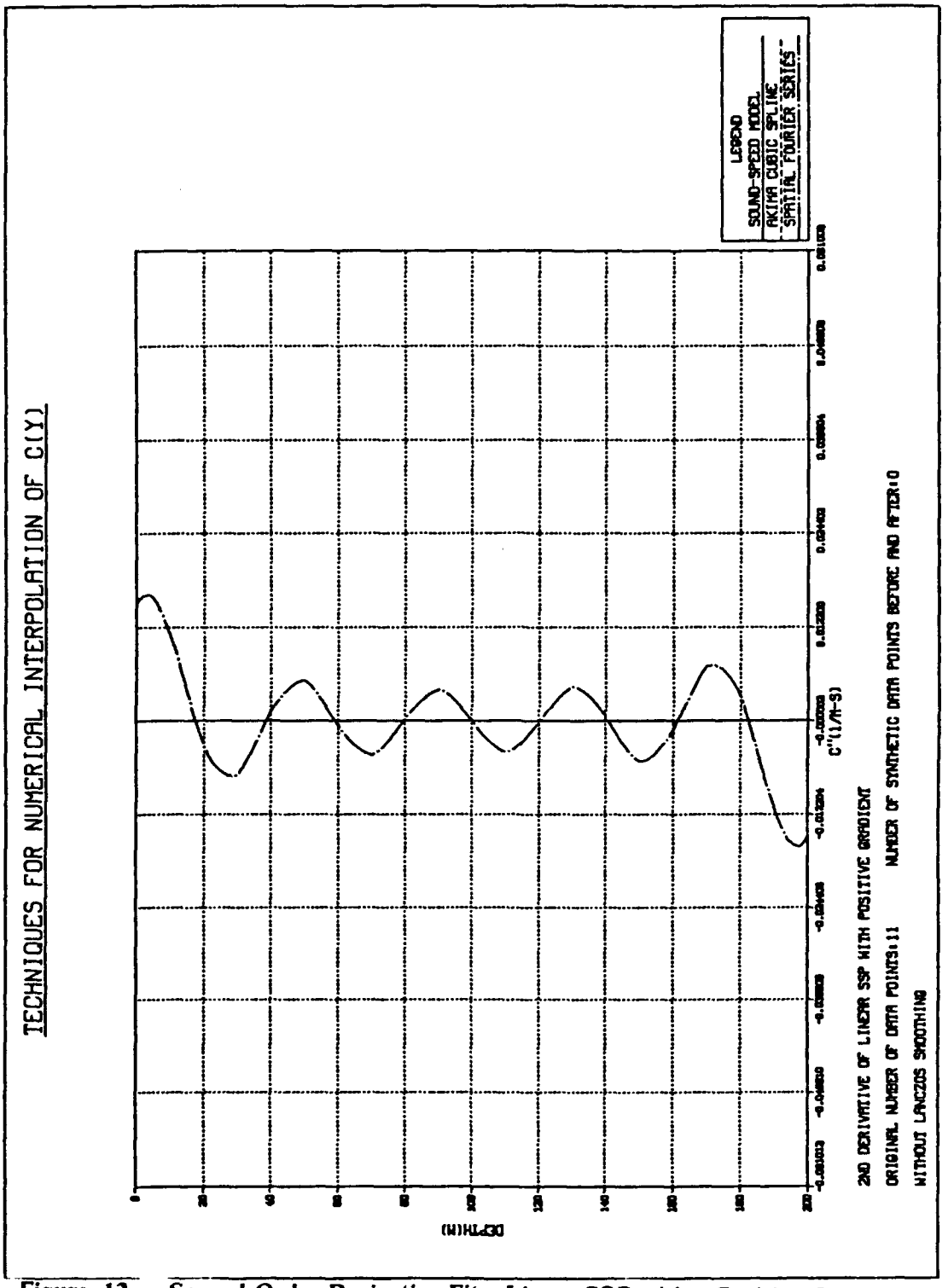

Figure 12. **Second Order Derivative Fit - Linear SSP with a Positive Gradient.**

Table 12. AKIMA CUBIC SPLINE RESULTS - LINEAR SSP WITH A NEGATIVE GRADIENT

LINEAR SOUND-SPEED PROFILE WITH A NEGATIVE GRADIENT

NUMBER OF ORIGINAL DATA POINTS = 11

TECHNIQUE: AKIMA CUBIC SPLINE FIT

DEPTH (M)	C(EXACT) (M/S)	C(FIT) (M/S)	% ERROR	CDOT(EXACT) (1/S)	CDOT(FIT) (1/S)	% ERROR	CDOT2(EXACT) (1/M-S)	CDOT2(FIT) (1/M-S)	% ERROR
0.00	1500.0	1500.0	0.000	-0.1700E-01	-0.1700E-01	0.000	0.0000E+00	0.1417E-15	0.000
10.00	1499.8	1499.8	0.000	-0.1700E-01	-0.1700E-01	0.000	0.0000E+00	0.1421E-15	0.000
20.00	1499.7	1499.7	0.000	-0.1700E-01	-0.1700E-01	0.000	0.0000E+00	0.4260E-15	0.000
30.00	1499.5	1499.5	0.000	-0.1700E-01	-0.1700E-01	0.000	0.0000E+00	0.4930E-31	0.000
40.00	1499.3	1499.3	0.000	-0.1700E-01	-0.1700E-01	0.000	0.0000E+00	-0.4267E-15	0.000
50.00	1499.1	1499.1	0.000	-0.1700E-01	-0.1700E-01	0.000	0.0000E+00	0.0000E+00	0.000
60.00	1499.0	1499.0	0.000	-0.1700E-01	-0.1700E-01	0.000	0.0000E+00	0.4260E-15	0.000
70.00	1498.8	1498.8	0.000	-0.1700E-01	-0.1700E-01	0.000	0.0000E+00	0.4930E-31	0.000
80.00	1498.6	1498.6	0.000	-0.1700E-01	-0.1700E-01	0.000	0.0000E+00	-0.4267E-15	0.000
90.00	1498.5	1498.5	0.000	-0.1700E-01	-0.1700E-01	0.000	0.0000E+00	0.0000E+00	0.000
100.00	1498.3	1498.3	0.000	-0.1700E-01	-0.1700E-01	0.000	0.0000E+00	0.4260E-15	0.000
110.00	1498.1	1498.1	0.000	-0.1700E-01	-0.1700E-01	0.000	0.0000E+00	0.4930E-31	0.000
120.00	1498.0	1498.0	0.000	-0.1700E-01	-0.1700F-01	0.000	0.0000E+00	-0.5689E-15	0.000
130.00	1497.8	1497.8	0.000	-0.1700E-01	-0.1700E-01	0.000	0.0000E+00	0.7108E-16	0.000
140.00	1497.6	1497.6	0.000	-0.1700E-01	-0.1700E-01	0.000	0.0000E+00	-0.5204E-18	0.000
150.00	1497.4	1497.4	0.000	-0.1700E-01	-0.1700E-01	0.000	0.0000E+00	-0.1204E-34	0.000
160.00	1497.3	1497.3	0.000	-0.1700E-01	-0.1700E-01	0.000	0.0000E+00	-0.5204E-18	0.000
170.00	1497.1	1497.1	0.000	-0.1700E-01	-0.1700E-01	0.000	0.0000E+00	-0.1204E-34	0.000
180.00	1496.9	1496.9	0.000	-0.1700E-01	-0.1700E-01	0.000	0.0000E+00	-0.4268E-15	0.000
190.00	1496.8	1496.8	0.000	-0.1700E-01	-0.1700E-01	0.000	0.0000E+00	-0.2132E-15	0.000
200.00	1496.6	1496.6	0.000	-0.1700E-01	-0.1700E-01	0.000	0.0000E+00	0.4337E-18	0.000

Table 13. FOURIER SERIES RESULTS - LINEAR SSP WITH A NEGATIVE GRADIENT

LINEAR SOUND-SPEED PROFILE WITH A NEGATIVE GRADIENT

NUMBER OF ORIGINAL DATA POINTS = 11
TECHNIQUE: SPATIAL FOURIER SERIES FIT

DEPTH (M)	C(EXACT) (M/S)	C(FIT) (M/S)	% ERROR	CDOT(EXACT) (1/S)	CDOT(FIT) (1/S)	% ERROR	CDOT2(EXACT) (1/M-S)	CDOT2(FIT) (1/M-S)	% ERROR
0.00	1500.0	1500.0	0.000	-0.1700E-01	0.1133E+00	-766.225	0.0000E+00	-0.1525E-01	********
10.00	1499.8	1500.3	0.035	-0.1700E-01	-0.3660E-01	115.297	0.0000E+00	-0.1133E-01	********
20.00	1499.7	1499.7	0.000	-0.1700E-01	-0.7633E-01	348.986	0.0000E+00	0.3185E-02	********
30.00	1499.5	1499.2	-0.020	-0.1700E-01	-0.1101E-01	-35.247	0.0000E+00	0.7101E-02	********
40.00	1499.3	1499.3	0.000	-0.1700E-01	0.2248E-01	-232.210	0.0000E+00	-0.1204E-02	********
50.00	1499.1	1499.4	0.015	-0.1700E-01	-0.1955E-01	14.998	0.0000E+00	-0.5323E-02	********
60.00	1499.0	1499.0	0.000	-0.1700E-01	-0.4820E-01	183.502	0.0000E+00	0.5433E-03	********
70.00	1498.8	1498.6	-0.012	-0.1700E-01	-0.1586E-01	-6.733	0.0000E+00	0.4498E-02	********
80.00	1498.6	1498.6	0.000	-0.1700E-01	0.1051E-01	-161.799	0.0000E+00	-0.2216E-03	********
90.00	1498.5	1498.6	0.011	-0.1700E-01	-0.1734E-01	2.007	0.0000E+00	-0.4159E-02	********
100.00	1498.3	1498.3	0.000	-0.1700E-01	-0.4344E-01	155.523	0.0000E+00	0.8815E-06	0.000
110.00	1498.1	1498.0	-0.011	-0.1700E-01	-0.1733E-01	1.920	0.0000E+00	0.4160E-02	********
120.00	1498.0	1498.0	0.000	-0.1700E-01	0.1052E-01	-161.887	0.0000E+00	0.2207E-03	********
130.00	1497.8	1498.0	0.012	-0.1700E-01	-0.1586E-01	-6.734	0.0000E+00	-0.4500E-02	********
140.00	1497.6	1497.6	0.000	-0.1700E-01	-0.4821E-01	183.592	0.0000E+00	-0.5443E-03	********
150.00	1497.4	1497.2	-0.015	-0.1700E-01	-0.1956E-01	15.086	0.0000E+00	0.5324E-02	********
160.00	1497.3	1497.3	0.000	-0.1700E-01	0.2248E-01	-232.216	0.0000E+00	0.1206E-02	********
170.00	1497.1	1497.4	0.020	-0.1700E-01	-0.1099E-01	-35.336	0.0000E+00	-0.7100E-02	********
180.00	1496.9	1496.9	0.000	-0.1700E-01	-0.7632E-01	348.914	0.0000E+00	-0.3187E-02	********
190.00	1496.8	1496.3	-0.035	-0.1700E-01	-0.3660E-01	115.304	0.0000E+00	0.1133E-01	********
200.00	1496.6	1496.6	0.000	-0.1700E-01	0.1133E+00	-766.181	0.0000E+00	0.1525E-01	********

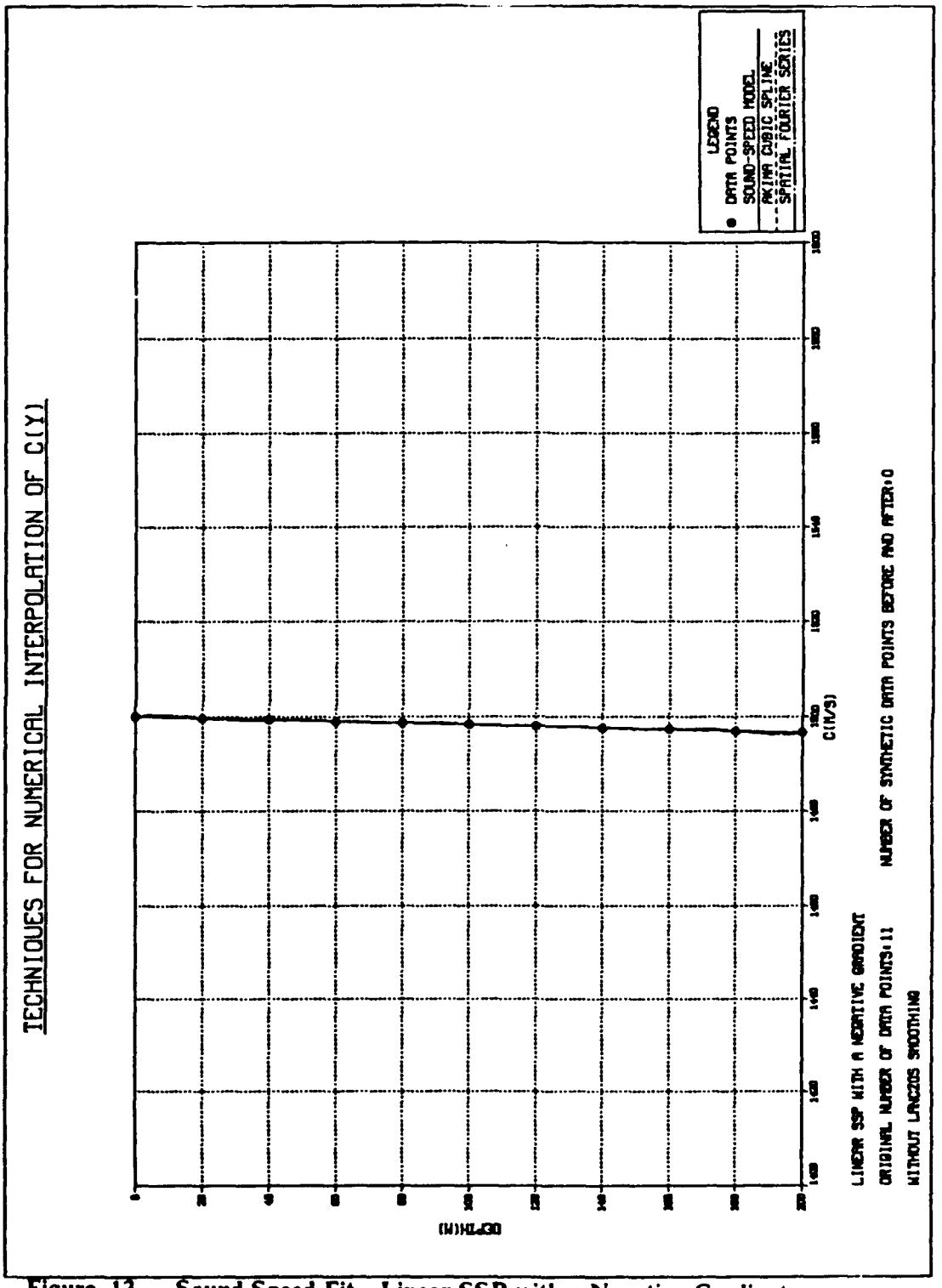

Figure 13. Sound Speed Fit - Linear SSP with a Negative Gradient.

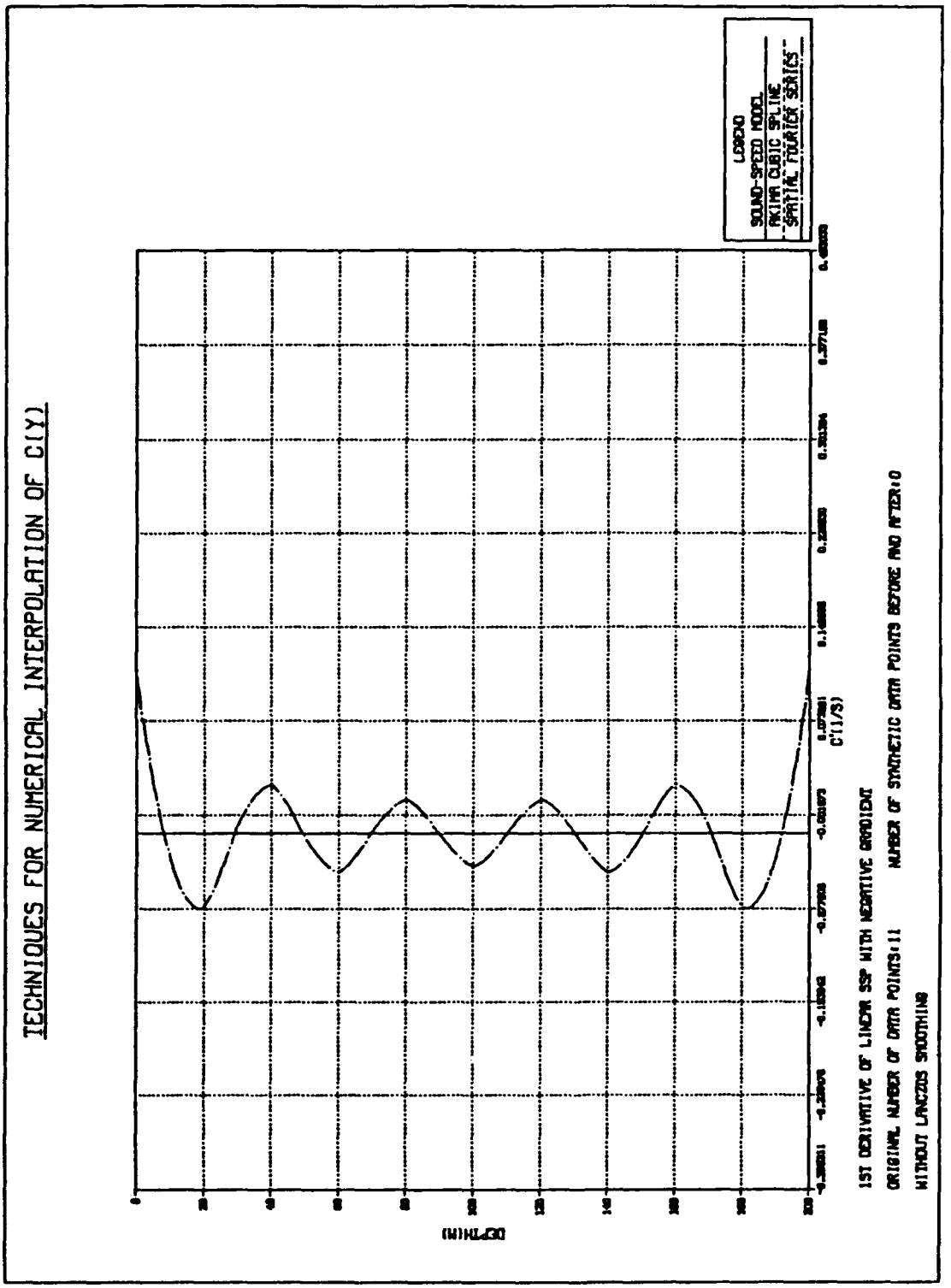

Figure 14. First-Order Derivative Fit - Linear SSP with a Negative Gradient.

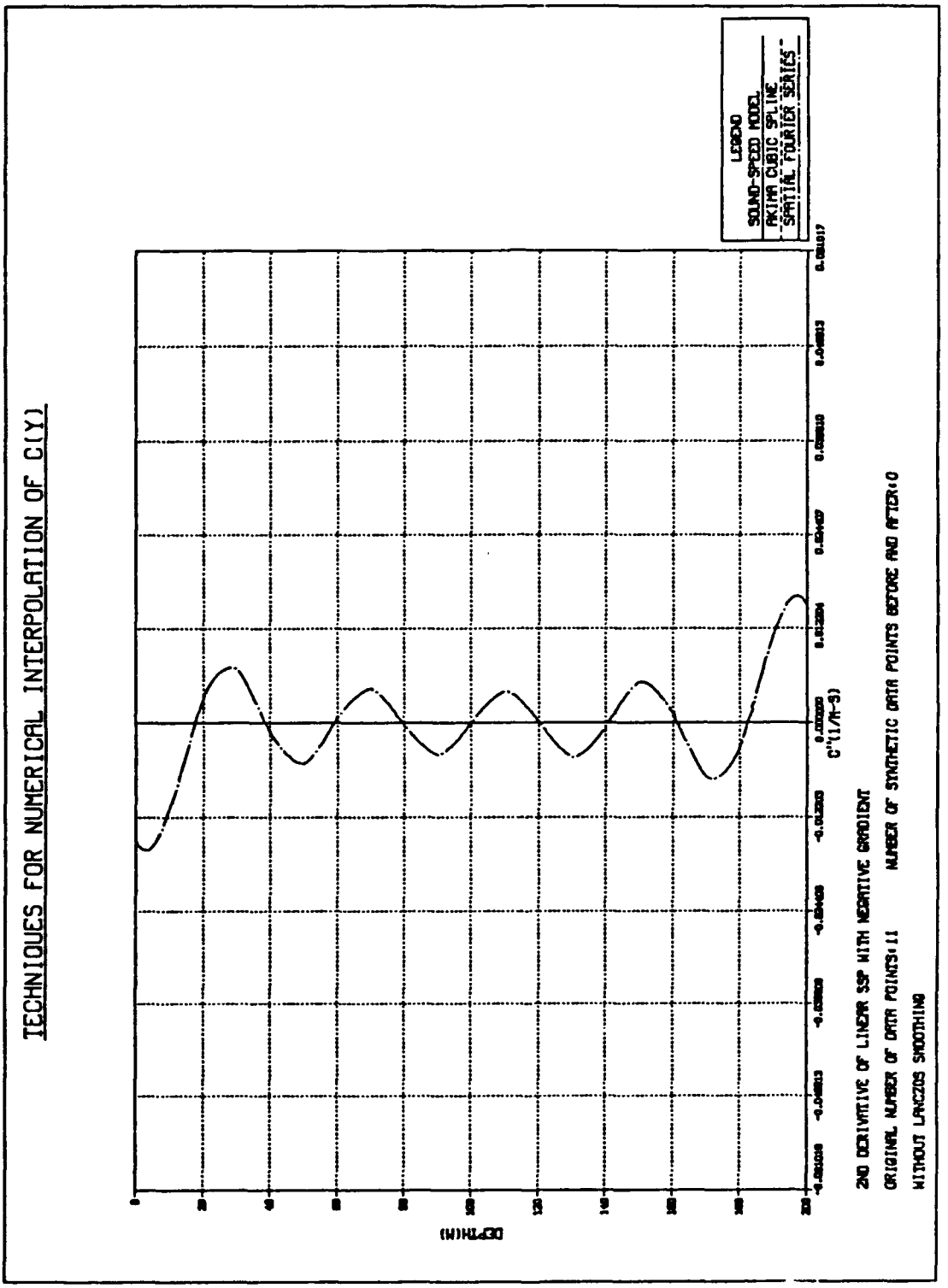

Figure 15. Second-Order Derivative Fit - Linear SSP with a Negative Gradient.

The above three exact sound-speed functions were used to compare the Fourier series representation with the Akima cubic spline since the Fourier fit can be expected to be at its worst since we are trying to form linear functions from trigonometric ones. The next two functions examined, however, are non-linear; the half-period sine wave and the parabola.

Tables 14 and 15 along with Figures 16, 17 and 18 compare the Akima cubic spline and Fourier series representations of sound-speed data generated from a half-period sine wave. Both techniques encounter some difficulty here, with the Fourier representation generally behaving better near the midpoint of the data than the Akima cubic spline fit for sound speed and both derivatives. However, near the surface and bottom, the errors in the Fourier representation become much larger than those of the Akima cubic spline fit.

Tables 16 and 17 along with Figures 19, 20 and 21 compare the Akima cubic spline and Fourier series representations of sound-speed data generated from a parabola. Surprisingly, the Akima cubic spline representation matches sound speed and derivatives very well. The Fourier representation behaves in a manner similar to its handling of the half-period sine wave. It produces small errors near the midpoint of the data and large discrepancies at either end for sound speed as well as in the first and second-order derivatives.

The disappointing performance of the Fourier series representation of sound speed and of the first and second-order derivatives of sound speed led to various attempts to salvage it. First, Lanczos smoothing as discussed in Chapter II, Section C, was implemented. This ameliorated the oscillations of the Fourier representation as shown in Tables 18 and 19 and Figures 22 through 27 for the half-period sine wave and parabolic SSPs. It can be seen that Lanczos smoothing results in a smoother fit for sound speed and for the derivatives to a point closer to the end points of the data but, nevertheless, leaves significant discrepancies near the end points.

Table 14. AKIMA CUBIC SPLINE RESULTS - HALF-PERIOD SINE WAVE SSP

HALF-PERIOD SINE WAVE SOUND-SPEED PROFILE

NUMBER OF ORIGINAL DATA POINTS = 11

TECHNIQUE: AKIMA CUBIC SPLINE FIT

DEPTH (M)	C(EXACT) (M/S)	C(FIT) (M/S)	% ERROR	CDOT(EXACT) (1/S)	CDOT(FIT) (1/S)	% ERROR	CDOT2(EXACT) (1/M-S)	CDOT2(FIT) (1/M-S)	% ERROR
0.00	1500.0	1500.0	0.000	-0.3927E+00	-0.4052E+00	3.177	0.0000E+00	0.2478E-02	********
10.00	1496.1	1496.1	-0.002	-0.3879E+00	-0.3848E+00	-0.790	0.9650E-03	0.1597E-02	65.468
20.00	1492.3	1492.3	0.000	-0.3735E+00	-0.3732E+00	-0.063	0.1906E-02	0.2969E-02	55.736
30.00	1488.7	1488.7	0.002	-0.3499E+00	-0.3472E+00	-0.761	0.2800E-02	0.2233E-02	-20.262
40.00	1485.3	1485.3	0.000	-0.3177E+00	-0.3286E+00	3.425	0.3626E-02	0.6627E-02	82.786
50.00	1482.3	1482.3	0.000	-0.2777E+00	-0.2730E+00	-1.692	0.4362E-02	0.4493E-02	3.000
60.00	1479.8	1479.8	0.000	-0.2308E+00	-0.2387E+00	3.425	0.4990E-02	0.7032E-02	40.903
70.00	1477.7	1477.7	-0.001	-0.1783E+00	-0.1753E+00	-1.692	0.5496E-02	0.5661E-02	3.000
80.00	1476.2	1476.2	0.000	-0.1214E+00	-0.1255E+00	3.425	0.5867E-02	0.6748E-02	15.018
90.00	1475.3	1475.3	-0.001	-0.6143E-01	-0.6039E-01	-1.692	0.6093E-02	0.6275E-02	3.000
100.00	1475.0	1475.0	0.000	-0.1112E-15	0.0000E+00	0.000	0.6169E-02	0.5803E-02	-5.924
110.00	1475.3	1475.3	-0.001	0.6143E-01	0.6039E-01	-1.692	0.6093E-02	0.6275E-02	3.000
120.00	1476.2	1476.2	0.000	0.1214E+00	0.1255E+00	3.425	0.5867E-02	0.4291E-02	-26.865
130.00	1477.7	1477.7	-0.001	0.1783E+00	0.1753E+00	-1.692	0.5496E-02	0.5661E-02	3.000
140.00	1479.8	1479.8	0.000	0.2308E+00	0.2387E+00	3.425	0.4990E-02	0.2358E-02	-52.750
150.00	1482.3	1482.3	0.000	0.2777E+00	0.2730E+00	-1.692	0.4362E-02	0.4493E-02	3.000
160.00	1485.3	1485.3	0.000	0.3177E+00	0.3286E+00	3.425	0.3626E-02	0.1497E-02	-58.699
170.00	1488.7	1488.7	0.002	0.3499E+00	0.3472E+00	-0.761	0.2800E-02	0.2233E-02	-20.262
180.00	1492.3	1492.3	0.000	0.3735E+00	0.3732E+00	-0.063	0.1906E-02	0.7152E-03	-62.480
190.00	1496.1	1496.1	-0.002	0.3879E+00	0.3848E+00	-0.790	0.9650E-03	0.1597E-02	65.468
200.00	1500.0	1500.0	0.000	0.3927E+00	0.4052E+00	3.177	0.2125E-17	0.2478E-02	********

Table 15. FOURIER SERIES RESULTS - HALF-PERIOD SINE WAVE SSP

HALF-PERIOD SINE WAVE SOUND-SPEED PROFILE

NUMBER OF ORIGINAL DATA POINTS = 11

TECHNIQUE: SPATIAL FOURIER SERIES FIT

DEPTH (M)	C(EXACT) (M/S)	C(FIT) (M/S)	% ERROR	CDOT(EXACT) (1/S)	CDOT(FIT) (1/S)	% ERROR	CDOT2(EXACT) (1/M-S)	CDOT2(FIT) (1/M-S)	% ERROR
0.00	1500.0	1500.0	0.000	-0.3927E+00	-0.2739E+00	-30.253	0.0000E+00	-0.2198E-01	********
10.00	1496.1	1496.4	0.023	-0.3879E+00	-0.4111E+00	5.985	0.9650E-03	-0.5383E-02	-657.801
20.00	1492.3	1492.3	0.000	-0.3735E+00	-0.4034E+00	7.998	0.1906E-02	0.5100E-02	167.575
30.00	1488.7	1488.5	-0.008	-0.3499E+00	-0.3446E+00	-1.506	0.2800E-02	0.5362E-02	91.470
40.00	1485.3	1485.3	0.000	-0.3177E+00	-0.3058E+00	-3.761	0.3626E-02	0.2661E-02	-26.619
50.00	1482.3	1482.4	0.003	-0.2777E+00	-0.2796E+00	0.706	0.4362E-02	0.3172E-02	-27.283
60.00	1479.8	1479.8	0.000	-0.2308E+00	-0.2363E+00	2.393	0.4990E-02	0.5416E-02	8.526
70.00	1477.7	1477.7	-0.002	-0.1783E+00	-0.1773E+00	-0.564	0.5496E-02	0.6050E-02	10.078
80.00	1476.2	1476.2	0.000	-0.1214E+00	-0.1191E+00	-1.878	0.5867E-02	0.5613E-02	-4.329
90.00	1475.3	1475.3	0.000	-0.6143E-01	-0.6213E-01	1.134	0.6093E-02	0.5928E-02	-2.700
100.00	1475.0	1475.0	0.000	-0.1112E-15	-0.3522E-05	********	0.6169E-02	0.6380E-02	3.425
110.00	1475.3	1475.3	0.000	0.6143E-01	0.6213E-01	1.134	0.6093E-02	0.5929E-02	-2.682
120.00	1476.2	1476.2	0.000	0.1214E+00	0.1191E+00	-1.872	0.5867E-02	0.5613E-02	-4.327
130.00	1477.7	1477.7	-0.002	0.1783E+00	0.1773E+00	-0.564	0.5496E-02	0.6049E-02	10.057
140.00	1479.8	1479.8	0.000	0.2308E+00	0.2363E+00	2.390	0.4990E-02	0.5416E-02	8.523
150.00	1482.3	1482.4	0.003	0.2777E+00	0.2796E+00	0.706	0.4362E-02	0.3173E-02	-27.249
160.00	1485.3	1485.3	0.000	0.3177E+00	0.3058E+00	-3.758	0.3626E-02	0.2661E-02	-26.608
170.00	1488.7	1488.5	-0.008	0.3499E+00	0.3446E+00	-1.505	0.2800E-02	0.5360E-02	91.398
180.00	1492.3	1492.3	0.000	0.3735E+00	0.4033E+00	7.993	0.1906E-02	0.5099E-02	167.497
190.00	1496.1	1496.4	0.023	0.3879E+00	0.4111E+00	5.980	0.9650E-03	-0.5381E-02	-657.599
200.00	1500.0	1500.0	0.000	0.3927E+00	0.2739E+00	-30.249	0.2125E-17	-0.2198E-01	********

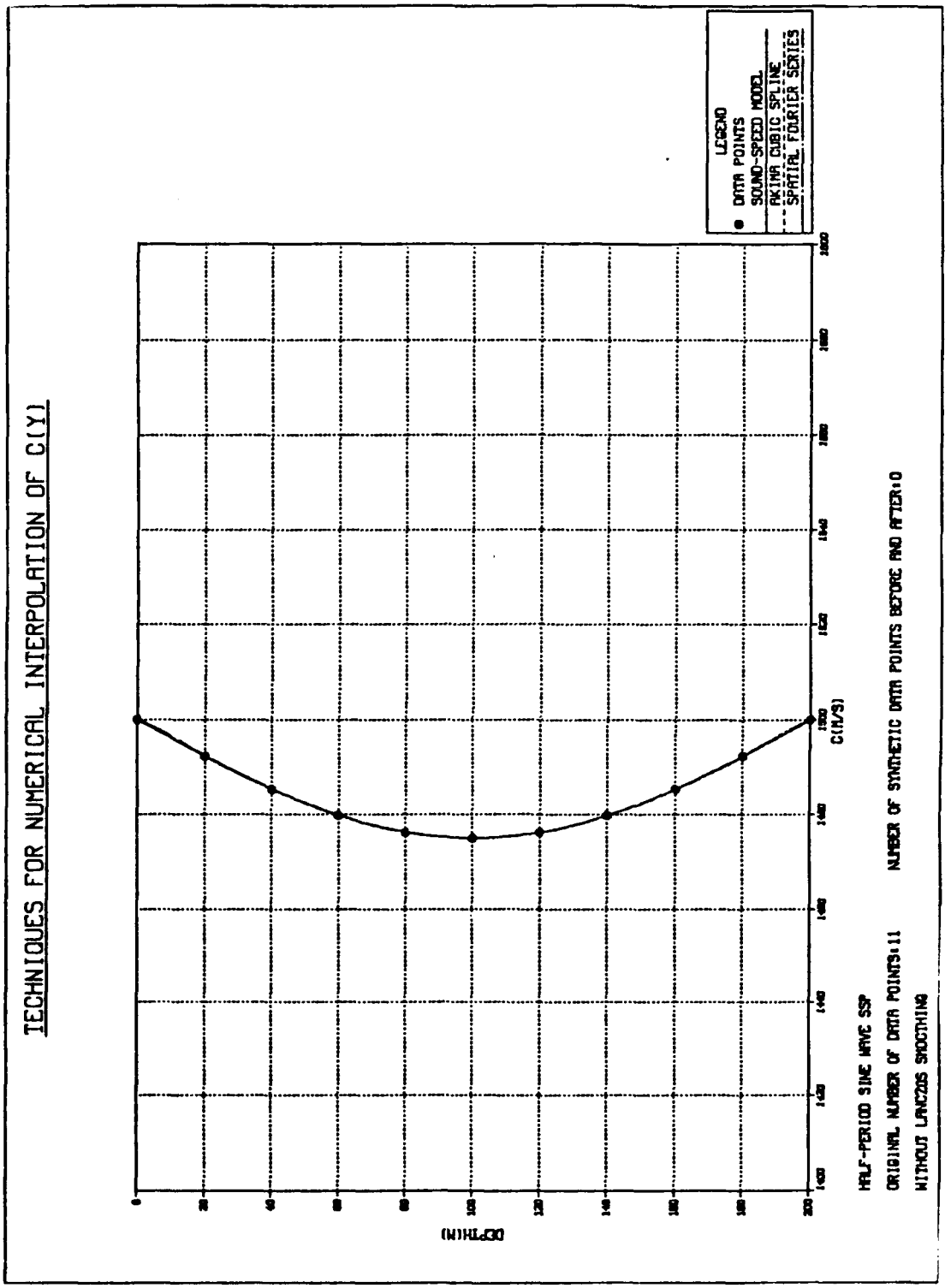

Figure 16. Sound Speed Fit - Half-Period Sine Wave SSP.

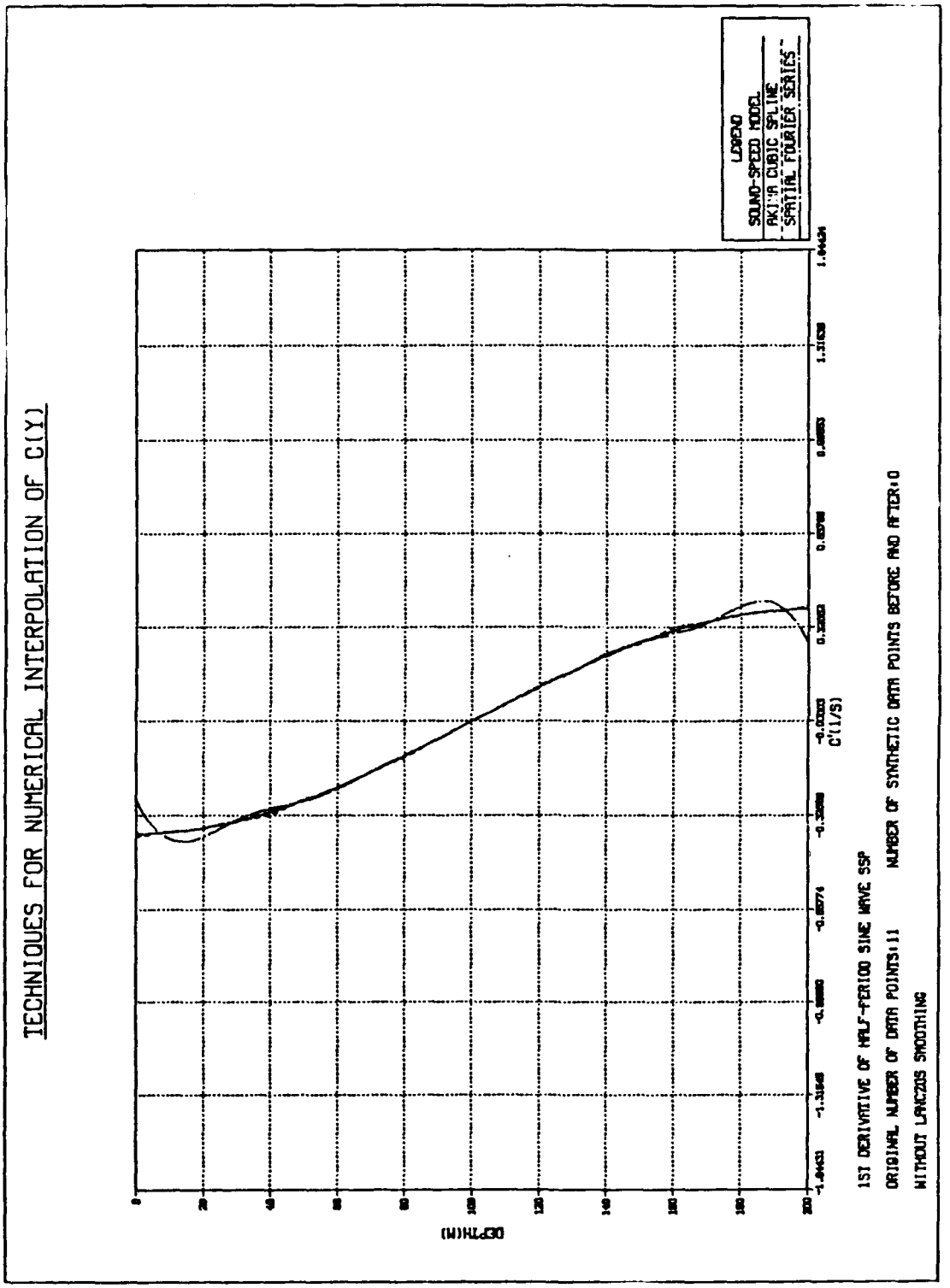

Figure 17. First-Order Derivative Fit - Half-Period Sine Wave SSP.

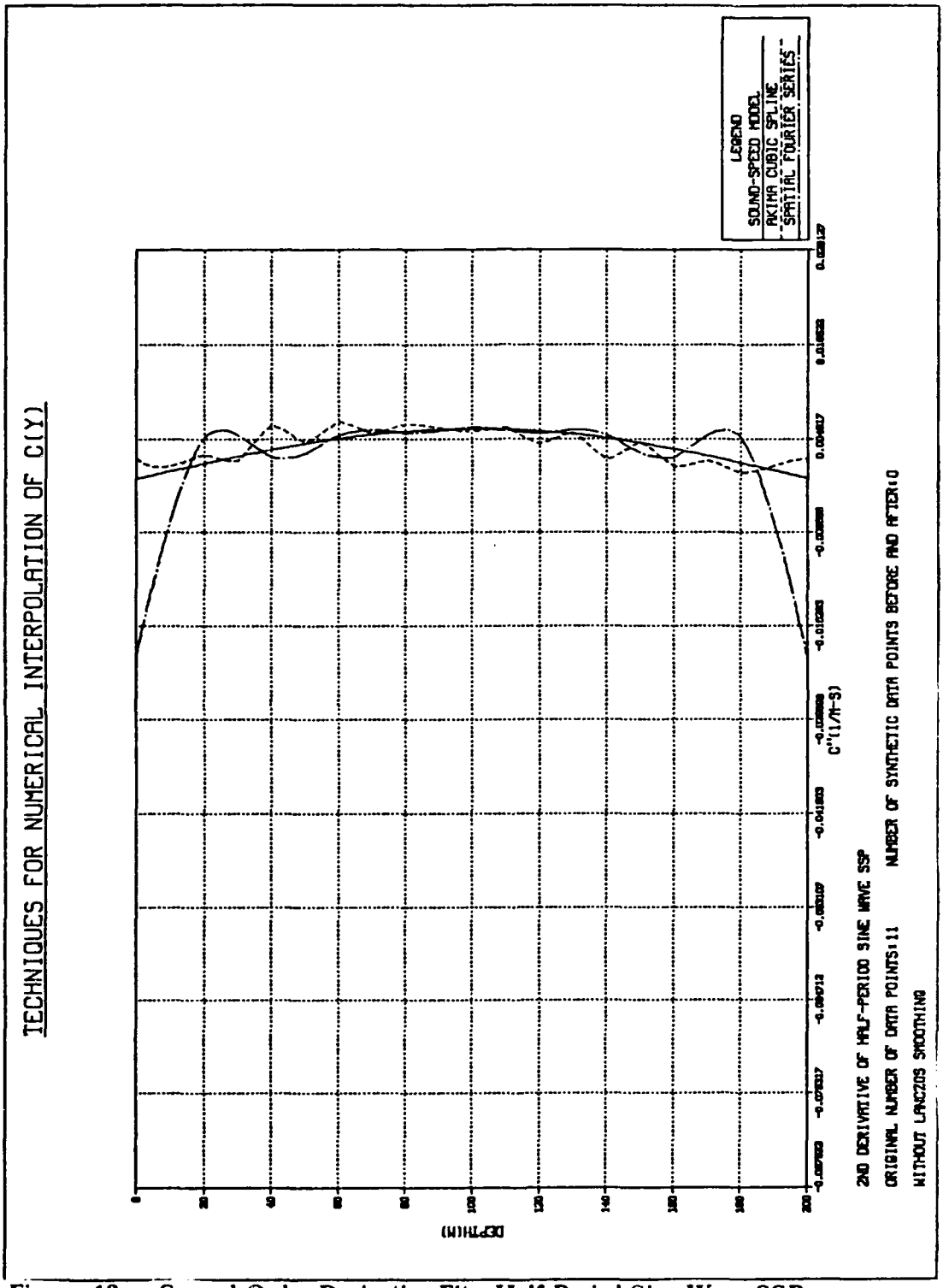

Figure 18. Second-Order Derivative Fit - Half-Period Sine Wave SSP.

Table 16. AKIMA CUBIC SPLINE RESULTS - PARABOLIC SSP

PARABOLIC SOUND-SPEED PROFILE

NUMBER OF ORIGINAL DATA POINTS = 11
TECHNIQUE: SPATIAL FOURIER SERIES FIT

DEPTH (M)	C(EXACT) (M/S)	C(FIT) (M/S)	% ERROR	CDOT(EXACT) (1/S)	CDOT(FIT) (1/S)	% ERROR	CDOT2(EXACT) (1/M-S)	CDOT2(FIT) (1/M-S)	% ERROR
0.00	1550.0	1550.0	0.000	-0.2000E+01	-0.1332E+01	-33.382	0.2000E-01	-0.1041E+00	-620.314
10.00	1531.0	1532.9	0.126	-0.1800E+01	-0.1930E+01	7.249	0.2000E-01	-0.1546E-01	-177.302
20.00	1514.0	1514.0	0.000	-0.1600E+01	-0.1767E+01	10.431	0.2000E-01	0.3791E-01	89.547
30.00	1499.0	1498.4	-0.043	-0.1400E+01	-0.1371E+01	-2.107	0.2000E-01	0.3428E-01	71.398
40.00	1486.0	1486.0	0.000	-0.1200E+01	-0.1133E+01	-5.549	0.2000E-01	0.1461E-01	-26.970
50.00	1475.0	1475.3	0.019	-0.1000E+01	-0.1011E+01	1.095	0.2000E-01	0.1338E-01	-33.111
60.00	1466.0	1466.0	0.000	-0.8000E+00	-0.8307E+00	3.840	0.2000E-01	0.2238E-01	11.876
70.00	1459.0	1458.9	-0.009	-0.6000E+00	-0.5944E+00	-0.938	0.2000E-01	0.2308E-01	15.379
80.00	1454.0	1454.0	0.000	-0.4000E+00	-0.3874E+00	-3.155	0.2000E-01	0.1858E-01	-7.104
90.00	1451.0	1451.0	0.003	-0.2000E+00	-0.2040E+00	1.976	0.2000E-01	0.1909E-01	-4.549
100.00	1450.0	1450.0	0.000	0.0000E+00	-0.6716E-14	0.000	0.2000E-01	0.2119E-01	5.929
110.00	1451.0	1451.0	0.003	0.2000E+00	0.2040E+00	1.976	0.2000E-01	0.1909E-01	-4.549
120.00	1454.0	1454.0	0.000	0.4000E+00	0.3874E+00	-3.155	0.2000E-01	0.1858E-01	-7.104
130.00	1459.0	1458.9	-0.009	0.6000E+00	0.5944E+00	-0.938	0.2000E-01	0.2308E-01	15.379
140.00	1466.0	1466.0	0.000	0.8000E+00	0.8307E+00	3.840	0.2000E-01	0.2238E-01	11.876
150.00	1475.0	1475.3	0.019	0.1000E+01	0.1011E+01	1.095	0.2000E-01	0.1338E-01	-33.111
160.00	1486.0	1486.0	0.000	0.1200E+01	0.1133E+01	-5.549	0.2000E-01	0.1461E-01	-26.970
170.00	1499.0	1498.4	-0.043	0.1400E+01	0.1371E+01	-2.107	0.2000E-01	0.3428E-01	71.398
180.00	1514.0	1514.0	0.000	0.1600E+01	0.1767E+01	10.431	0.2000E-01	0.3791E-01	89.547
190.00	1531.0	1532.9	0.126	0.1800E+01	0.1930E+01	7.249	0.2000E-01	-0.1546E-01	-177.302
200.00	1550.0	1550.0	0.000	0.2000E+01	0.1332E+01	-33.382	0.2000E-01	-0.1041E+00	-620.314

Table 17. FOURIER SERIES RESULTS - PARABOLIC SSP

PARABOLIC SOUND-SPEED PROFILE

NUMBER OF ORIGINAL DATA POINTS = 11

TECHNIQUE: AKIMA CUBIC SPLINE FIT

DEPTH (M)	C(EXACT) (M/S)	C(FIT) (M/S)	% ERROR	CDOT(EXACT) (1/S)	CDOT(FIT) (1/S)	% ERROR	CDOT2(EXACT) (1/M-S)	CDOT2(FIT) (1/M-S)	% ERROR
0.00	1550.0	1550.0	0.000	-0.2000E+01	-0.2000E+01	0.000	0.2000E-01	0.2000E-01	0.000
10.00	1531.0	1531.0	0.000	-0.1800E+01	-0.1800E+01	0.000	0.2000E-01	0.2000E-01	0.000
20.00	1514.0	1514.0	0.000	-0.1600E+01	-0.1600E+01	0.000	0.2000E-01	0.2000E-01	0.000
30.00	1499.0	1499.0	0.000	-0.1400E+01	-0.1400E+01	0.000	0.2000E-01	0.2000E-01	0.000
40.00	1486.0	1486.0	0.000	-0.1200E+01	-0.1200E+01	0.000	0.2000E-01	0.2000E-01	0.000
50.00	1475.0	1475.0	0.000	-0.1000E+01	-0.1000E+01	0.000	0.2000E-01	0.2000E-01	0.000
60.00	1466.0	1466.0	0.000	-0.8000E+00	-0.8000E+00	0.000	0.2000E-01	0.2000E-01	0.000
70.00	1459.0	1459.0	0.000	-0.6000E+00	-0.6000E+00	0.000	0.2000E-01	0.2000E-01	0.000
80.00	1454.0	1454.0	0.000	-0.4000E+00	-0.4000E+00	0.000	0.2000E-01	0.2000E-01	0.000
90.00	1451.0	1451.0	0.000	-0.2000E+00	-0.2000E+00	0.000	0.2000E-01	0.2000E-01	0.000
100.00	1450.0	1450.0	0.000	0.0000E+00	0.0000E+00	0.000	0.2000E-01	0.2000E-01	0.000
110.00	1451.0	1451.0	0.000	0.2000E+00	0.2000E+00	0.000	0.2000E-01	0.2000E-01	0.000
120.00	1454.0	1454.0	0.000	0.4000E+00	0.4000E+00	0.000	0.2000E-01	0.2000E-01	0.000
130.00	1459.0	1459.0	0.000	0.6000E+00	0.6000E+00	0.000	0.2000E-01	0.2000E-01	0.000
140.00	1466.0	1466.0	0.000	0.8000E+00	0.8000E+00	0.000	0.2000E-01	0.2000E-01	0.000
150.00	1475.0	1475.0	0.000	0.1000E+01	0.1000E+01	0.000	0.2000E-01	0.2000E-01	0.000
160.00	1486.0	1486.0	0.000	0.1200E+01	0.1200E+01	0.000	0.2000E-01	0.2000E-01	0.000
170.00	1499.0	1499.0	0.000	0.1400E+01	0.1400E+01	0.000	0.2000E-01	0.2000E-01	0.000
180.00	1514.0	1514.0	0.000	0.1600E+01	0.1600E+01	0.000	0.2000E-01	0.2000E-01	0.000
190.00	1531.0	1531.0	0.000	0.1800E+01	0.1800E+01	0.000	0.2000E-01	0.2000E-01	0.000
200.00	1550.0	1550.0	0.000	0.2000E+01	0.2000E+01	0.000	0.2000E-01	0.2000E-01	0.000

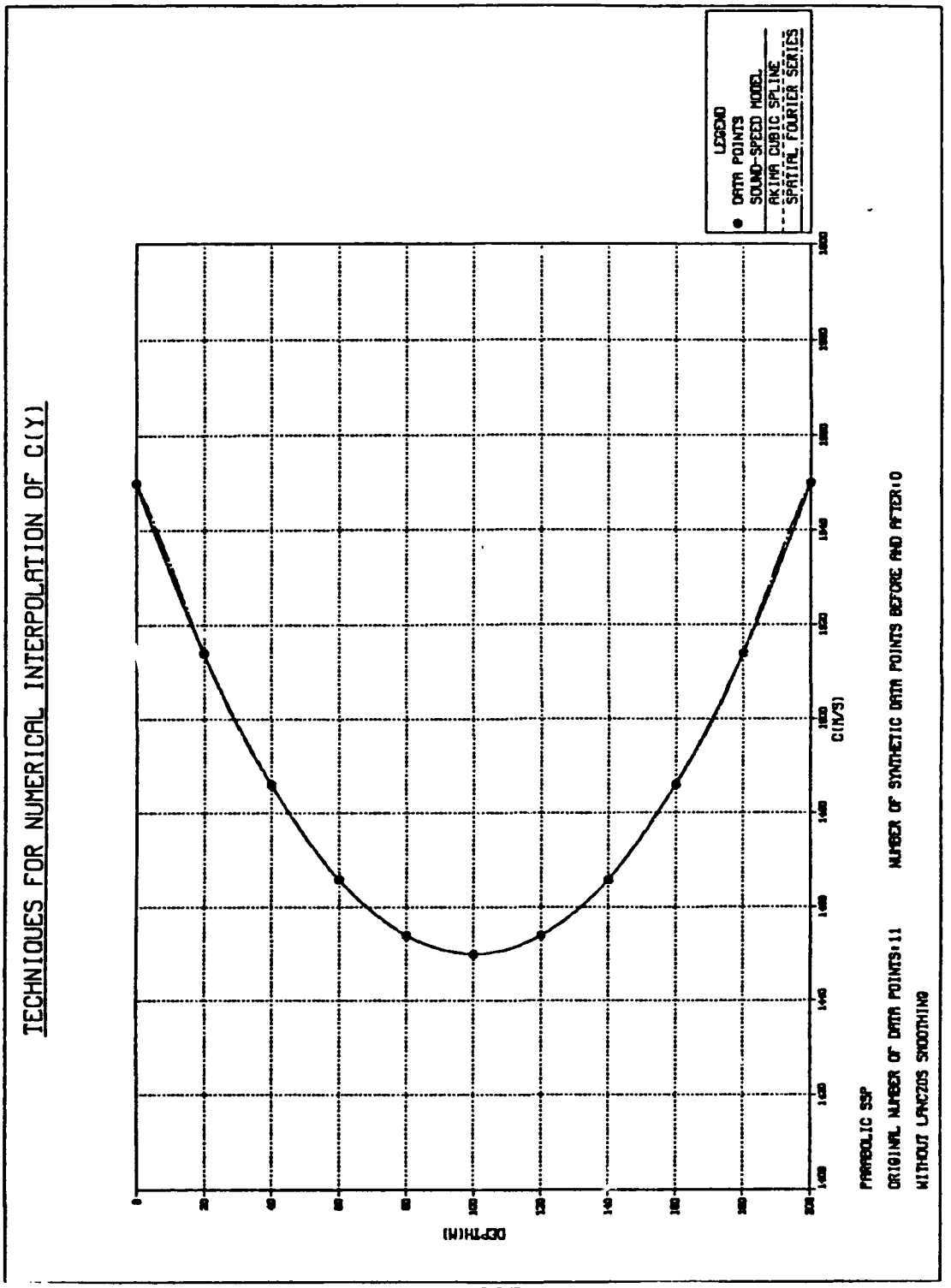

Figure 19. Sound Speed Fit - Parabolic SSP.

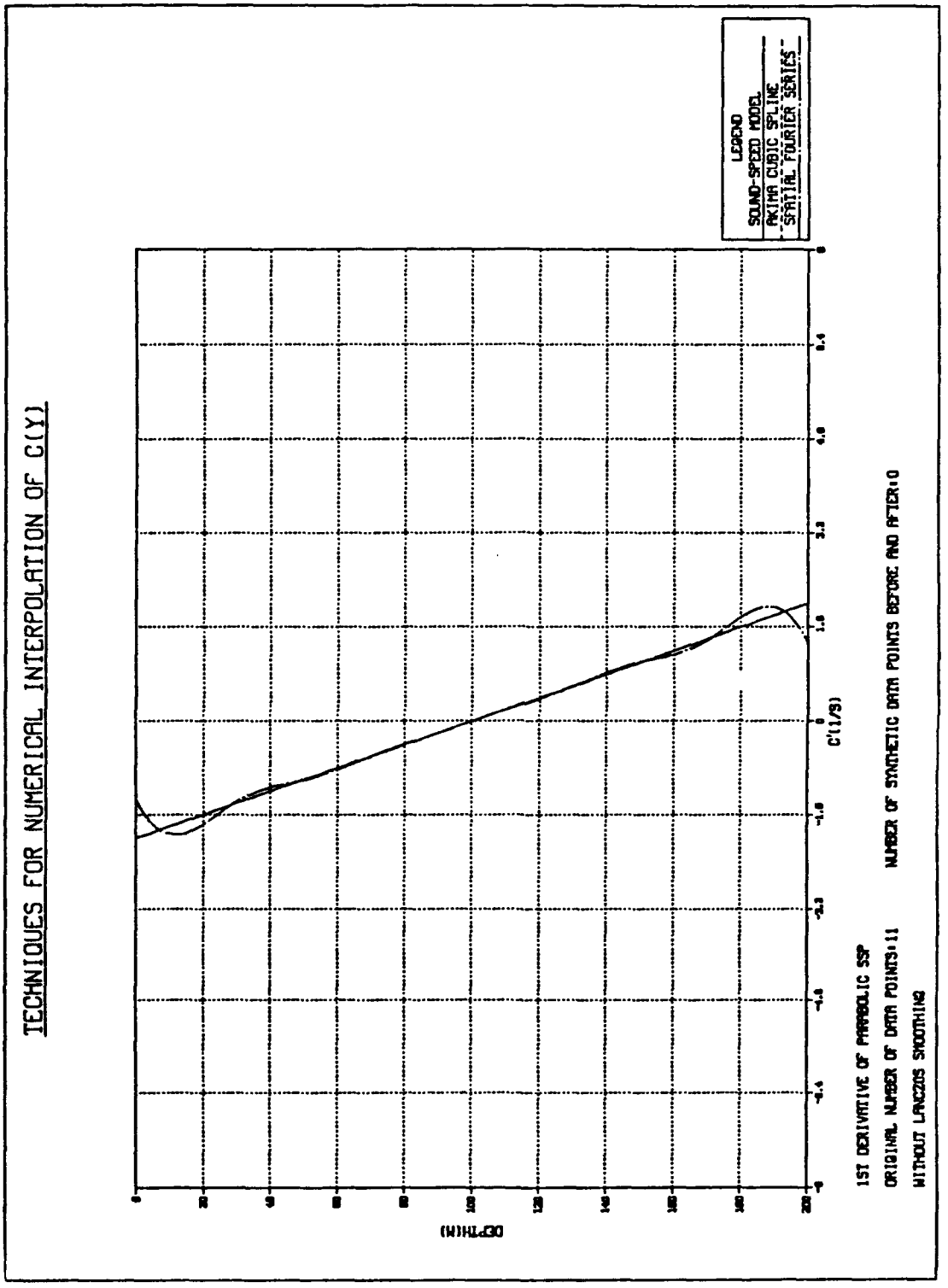

Figure 20. First-Order Derivative Fit - Parabolic SSP.

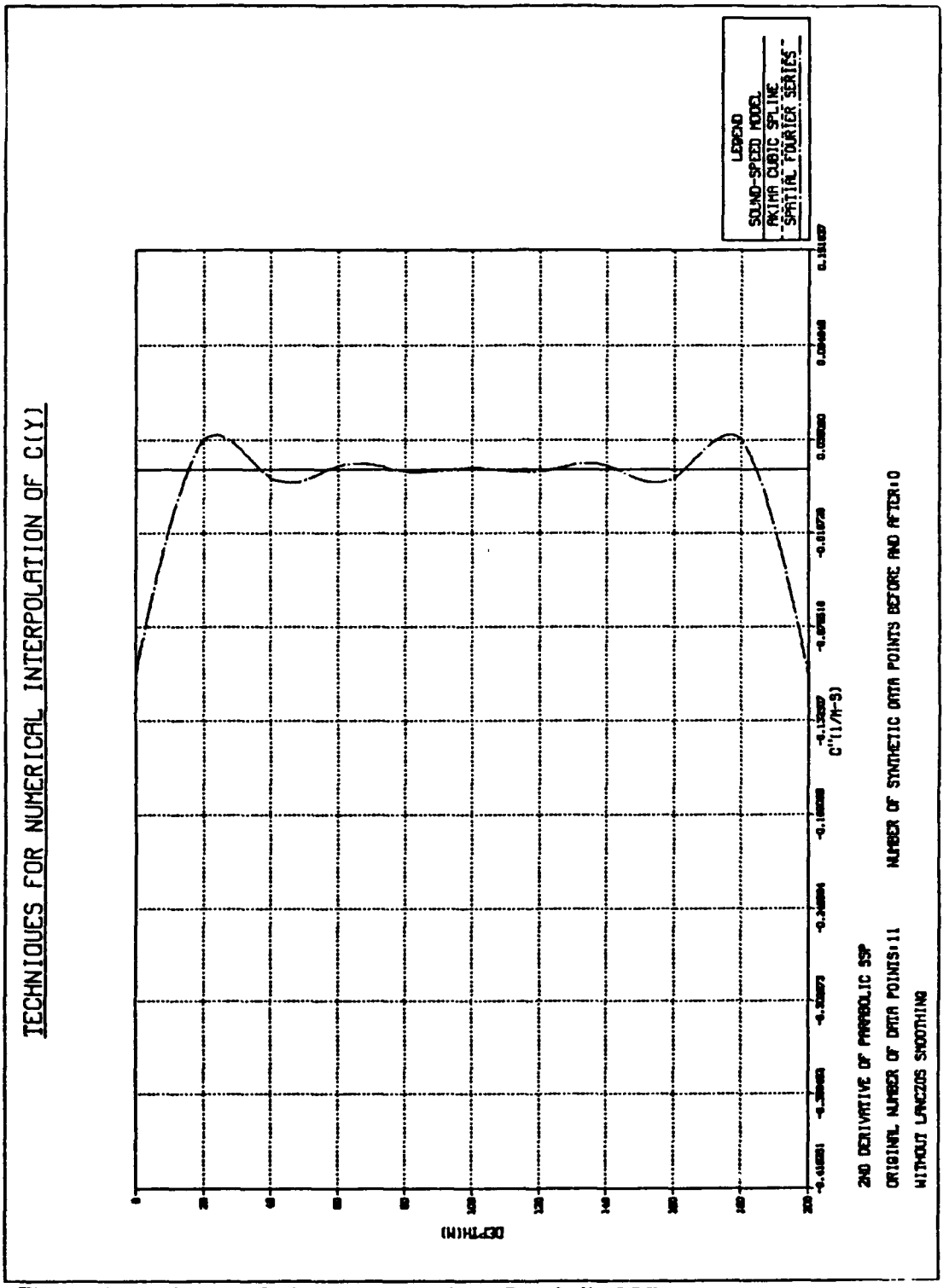

Figure 21. Second-Order Derivative Fit - Parabolic SSP.

Table 18. FOURIER SERIES RESULTS WITH LANCZOS SMOOTHING - HALF-PERIOD SINE WAVE SSP

HALF-PERIOD SINE WAVE SOUND-SPEED PROFILE

NUMBER OF ORIGINAL DATA POINTS = 11
TECHNIQUE: SPATIAL FOURIER SERIES FIT WITH LANCZOS SMOOTHING

DEPTH (M)	C(EXACT) (M/S)	C(FIT) (M/S)	% ERROR	CDOT(EXACT) (1/S)	CDOT(FIT) (1/S)	% ERROR	CDOT2(EXACT) (1/M-S)	CDOT2(FIT) (1/M-S)	% ERROR
0.00	1500.0	1498.8	-0.077	-0.3927E+00	-0.2038E+00	-48.112	0.0000E+00	-0.1763E-01	********
10.00	1496.1	1496.1	-0.001	-0.3879E+00	-0.3350E+00	-13.638	0.9650E-03	-0.8281E-02	-958.203
20.00	1492.3	1492.5	0.013	-0.3735E+00	-0.3735E+00	0.010	0.1906E-02	-0.5531E-04	-102.902
30.00	1488.7	1488.8	0.010	-0.3499E+00	-0.3518E+00	0.542	0.2800E-02	0.3636E-02	29.823
40.00	1485.3	1485.5	0.012	-0.3177E+00	-0.3118E+00	-1.847	0.3626E-02	0.4068E-02	12.191
50.00	1482.3	1482.6	0.017	-0.2777E+00	-0.2717E+00	-2.163	0.4362E-02	0.4056E-02	-7.018
60.00	1479.8	1480.1	0.019	-0.2308E+00	-0.2283E+00	-1.110	0.4990E-02	0.4719E-02	-5.441
70.00	1477.7	1478.0	0.021	-0.1783E+00	-0.1769E+00	-0.783	0.5496E-02	0.5513E-02	0.301
80.00	1476.2	1476.5	0.022	-0.1214E+00	-0.1194E+00	-1.579	0.5867E-02	0.5904E-02	0.633
90.00	1475.3	1475.6	0.023	-0.6143E-01	-0.5986E-01	-2.564	0.6093E-02	0.5983E-02	-1.790
100.00	1475.0	1475.3	0.024	-0.1112E-15	-0.3282E-06	0.000	0.6169E-02	0.5986E-02	-2.962
110.00	1475.3	1475.6	0.023	0.6143E-01	0.5986E-01	-2.563	0.6093E-02	0.5984E-02	-1.789
120.00	1476.2	1476.5	0.022	0.1214E+00	0.1194E+00	-1.578	0.5867E-02	0.5904E-02	0.633
130.00	1477.7	1478.0	0.021	0.1783E+00	0.1769E+00	-0.784	0.5496E-02	0.5513E-02	0.299
140.00	1479.8	1480.1	0.019	0.2308E+00	0.2283E+00	-1.111	0.4990E-02	0.4719E-02	-5.440
150.00	1482.3	1482.6	0.017	0.2777E+00	0.2717E+00	-2.162	0.4362E-02	0.4056E-02	-7.014
160.00	1485.3	1485.5	0.012	0.3177E+00	0.3118E+00	-1.846	0.3626E-02	0.4068E-02	12.185
170.00	1488.7	1488.8	0.010	0.3499E+00	0.3518E+00	0.541	0.2800E-02	0.3635E-02	29.802
180.00	1492.3	1492.5	0.013	0.3735E+00	0.3735E+00	0.008	0.1906E-02	-0.5544E-04	-102.908
190.00	1496.1	1496.1	-0.001	0.3879E+00	0.3350E+00	-13.639	0.9650E-03	-0.8281E-02	-958.114
200.00	1500.0	1498.8	-0.077	0.3927E+00	0.2038E+00	-48.111	0.2125E-17	-0.1763E-01	********

Table 19. FOURIER SERIES RESULTS WITH LANCZOS SMOOTHING - PARABOLIC SSP

PARABOLIC SOUND-SPEED PROFILE

NUMBER OF ORIGINAL DATA POINTS = 11
TECHNIQUE: SPATIAL FOURIER SERIES FIT WITH LANCZOS SMOOTHING

DEPTH (M)	C(EXACT) (M/S)	C(FIT) (M/S)	% ERROR	CDOT(EXACT) (1/S)	CDOT(FIT) (1/S)	% ERROR	CDOT2(EXACT) (1/M-S)	CDOT2(FIT) (1/M-S)	% ERROR
0.00	1550.0	1544.6	-0.349	-0.2000E+01	-0.9566E+00	-52.171	0.2000E-01	-0.8113E-01	-505.645
10.00	1531.0	1531.7	0.048	-0.1800E+01	-0.1531E+01	-14.922	0.2000E-01	-0.3227E-01	-261.349
20.00	1514.0	1515.6	0.105	-0.1600E+01	-0.1629E+01	1.814	0.2000E-01	0.9126E-02	-54.370
30.00	1499.0	1500.1	0.075	-0.1400E+01	-0.1438E+01	2.687	0.2000E-01	0.2490E-01	24.501
40.00	1486.0	1487.0	0.067	-0.1200E+01	-0.1192E+01	-0.695	0.2000E-01	0.2275E-01	13.750
50.00	1475.0	1476.1	0.077	-0.1000E+01	-0.9878E+00	-1.219	0.2000E-01	0.1863E-01	-6.869
60.00	1466.0	1467.2	0.080	-0.8000E+00	-0.8034E+00	0.427	0.2000E-01	0.1887E-01	-5.657
70.00	1459.0	1460.1	0.076	-0.6000E+00	-0.6059E+00	0.983	0.2000E-01	0.2051E-01	2.560
80.00	1454.0	1455.1	0.075	-0.4000E+00	-0.3987E+00	-0.335	0.2000E-01	0.2066E-01	3.277
90.00	1451.0	1452.1	0.077	-0.2000E+00	-0.1960E+00	-2.017	0.2000E-01	0.1986E-01	-0.694
100.00	1450.0	1451.1	0.079	0.0000E+00	0.4955E-14	0.000	0.2000E-01	0.1946E-01	-2.706
110.00	1451.0	1452.1	0.077	0.2000E+00	0.1960E+00	-2.017	0.2000E-01	0.1986E-01	-0.694
120.00	1454.0	1455.1	0.075	0.4000E+00	0.3987E+00	-0.335	0.2000E-01	0.2066E-01	3.277
130.00	1459.0	1460.1	0.076	0.6000E+00	0.6059E+00	0.983	0.2000E-01	0.2051E-01	2.560
140.00	1466.0	1467.2	0.080	0.8000E+00	0.8034E+00	0.427	0.2000E-01	0.1887E-01	-5.657
150.00	1475.0	1476.1	0.077	0.1000E+01	0.9878E+00	-1.219	0.2000E-01	0.1863E-01	-6.869
160.00	1486.0	1487.0	0.067	0.1200E+01	0.1192E+01	-0.695	0.2000E-01	0.2275E-01	13.750
170.00	1499.0	1500.1	0.075	0.1400E+01	0.1438E+01	2.687	0.2000E-01	0.2490E-01	24.501
180.00	1514.0	1515.6	0.105	0.1600E+01	0.1629E+01	1.814	0.2000E-01	0.9126E-02	-54.370
190.00	1531.0	1531.7	0.048	0.1800E+01	0.1531E+01	-14.922	0.2000E-01	-0.3227E-01	-261.349
200.00	1550.0	1544.6	-0.349	0.2000E+01	0.9566E+00	-52.171	0.2000E-01	-0.8113E-01	-505.645

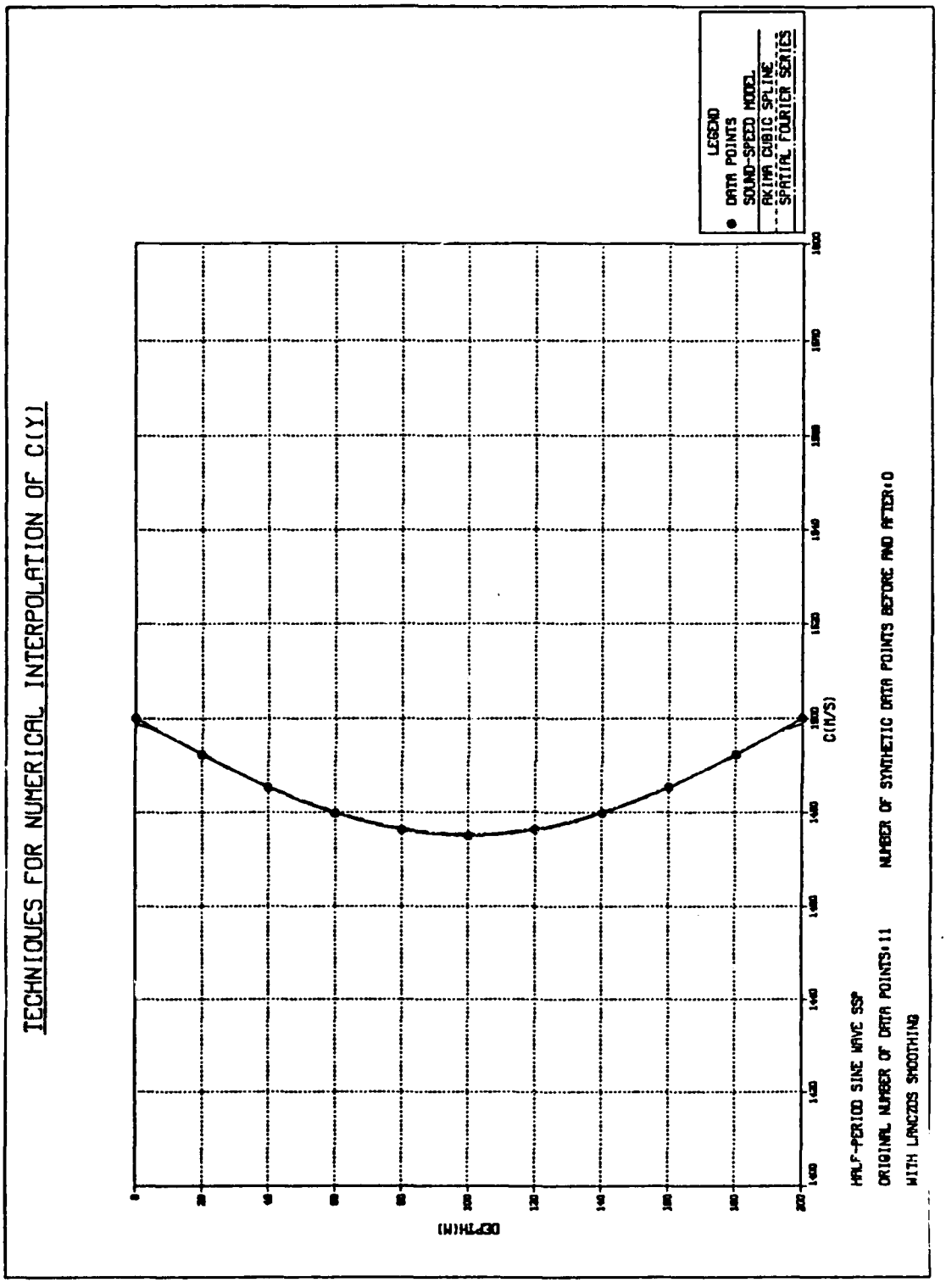

Figure 22. Sound Speed Fit with Lanczos Smoothing - Half-Period Sine Wave SSP.

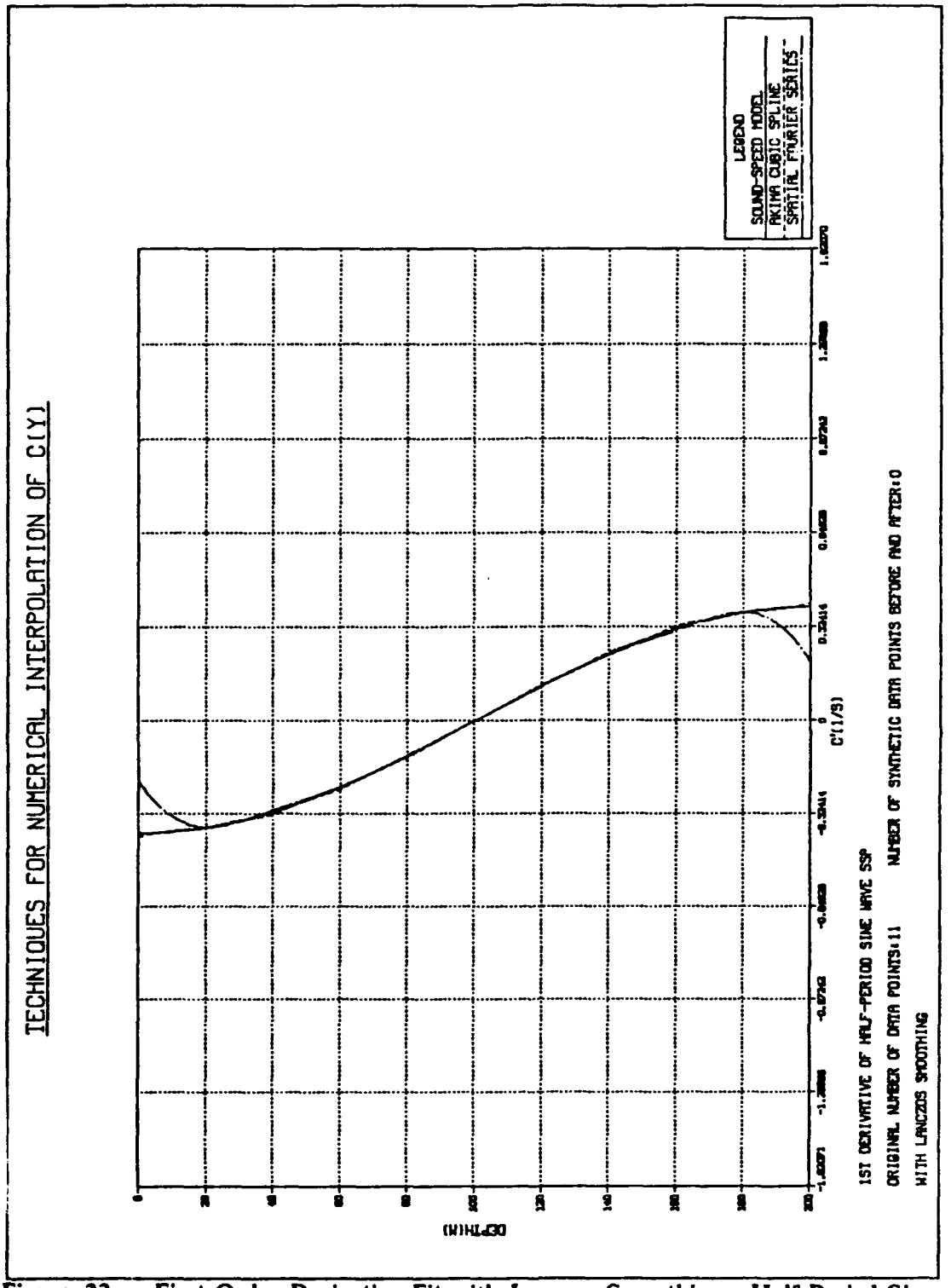

Figure 23. First-Order Derivative Fit with Lanczos Smoothing - Half-Period Sine Wave SSP.

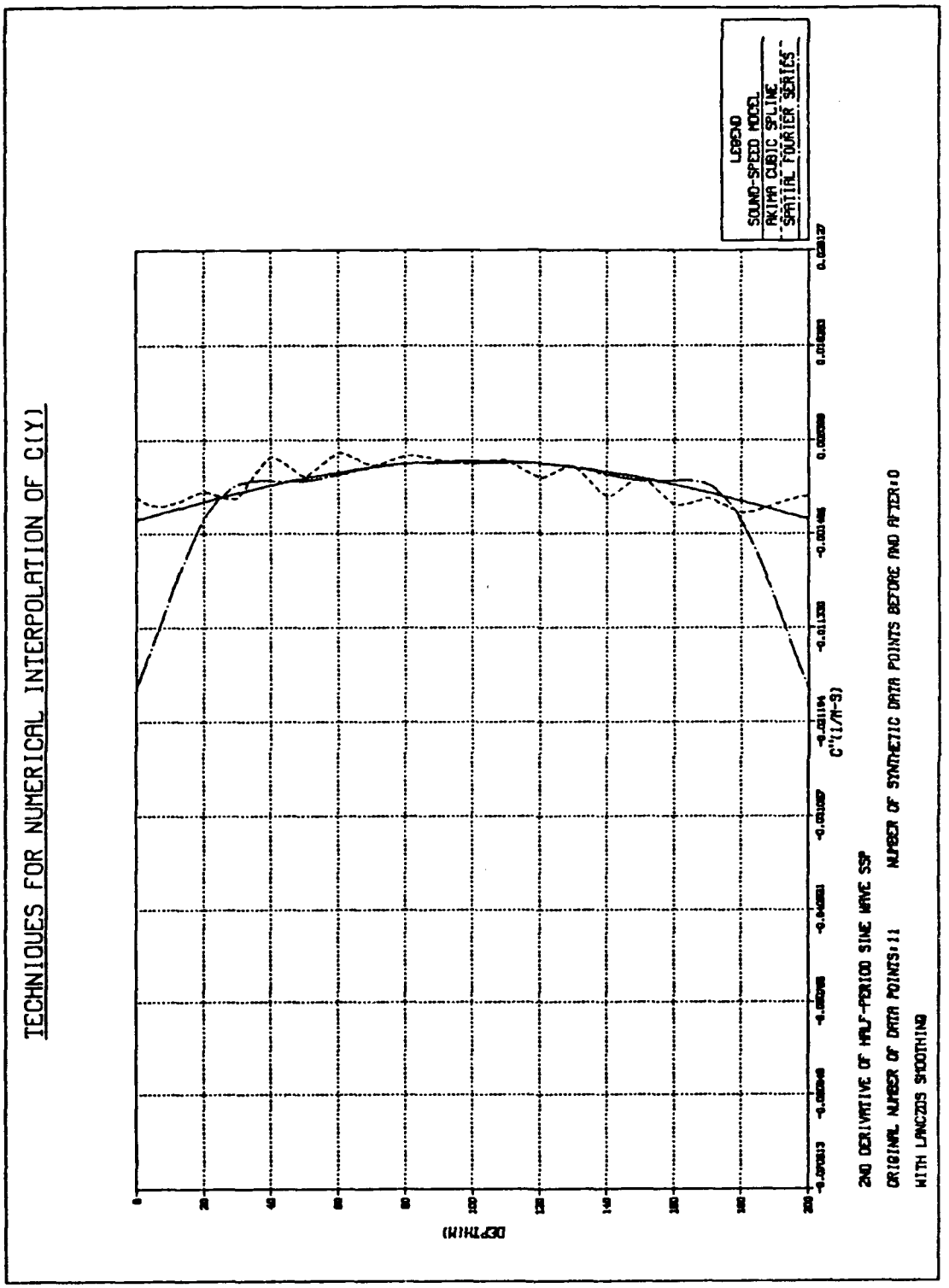

Figure 24. Second-Order Derivative Fit with Lanczos Smoothing - Half-Period Sine Wave SSP.

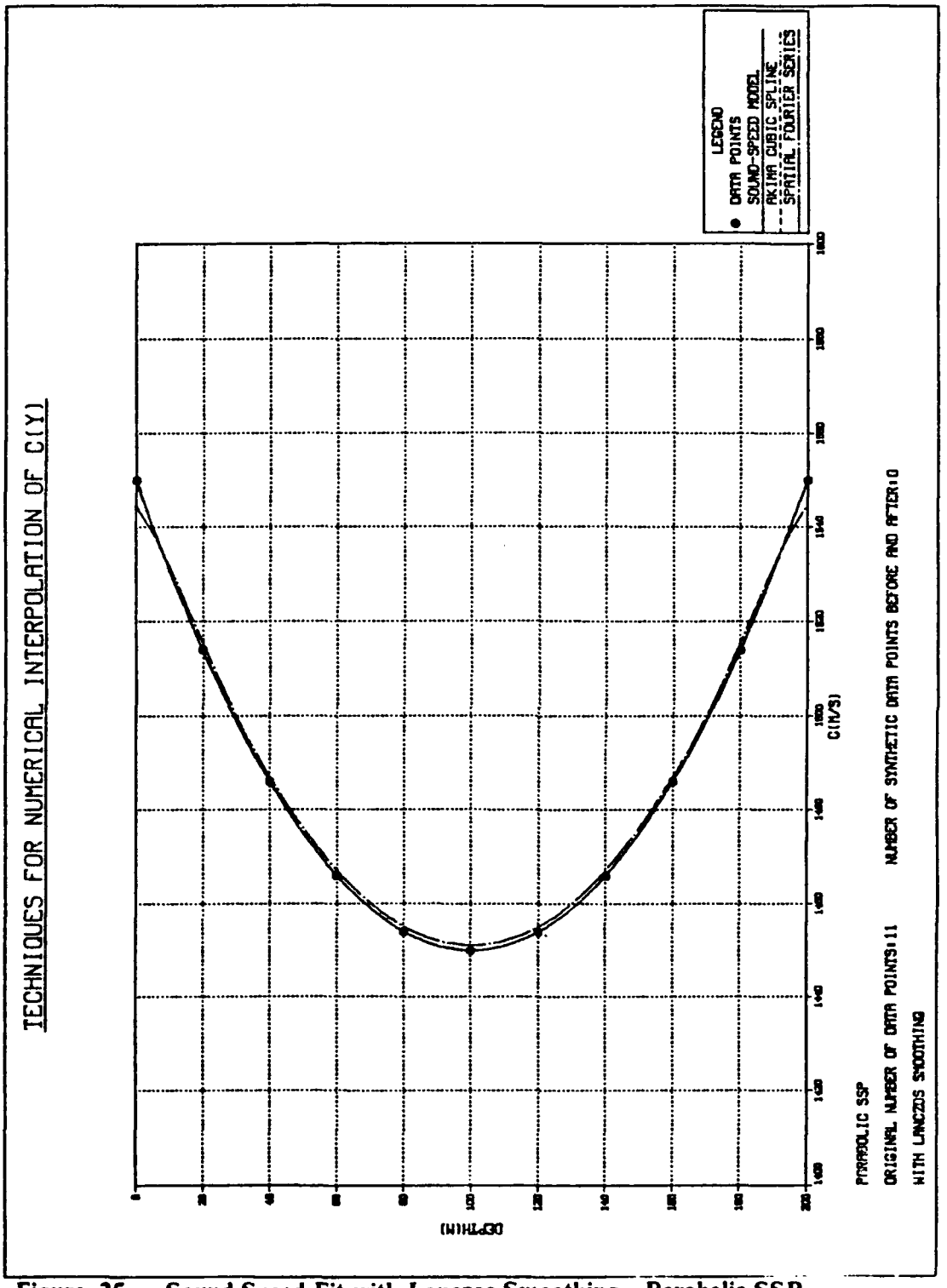

Figure 25. Sound Speed Fit with Lanczos Smoothing - Parabolic SSP.

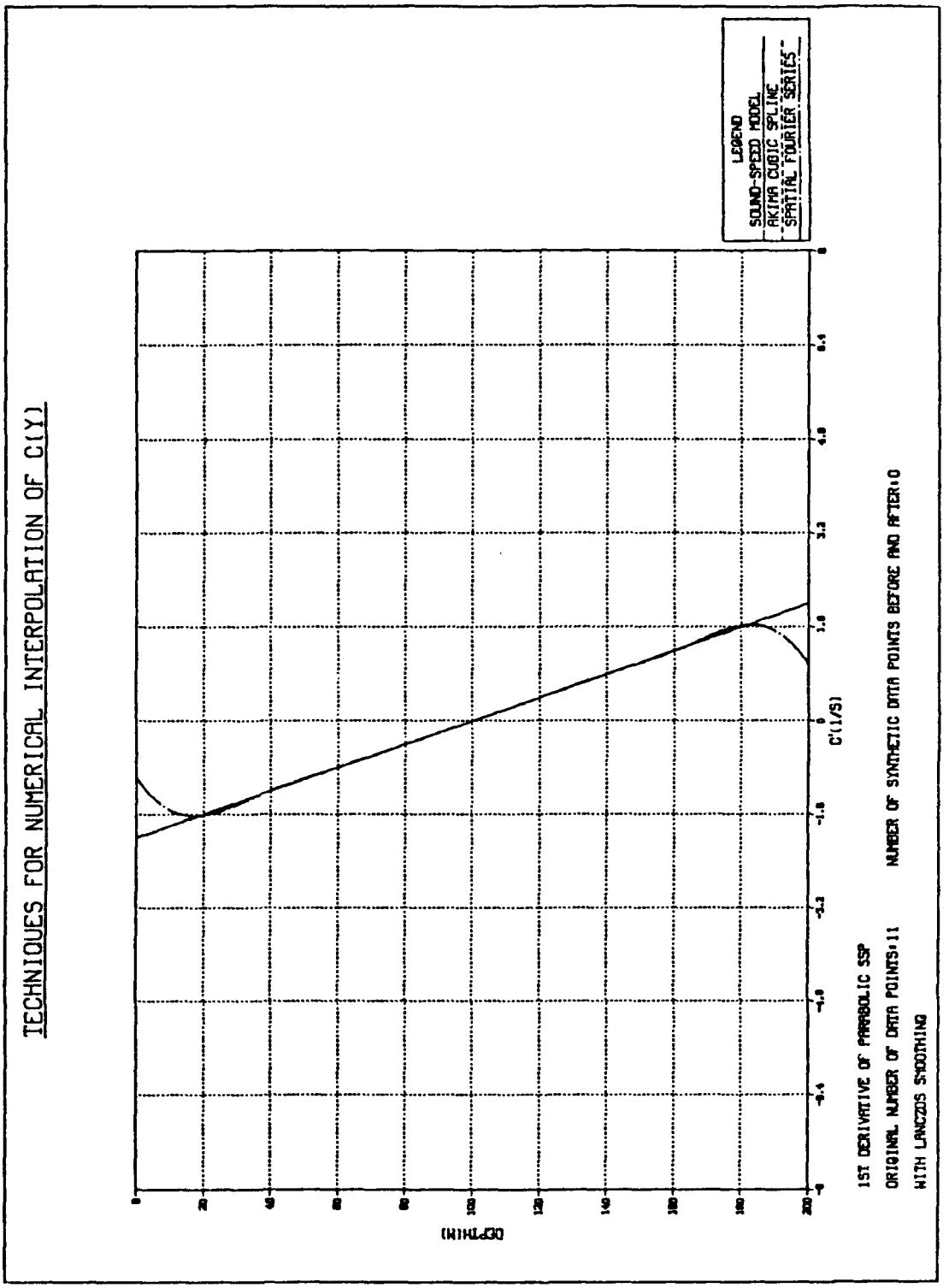

Figure 26. First-Order Derivative Fit with Lanczos Smoothing - Parabolic SSP.

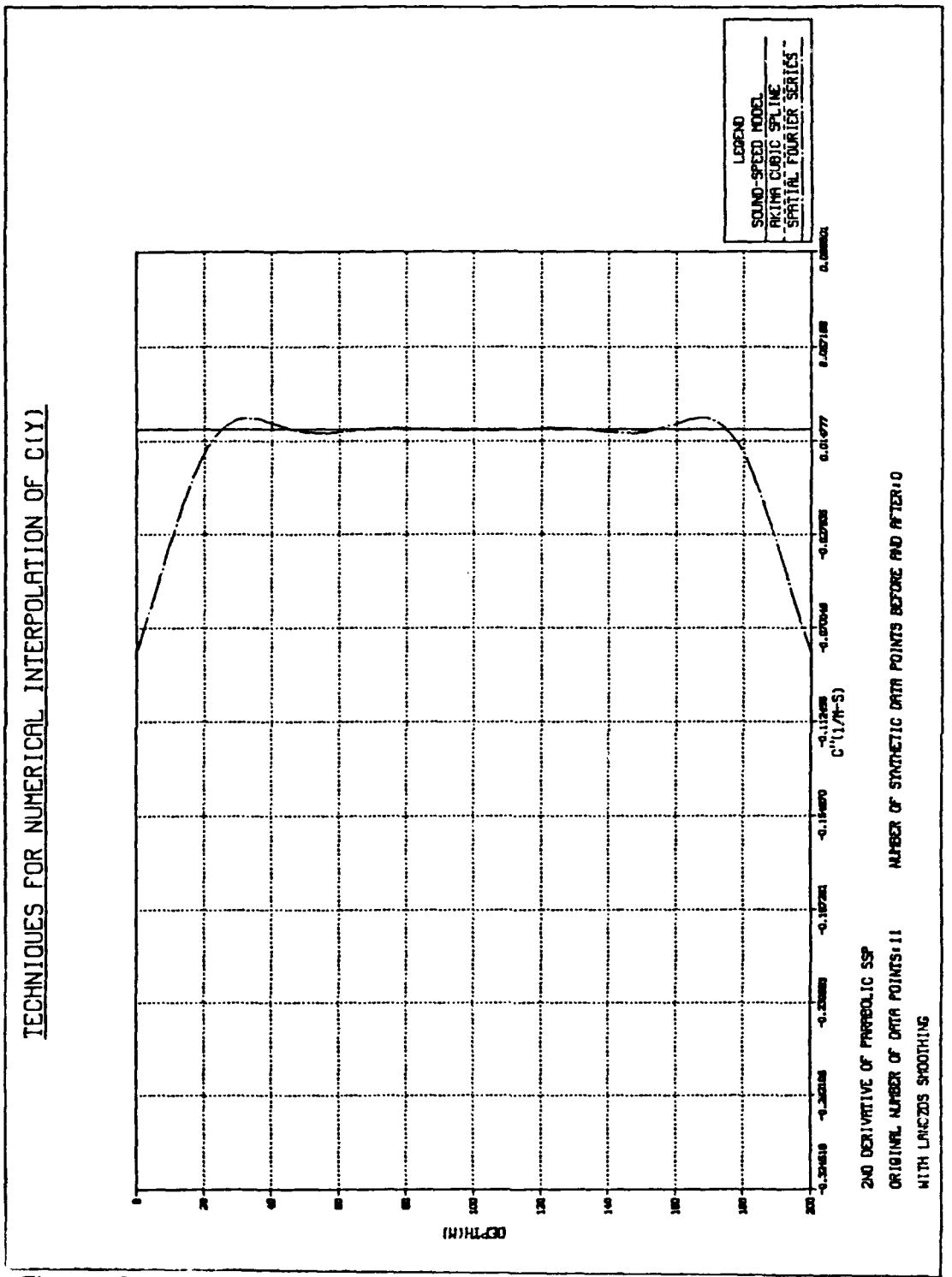

Figure 27. Second-Order Derivative Fit with Lanczos Smoothing - Parabolic SSP.

The difficulty in achieving a good fit at or near the end points of the data using a spatial Fourier series representation is a result of the instantaneous commencement and cessation of sound-speed data at the ocean surface and bottom. Therefore, an attempt to overcome this difficulty was made by adding synthetic data points above the ocean surface and below the ocean bottom so as to enable the Fourier series to "settle down" before the real data begins.

Synthetic data was created by first examining the three data points nearest the ocean surface and bottom. Similar procedures were used to generate synthetic data both above the surface and below the bottom. Therefore, only the surface case will be examined.

Let

$$m_{10} = \frac{c(y_1) - c(0)}{y_1} \tag{4.1}$$

where $c(0) = c(y = 0)$, and

$$m_{21} = \frac{c(y_2) - c(y_1)}{y_2 - y_1} \tag{4.2}$$

where y_i is depth in meters at the ith data point. If we let

$$\Delta m = m_{21} - m_{10} \tag{4.3}$$

and if

$$|\Delta m| = |m_{21} - m_{10}| < \varepsilon \tag{4.4}$$

for some arbitrarily small ε, then linear extrapolation is used, i.e.,

$$c(y_{-i}) = c(0) + m_{10} y_{-i}, \quad i = 1,2,...,SYNPTS \tag{4.5}$$

where

$$y_{-i} = -y_i \tag{4.6}$$

and $SYNPTS$ is the number of synthetic data points desired.

If the test at Equation 4.4 fails, and if

$$|m_{10}| < |m_{21}| , \tag{4.7}$$

then mirror imaging about the ocean surface is appropriate, i.e.,

$$c(y_{-i}) = c(y_i) , \; i = 1,2,...,SYNPTS . \tag{4.8}$$

If both of the tests at Equations 4.4 and 4.7 fail, then neither linear extrapolation nor mirror imaging is appropriate. Under these circumstances it is appropriate to reverse the rate of change of the slope and let

$$c(y_{-i}) = c(0) + (m_{10} - i\,\Delta m)y_{-i} , \; i = 1,2,...,SYNPTS . \tag{4.9}$$

This methodology of extending the real data was implemented using five synthetic data points both above the surface and below the bottom. The results are shown in Tables 20 through 24 and Figures 28 through 42.

A substantial improvement in the accuracy of the Fourier series representation can be seen with respect to all the functions examined. Nevertheless, some difficulty is still evident near the ends of the original data. A final attempt to resolve this discrepancy was made by using the Akima cubic spline representation of sound speed as input to the Fourier algorithm, and sampling the SSP generated by the Akima cubic spline fit at some arbitrarily high frequency. This was attempted using a sampling rate ten times greater than available from the original data. The synthetic data as described above was not fit using the Akima cubic spline method. Results for the half-period sine wave and parabolic SSPs are presented in Tables 25 and 26 and Figures 43 to 48.

These results are once again an improvement on previous work. Nonetheless, some inaccuracies remain. Unfortunately, time constraints precluded further, more sophisticated attempts to further improve the accuracy of the Fourier representation.

Table 20. FOURIER SERIES RESULTS WITH LANCZOS SMOOTHING AND SYNTHETIC DATA - CONSTANT SPEED OF SOUND

CONSTANT SPEED OF SOUND

NUMBER OF ORIGINAL DATA POINTS = 11
NUMBER OF SYNTHETIC DATA POINTS = 5
TECHNIQUE: SPATIAL FOURIER SERIES FIT WITH LANCZOS SMOOTHING

DEPTH (M)	C(EXACT) (M/S)	C(FIT) (M/S)	% ERROR	CDOT(EXACT) (1/S)	CDOT(FIT) (1/S)	% ERROR	CDOT2(EXACT) (1/M-S)	CDOT2(FIT) (1/M-S)	% ERROR
0.00	1500.0	1500.0	0.000	0.0000E+00	0.3008E-14	0.000	0.0000E+00	0.6207E-16	0.000
10.00	1500.0	1500.0	0.000	0.0000E+00	0.6672E-14	0.000	0.0000E+00	0.6741E-15	0.000
20.00	1500.0	1500.0	0.000	0.0000E+00	0.1371E-13	0.000	0.0000E+00	0.5155E-15	0.000
30.00	1500.0	1500.0	0.000	0.0000E+00	0.1386E-13	0.000	0.0000E+00	-0.5082E-15	0.000
40.00	1500.0	1500.0	0.000	0.0000E+00	0.6059E-14	0.000	0.0000E+00	-0.8328E-15	0.000
50.00	1500.0	1500.0	0.000	0.0000E+00	0.8560E-15	0.000	0.0000E+00	-0.1328E-15	0.000
60.00	1500.0	1500.0	0.000	0.0000E+00	0.2210E-14	0.000	0.0000E+00	0.2505E-15	0.000
70.00	1500.0	1500.0	0.000	0.0000E+00	0.3057E-14	0.000	0.0000E+00	-0.1461E-15	0.000
80.00	1500.0	1500.0	0.000	0.0000E+00	0.4528E-16	0.000	0.0000E+00	-0.3482E-15	0.000
90.00	1500.0	1500.0	0.000	0.0000E+00	-0.2063E-14	0.000	0.0000E+00	-0.4634E-16	0.000
100.00	1500.0	1500.0	0.000	0.0000E+00	-0.1916E-14	0.000	0.0000E+00	-0.1959E-16	0.000
110.00	1500.0	1500.0	0.000	0.0000E+00	-0.3624E-14	0.000	0.0000E+00	-0.3021E-15	0.000
120.00	1500.0	1500.0	0.000	0.0000E+00	-0.6000E-14	0.000	0.0000E+00	-0.4111E-16	0.000
130.00	1500.0	1500.0	0.000	0.0000E+00	-0.2924E-14	0.000	0.0000E+00	0.6327E-15	0.000
140.00	1500.0	1500.0	0.000	0.0000E+00	0.4260E-14	0.000	0.0000E+00	0.6369E-15	0.000
150.00	1500.0	1500.0	0.000	0.0000E+00	0.7514E-14	0.000	0.0000E+00	0.3708E-18	0.000
160.00	1500.0	1500.0	0.000	0.0000E+00	0.6050E-14	0.000	0.0000E+00	-0.1502E-15	0.000
170.00	1500.0	1500.0	0.000	0.0000E+00	0.6425E-14	0.000	0.0000E+00	0.2238E-15	0.000
180.00	1500.0	1500.0	0.000	0.0000E+00	0.8611E-14	0.000	0.0000E+00	0.7703E-16	0.000
190.00	1500.0	1500.0	0.000	0.0000E+00	0.6570E-14	0.000	0.0000E+00	-0.4393E-15	0.000
200.00	1500.0	1500.0	0.000	0.0000E+00	0.2750E-14	0.000	0.0000E+00	-0.1478E-15	0.000

Table 21. FOURIER SERIES RESULTS WITH LANCZOS SMOOTHING AND SYNTHETIC DATA - LINEAR SSP WITH POSITIVE GRADIENT

LINEAR SOUND-SPEED PROFILE WITH A POSITIVE GRADIENT

NUMBER OF ORIGINAL DATA POINTS = 11
NUMBER OF SYNTHETIC DATA POINTS = 5
TECHNIQUE: SPATIAL FOURIER SERIES FIT WITH LANCZOS SMOOTHING

DEPTH (M)	C(EXACT) (M/S)	C(FIT) (M/S)	% ERROR	CDOT(EXACT) (1/S)	CDOT(FIT) (1/S)	% ERROR	CDOT2(EXACT) (1/M-S)	CDOT2(FIT) (1/M-S)	% ERROR
0.00	1500.0	1500.0	-0.001	0.1700E-01	0.1875E-01	10.323	0.0000E+00	0.2390E-03	********
10.00	1500.2	1500.2	0.001	0.1700E-01	0.1829E-01	7.560	0.0000E+00	-0.2860E-03	********
20.00	1500.3	1500.3	0.000	0.1700E-01	0.1544E-01	-9.156	0.0000E+00	-0.1553E-03	********
30.00	1500.5	1500.5	-0.001	0.1700E-01	0.1616E-01	-4.956	0.0000E+00	0.2508E-03	********
40.00	1500.7	1500.7	0.000	0.1700E-01	0.1842E-01	8.352	0.0000E+00	0.1005E-03	********
50.00	1500.8	1500.9	0.001	0.1700E-01	0.1753E-01	3.111	0.0000E+00	-0.2292E-03	********
60.00	1501.0	1501.0	0.000	0.1700E-01	0.1566E-01	-7.880	0.0000E+00	-0.6049E-04	********
70.00	1501.2	1501.2	-0.001	0.1700E-01	0.1671E-01	-1.725	0.0000E+00	0.2169E-03	********
80.00	1501.4	1501.4	0.000	0.1700E-01	0.1830E-01	7.625	0.0000E+00	0.2876E-04	********
90.00	1501.5	1501.5	0.001	0.1700E-01	0.1710E-01	0.574	0.0000E+00	-0.2111E-03	********
100.00	1501.7	1501.7	0.000	0.1700E-01	0.1572E-01	-7.520	0.0000E+00	-0.4325E-06	0.000
110.00	1501.9	1501.9	-0.001	0.1700E-01	0.1709E-01	0.533	0.0000E+00	0.2107E-03	********
120.00	1502.0	1502.0	0.000	0.1700E-01	0.1829E-01	7.585	0.0000E+00	-0.2829E-04	********
130.00	1502.2	1502.2	0.001	0.1700E-01	0.1671E-01	-1.722	0.0000E+00	-0.2161E-03	********
140.00	1502.4	1502.4	0.000	0.1700E-01	0.1567E-01	-7.840	0.0000E+00	0.6081E-04	********
150.00	1502.5	1502.5	-0.001	0.1700E-01	0.1753E-01	3.146	0.0000E+00	0.2287E-03	********
160.00	1502.7	1502.7	0.000	0.1700E-01	0.1842E-01	8.350	0.0000E+00	-0.1011E-03	********
170.00	1502.9	1502.9	0.001	0.1700E-01	0.1615E-01	-4.977	0.0000E+00	-0.2508E-03	********
180.00	1503.1	1503.1	0.000	0.1700E-01	0.1544E-01	-9.159	0.0000E+00	0.1559E-03	********
190.00	1503.2	1503.2	-0.001	0.1700E-01	0.1829E-01	7.591	0.0000E+00	0.2864E-03	********
200.00	1503.4	1503.4	0.001	0.1700E-01	0.1876E-01	10.361	0.0000E+00	-0.2391E-03	********

Table 22. FOURIER SERIES RESULTS WITH LANCZOS SMOOTHING AND SYNTHETIC DATA - LINEAR SSP WITH NEGATIVE GRADIENT

LINEAR SOUND-SPEED PROFILE WITH A NEGATIVE GRADIENT

NUMBER OF ORIGINAL DATA POINTS = 11
NUMBER OF SYNTHETIC DATA POINTS = 5
TECHNIQUE: SPATIAL FOURIER SERIES FIT WITH LANCZOS SMOOTHING

DEPTH (M)	C(EXACT) (M/S)	C(FIT) (M/S)	% ERROR	CDOT(EXACT) (1/S)	CDOT(FIT) (1/S)	% ERROR	CDOT2(EXACT) (1/M-S)	CDOT2(FIT) (1/M-S)	% ERROR
0.00	1500.0	1500.0	0.001	-0.1700E-01	-0.1876E-01	10.362	0.0000E+00	-0.2393E-03	*********
10.00	1499.8	1499.8	-0.001	-0.1700E-01	-0.1829E-01	7.608	0.0000E+00	0.2861E-03	*********
20.00	1499.7	1499.7	0.000	-0.1700E-01	-0.1545E-01	-9.123	0.0000E+00	0.1557E-03	*********
30.00	1499.5	1499.5	0.001	-0.1700E-01	-0.1616E-01	-4.942	0.0000E+00	-0.2505E-03	*********
40.00	1499.3	1499.3	0.000	-0.1700E-01	-0.1842E-01	8.353	0.0000E+00	-0.1004E-03	*********
50.00	1499.1	1499.1	-0.001	-0.1700E-01	-0.1753E-01	3.109	0.0000E+00	0.2292E-03	*********
60.00	1499.0	1499.0	0.000	-0.1700E-01	-0.1566E-01	-7.881	0.0000E+00	0.6045E-04	*********
70.00	1498.8	1498.8	0.001	-0.1700E-01	-0.1671E-01	-1.724	0.0000E+00	-0.2170E-03	*********
80.00	1498.6	1498.6	0.000	-0.1700E-01	-0.1830E-01	7.626	0.0000E+00	-0.2873E-04	*********
90.00	1498.5	1498.5	-0.001	-0.1700E-01	-0.1710E-01	0.573	0.0000E+00	0.2111E-03	*********
100.00	1498.3	1498.3	0.000	-0.1700E-01	-0.1572E-01	-7.521	0.0000E+00	0.4083E-06	0.000
110.00	1498.1	1498.1	0.001	-0.1700E-01	-0.1709E-01	0.534	0.0000E+00	-0.2107E-03	*********
120.00	1498.0	1498.0	0.000	-0.1700E-01	-0.1829E-01	7.586	0.0000E+00	0.2832E-04	*********
130.00	1497.8	1497.8	-0.001	-0.1700E-01	-0.1671E-01	-1.724	0.0000E+00	0.2162E-03	*********
140.00	1497.6	1497.6	0.000	-0.1700E-01	-0.1567E-01	-7.842	0.0000E+00	-0.6085E-04	*********
150.00	1497.4	1497.5	0.001	-0.1700E-01	-0.1754E-01	3.148	0.0000E+00	-0.2288E-03	*********
160.00	1497.3	1497.3	0.000	-0.1700E-01	-0.1842E-01	8.352	0.0000E+00	0.1012E-03	*********
170.00	1497.1	1497.1	-0.001	-0.1700E-01	-0.1615E-01	-4.981	0.0000E+00	0.2509E-03	*********
180.00	1496.9	1496.9	0.000	-0.1700E-01	-0.1544E-01	-9.162	0.0000E+00	-0.1560E-03	*********
190.00	1496.8	1496.8	0.001	-0.1700E-01	-0.1829E-01	7.606	0.0000E+00	-0.2868E-03	*********
200.00	1496.6	1496.6	-0.001	-0.1700E-01	-0.1877E-01	10.400	0.0000E+00	0.2388E-03	*********

Table 23. FOURIER SERIES RESULTS WITH LANCZOS SMOOTHING AND SYNTHETIC DATA - HALF-PERIOD SINE WAVE SSP

HALF-PERIOD SINE WAVE SOUND-SPEED PROFILE

NUMBER OF ORIGINAL DATA POINTS = 11
NUMBER OF SYNTHETIC DATA POINTS = 5
TECHNIQUE: SPATIAL FOURIER SERIES FIT WITH LANCZOS SMOOTHING

DEPTH (M)	C(EXACT) (M/S)	C(FIT) (M/S)	% ERROR	CDOT(EXACT) (1/S)	CDOT(FIT) (1/S)	% ERROR	CDOT2(EXACT) (1/M-S)	CDOT2(FIT) (1/M-S)	% ERROR
0.00	1500.0	1499.9	-0.008	-0.3927E+00	-0.3684E+00	-6.186	0.0000E+00	-0.1683E-02	********
10.00	1496.1	1496.1	0.003	-0.3879E+00	-0.3768E+00	-2.843	0.9650E-03	0.2498E-04	-97.411
20.00	1492.3	1492.4	0.008	-0.3735E+00	-0.3682E+00	-1.407	0.1906E-02	0.1644E-02	-13.748
30.00	1488.7	1488.8	0.011	-0.3499E+00	-0.3454E+00	-1.276	0.2800E-02	0.2835E-02	1.221
40.00	1485.3	1485.5	0.015	-0.3177E+00	-0.3129E+00	-1.523	0.3626E-02	0.3634E-02	0.220
50.00	1482.3	1482.6	0.018	-0.2777E+00	-0.2733E+00	-1.589	0.4362E-02	0.4276E-02	-1.976
60.00	1479.8	1480.1	0.020	-0.2308E+00	-0.2274E+00	-1.473	0.4990E-02	0.4888E-02	-2.054
70.00	1477.7	1478.1	0.022	-0.1783E+00	-0.1758E+00	-1.412	0.5496E-02	0.5423E-02	-1.340
80.00	1476.2	1476.6	0.024	-0.1214E+00	-0.1195E+00	-1.511	0.5867E-02	0.5797E-02	-1.185
90.00	1475.3	1475.7	0.025	-0.6143E-01	-0.6040E-01	-1.673	0.6093E-02	0.5999E-02	-1.534
100.00	1475.0	1475.4	0.025	-0.1112E-15	-0.1068E-05	********	0.6169E-02	0.6061E-02	-1.748
110.00	1475.3	1475.7	0.025	0.6143E-01	0.6040E-01	-1.672	0.6093E-02	0.5999E-02	-1.529
120.00	1476.2	1476.6	0.024	0.1214E+00	0.1195E+00	-1.509	0.5867E-02	0.5797E-02	-1.186
130.00	1477.7	1478.1	0.022	0.1783E+00	0.1758E+00	-1.412	0.5496E-02	0.5422E-02	-1.347
140.00	1479.8	1480.1	0.020	0.2308E+00	0.2274E+00	-1.474	0.4990E-02	0.4888E-02	-2.051
150.00	1482.3	1482.6	0.018	0.2777E+00	0.2733E+00	-1.589	0.4362E-02	0.4276E-02	-1.967
160.00	1485.3	1485.5	0.015	0.3177E+00	0.3129E+00	-1.523	0.3626E-02	0.3633E-02	0.212
170.00	1488.7	1488.8	0.011	0.3499E+00	0.3454E+00	-1.277	0.2800E-02	0.2834E-02	1.194
180.00	1492.3	1492.4	0.008	0.3735E+00	0.3682E+00	-1.409	0.1906E-02	0.1644E-02	-13.755
190.00	1496.1	1496.1	0.003	0.3879E+00	0.3768E+00	-2.844	0.9650E-03	0.2539E-04	-97.369
200.00	1500.0	1499.9	-0.008	0.3927E+00	0.3684E+00	-6.187	0.2125E-17	-0.1683E-02	********

Table 24. FOURIER SERIES RESULTS WITH LANCZOS SMOOTHING AND SYNTHETIC DATA - PARABOLIC SSP

PARABOLIC SOUND-SPEED PROFILE

NUMBER OF ORIGINAL DATA POINTS = 11
NUMBER OF SYNTHETIC DATA POINTS = 5
TECHNIQUE: SPATIAL FOURIER SERIES FIT WITH LANCZOS SMOOTHING

DEPTH (M)	C(EXACT) (M/S)	C(FIT) (M/S)	% ERROR	CDOT(EXACT) (1/S)	CDOT(FIT) (1/S)	% ERROR	CDOT2(EXACT) (1/M-S)	CDOT2(FIT) (1/M-S)	% ERROR
0.00	1550.0	1548.7	-0.086	-0.2000E+01	-0.1611E+01	-19.431	0.2000E-01	-0.1699E-01	-184.953
10.00	1531.0	1532.0	0.066	-0.1800E+01	-0.1692E+01	-5.984	0.2000E-01	0.8243E-03	-95.879
20.00	1514.0	1515.4	0.092	-0.1600E+01	-0.1607E+01	0.411	0.2000E-01	0.1521E-01	-23.967
30.00	1499.0	1500.2	0.082	-0.1400E+01	-0.1416E+01	1.121	0.2000E-01	0.2156E-01	7.795
40.00	1486.0	1487.2	0.078	-0.1200E+01	-0.1198E+01	-0.182	0.2000E-01	0.2132E-01	6.600
50.00	1475.0	1476.2	0.082	-0.1000E+01	-0.9941E+00	-0.590	0.2000E-01	0.1955E-01	-2.236
60.00	1466.0	1467.2	0.085	-0.8000E+00	-0.8010E+00	0.126	0.2000E-01	0.1937E-01	-3.167
70.00	1459.0	1460.2	0.083	-0.6000E+00	-0.6034E+00	0.560	0.2000E-01	0.2018E-01	0.877
80.00	1454.0	1455.2	0.082	-0.4000E+00	-0.3996E+00	-0.106	0.2000E-01	0.2042E-01	2.114
90.00	1451.0	1452.2	0.084	-0.2000E+00	-0.1974E+00	-1.286	0.2000E-01	0.1995E-01	-0.246
100.00	1450.0	1451.2	0.085	0.0000E+00	-0.8648E-15	0.000	0.2000E-01	0.1963E-01	-1.853
110.00	1451.0	1452.2	0.084	0.2000E+00	0.1974E+00	-1.286	0.2000E-01	0.1995E-01	-0.246
120.00	1454.0	1455.2	0.082	0.4000E+00	0.3996E+00	-0.106	0.2000E-01	0.2042E-01	2.114
130.00	1459.0	1460.2	0.083	0.6000E+00	0.6034E+00	0.560	0.2000E-01	0.2018E-01	0.877
140.00	1466.0	1467.2	0.085	0.8000E+00	0.8010E+00	0.126	0.2000E-01	0.1937E-01	-3.167
150.00	1475.0	1476.2	0.082	0.1000E+01	0.9941E+00	-0.590	0.2000E-01	0.1955E-01	-2.236
160.00	1486.0	1487.2	0.078	0.1200E+01	0.1198E+01	-0.182	0.2000E-01	0.2132E-01	6.600
170.00	1499.0	1500.2	0.082	0.1400E+01	0.1416E+01	1.121	0.2000E-01	0.2156E-01	7.795
180.00	1514.0	1515.4	0.092	0.1600E+01	0.1607E+01	0.411	0.2000E-01	0.1521E-01	-23.967
190.00	1531.0	1532.0	0.066	0.1800E+01	0.1692E+01	-5.984	0.2000E-01	0.8243E-03	-95.879
200.00	1550.0	1548.7	-0.086	0.2000E+01	0.1611E+01	-19.431	0.2000E-01	-0.1699E-01	-184.953

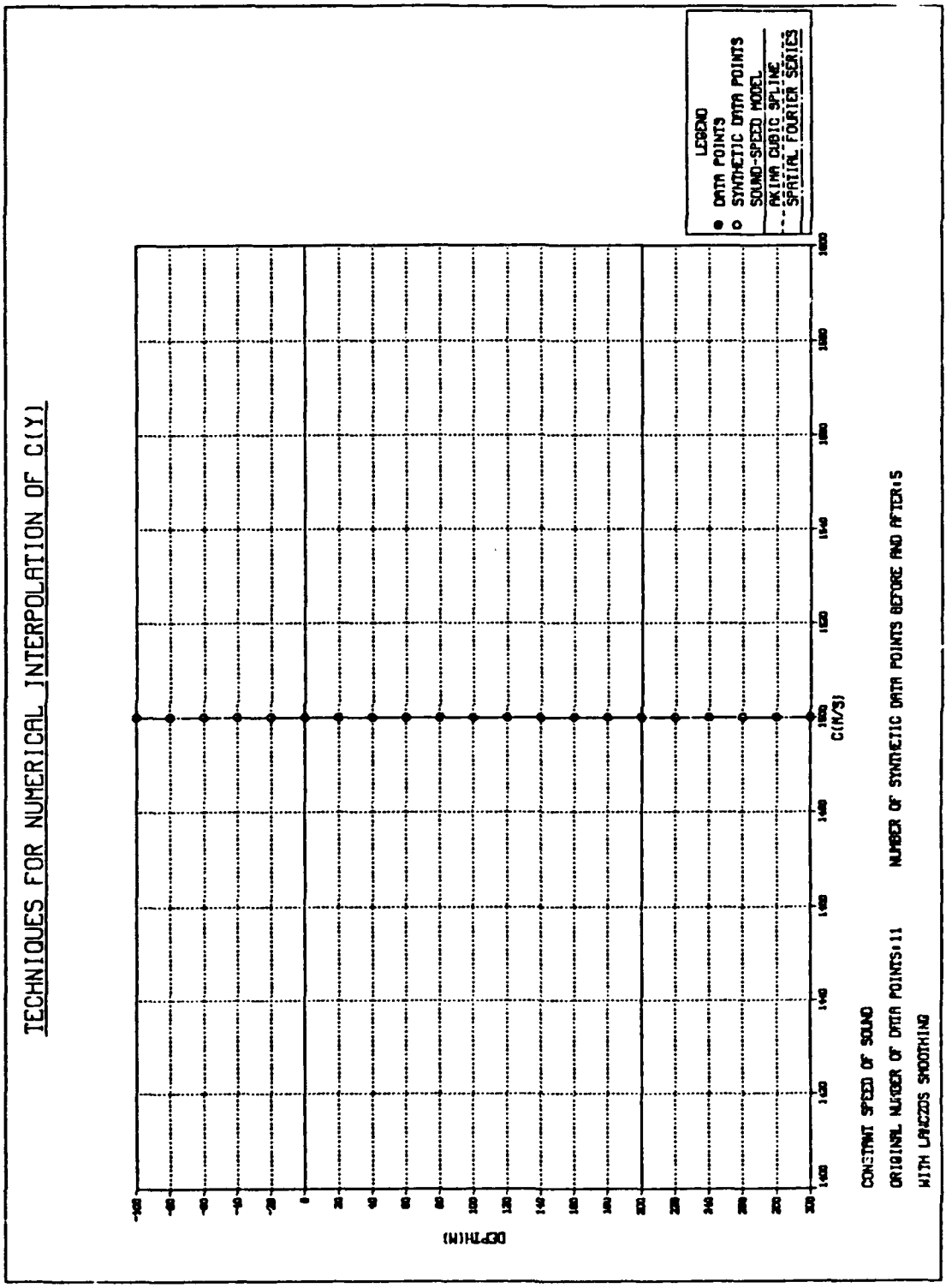

Figure 28. Sound-Speed Fit - Constant Speed of Sound with Synthetic Data.

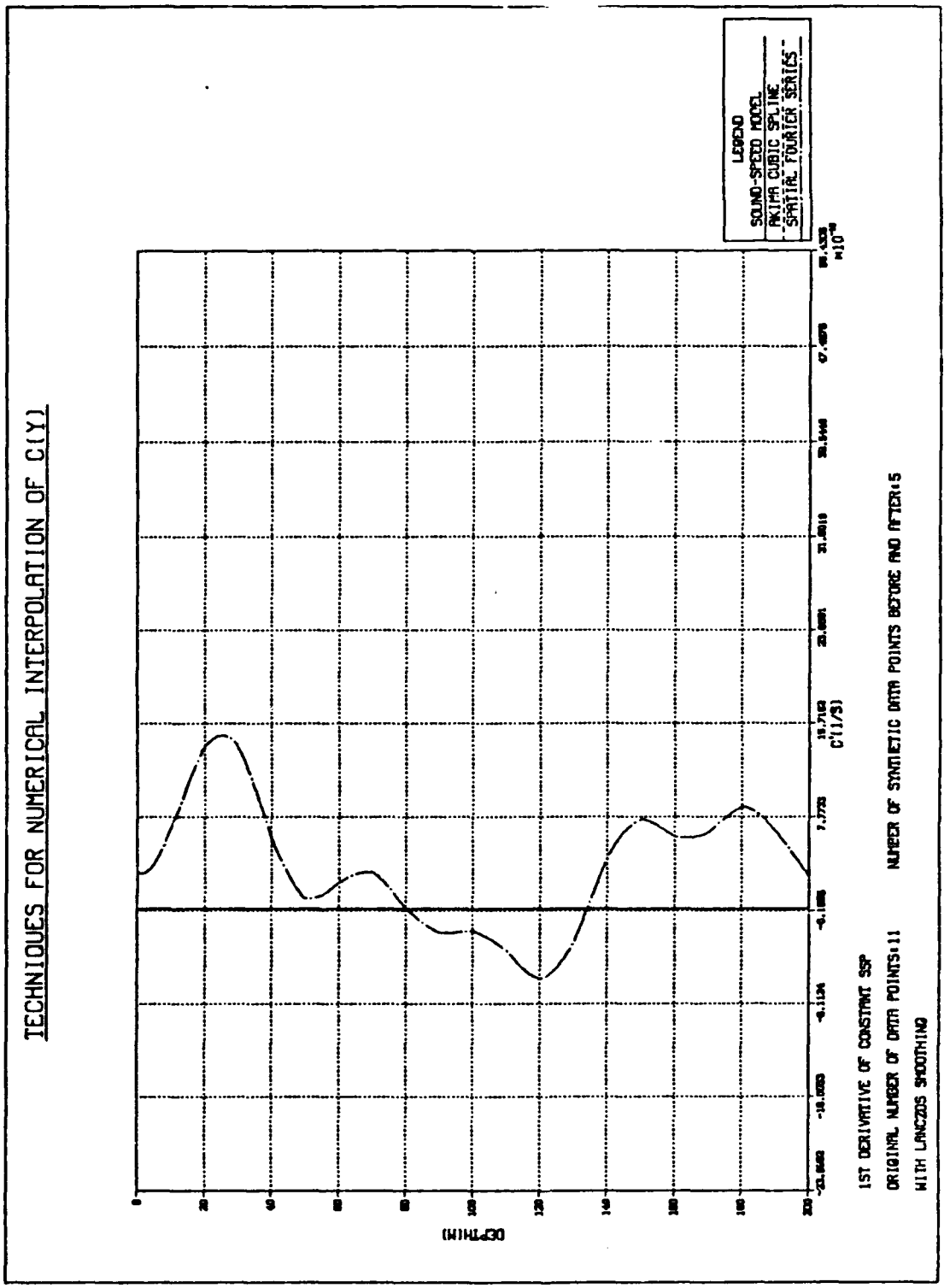

Figure 29. First-Order Derivative Fit - Constant Speed of Sound with Synthetic Data.

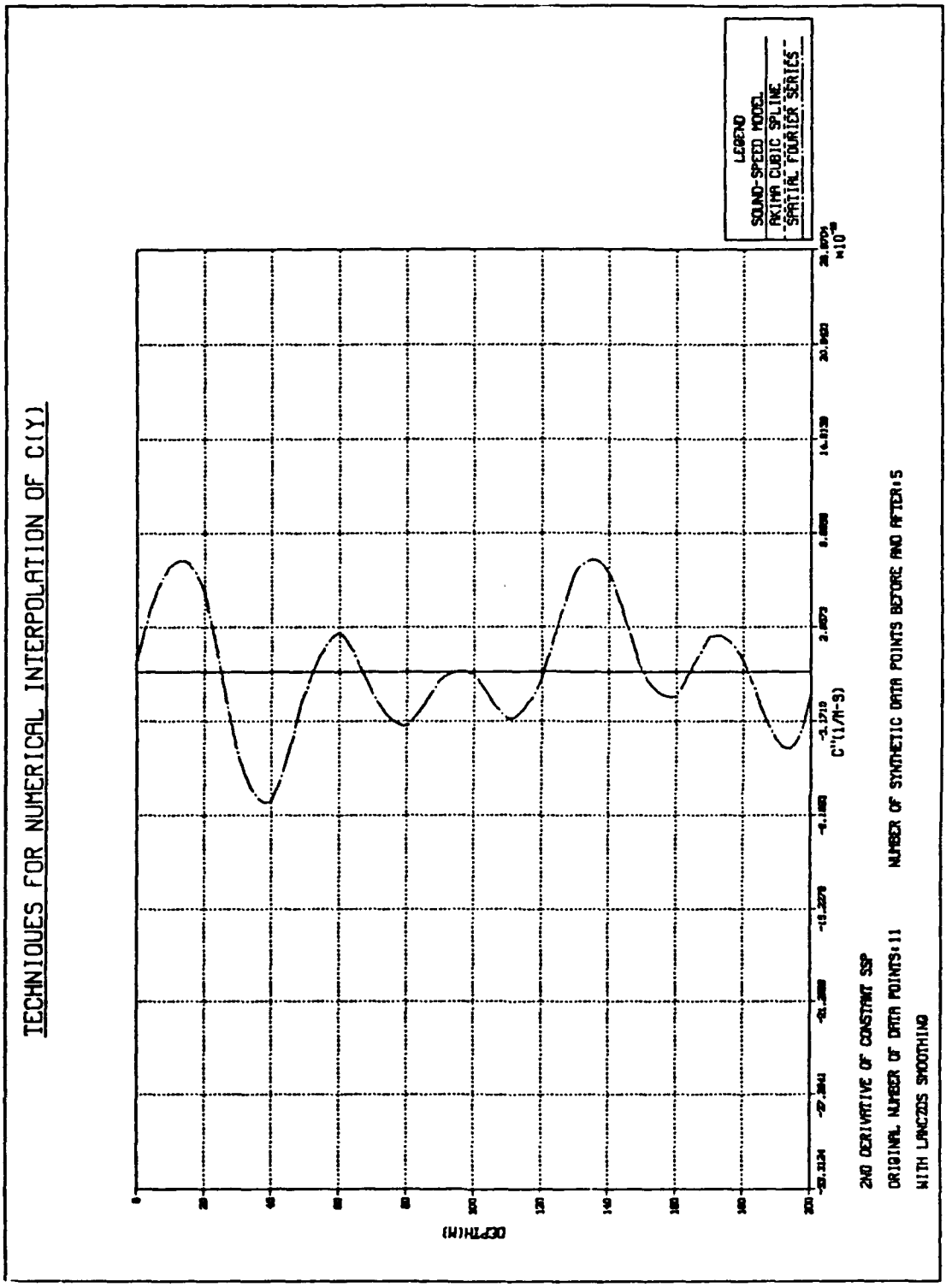

Figure 30. Second-Order Derivative Fit - Constant Speed of Sound with Synthetic Data.

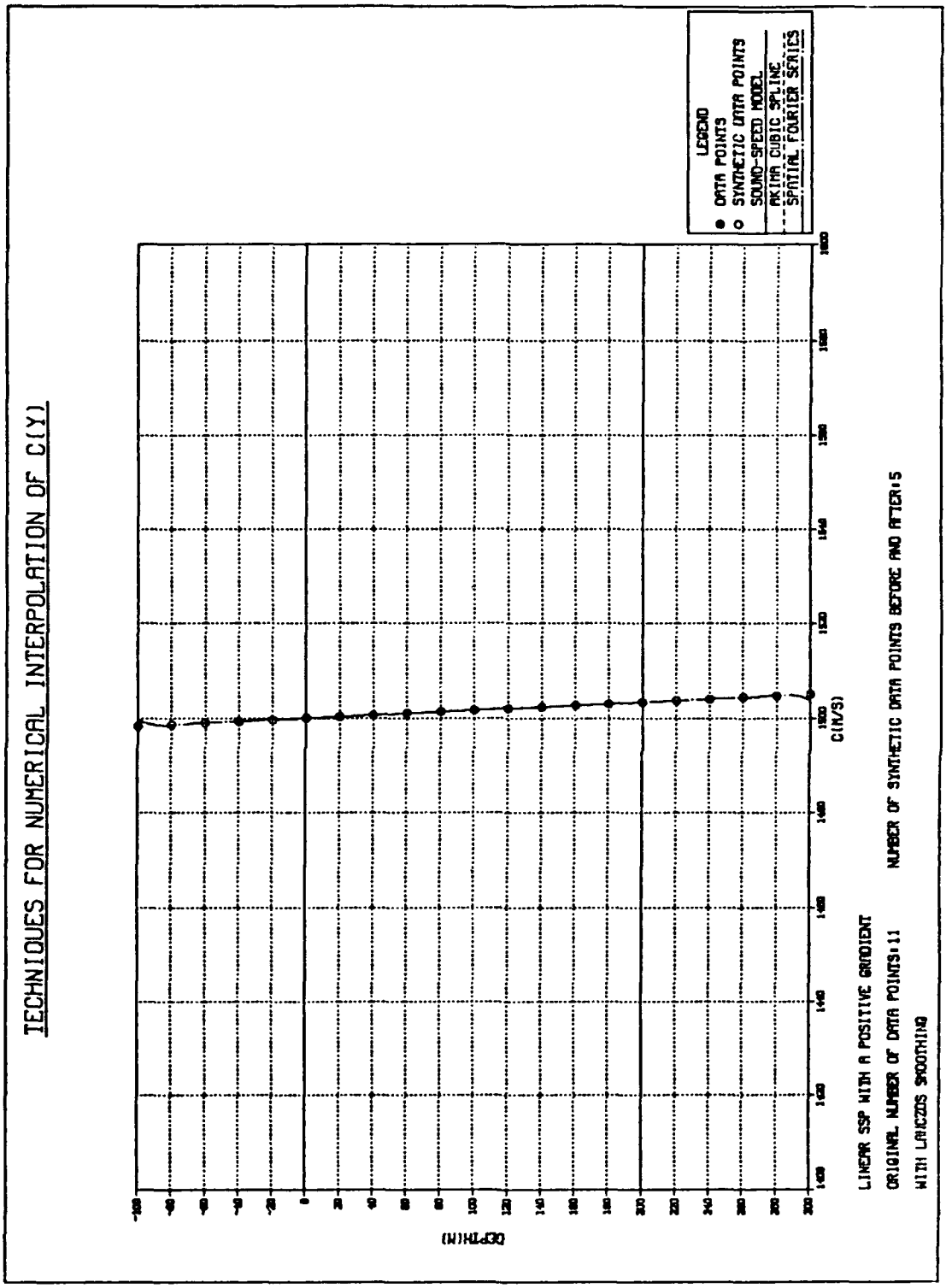

Figure 31. Sound-Speed Fit - Linear SSP with a Positive Gradient and Synthetic Data.

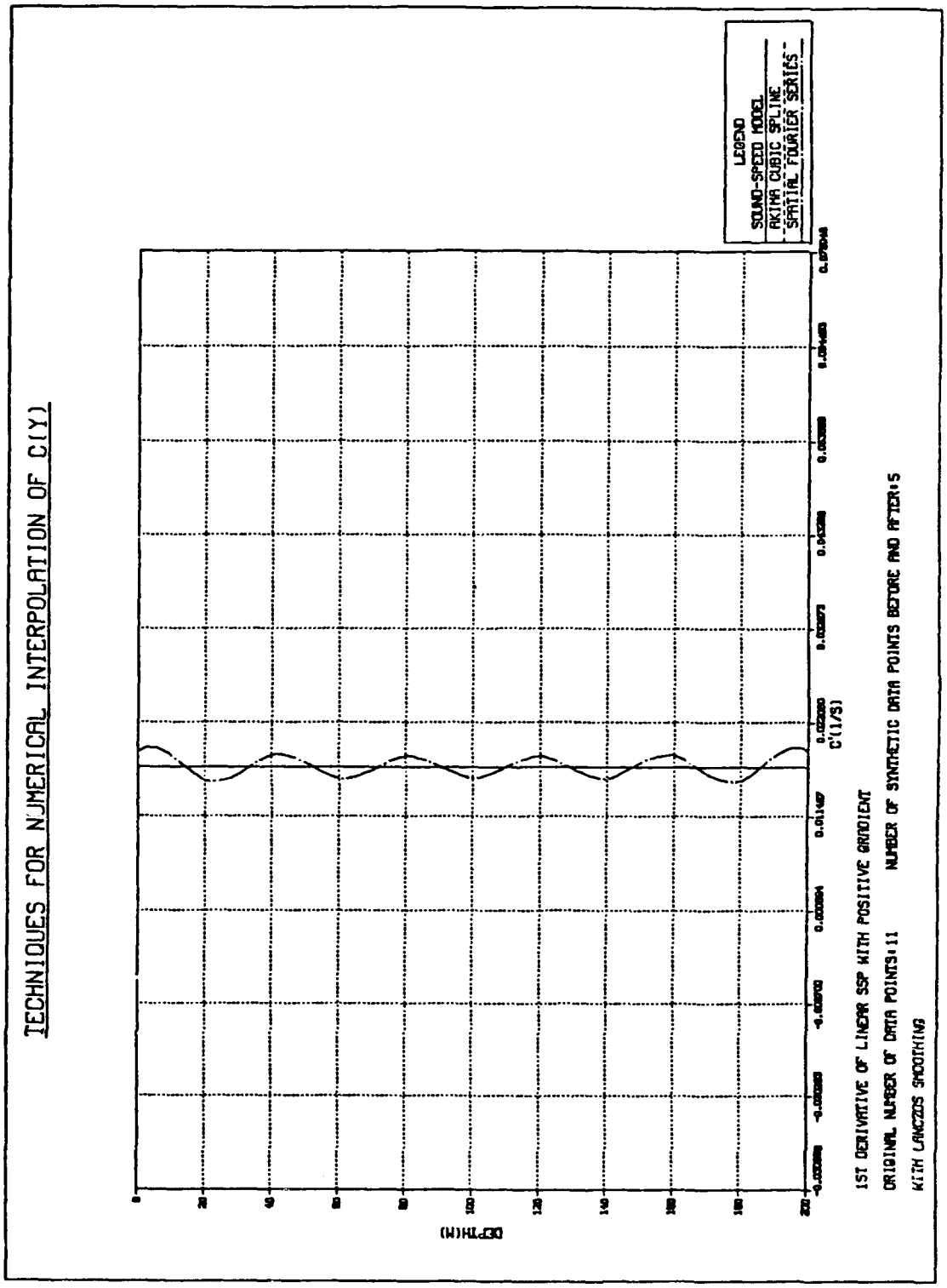

Figure 32. First-Order Derivative Fit - Linear SSP with a Positive Gradient and Synthetic Data.

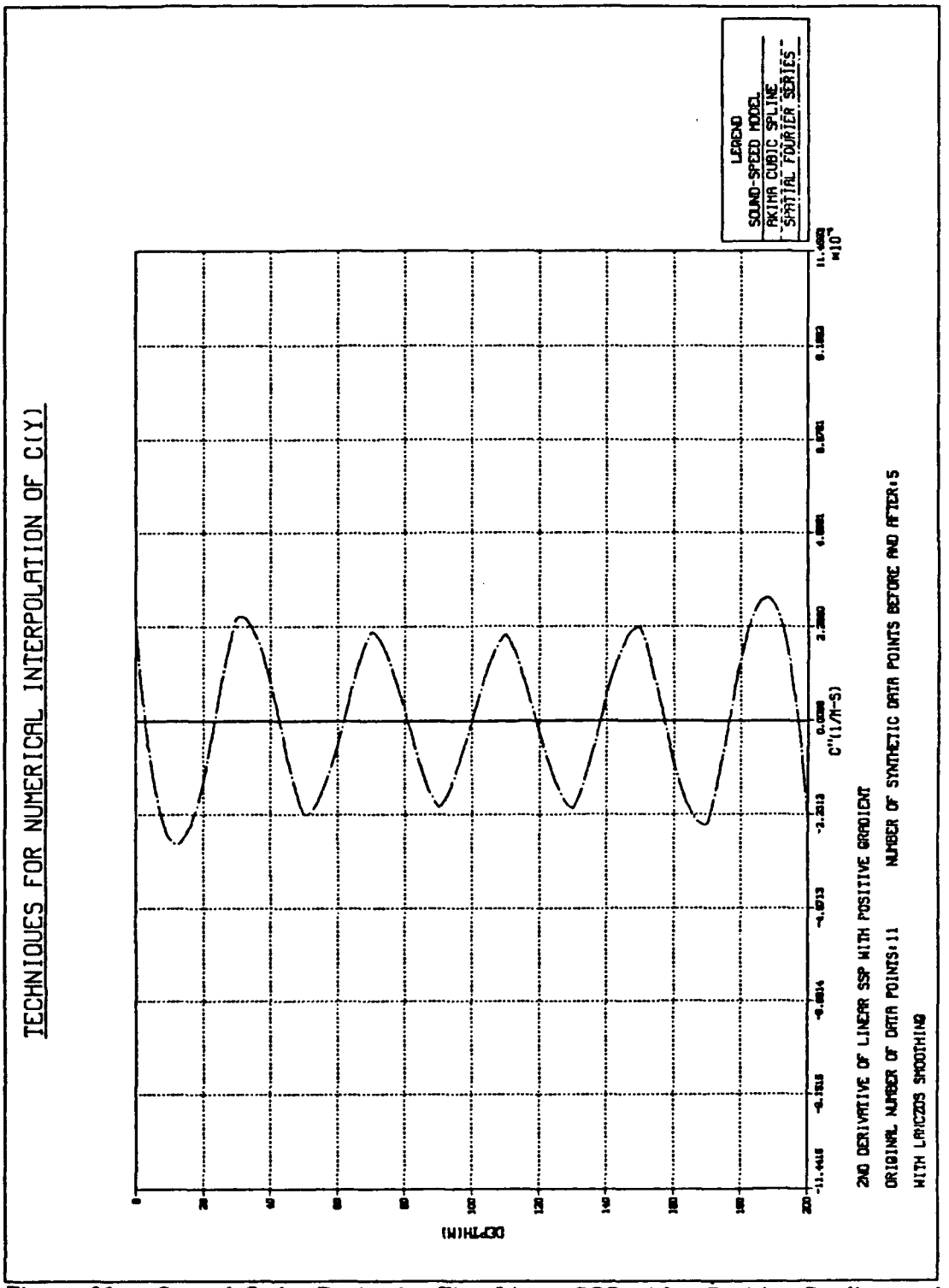

Figure 33. Second-Order Derivative Fit - Linear SSP with a Positive Gradient and Synthetic Data.

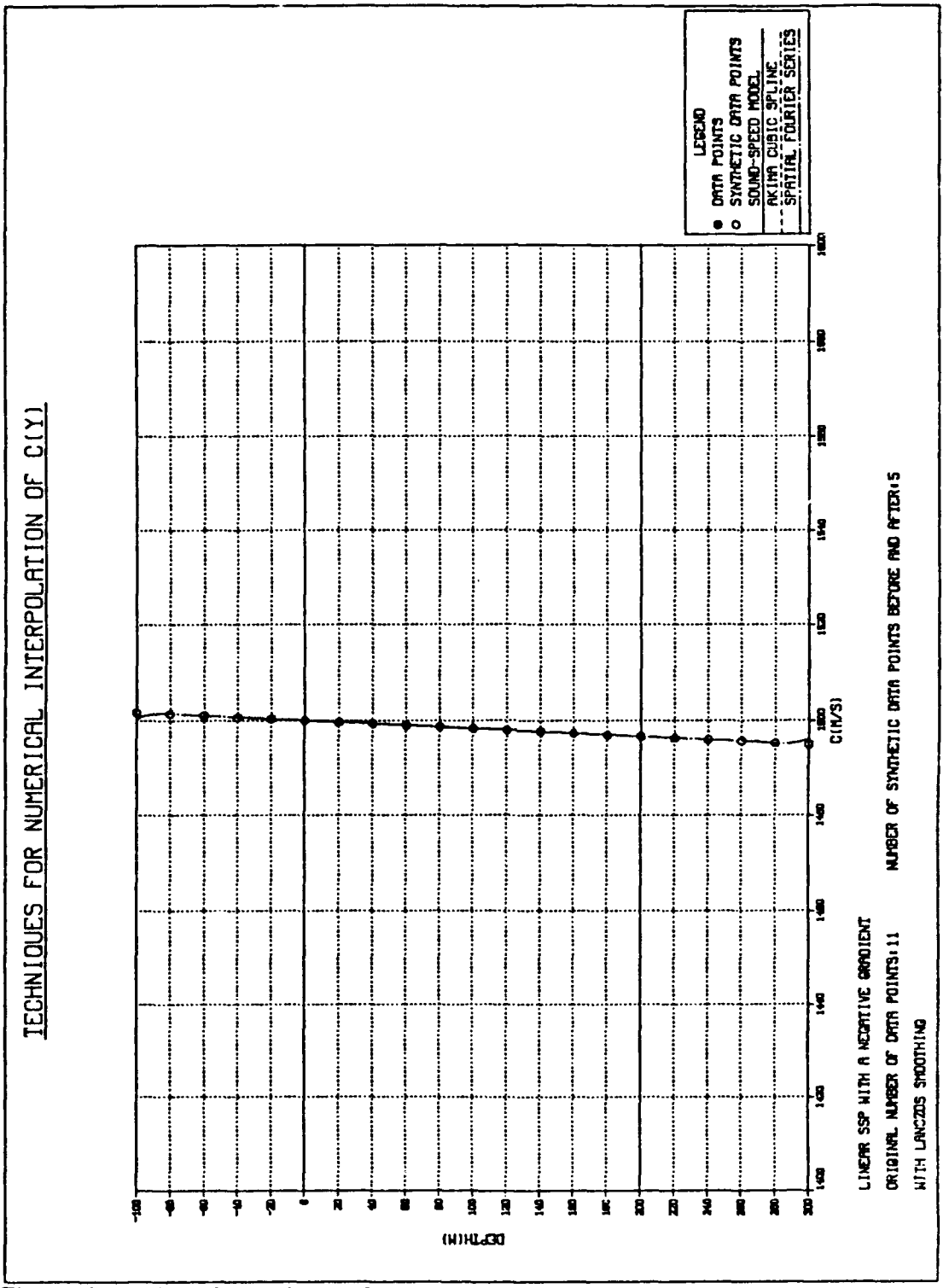

Figure 34. Sound-Speed Fit - Linear SSP with a Negative Gradient and Synthetic Data.

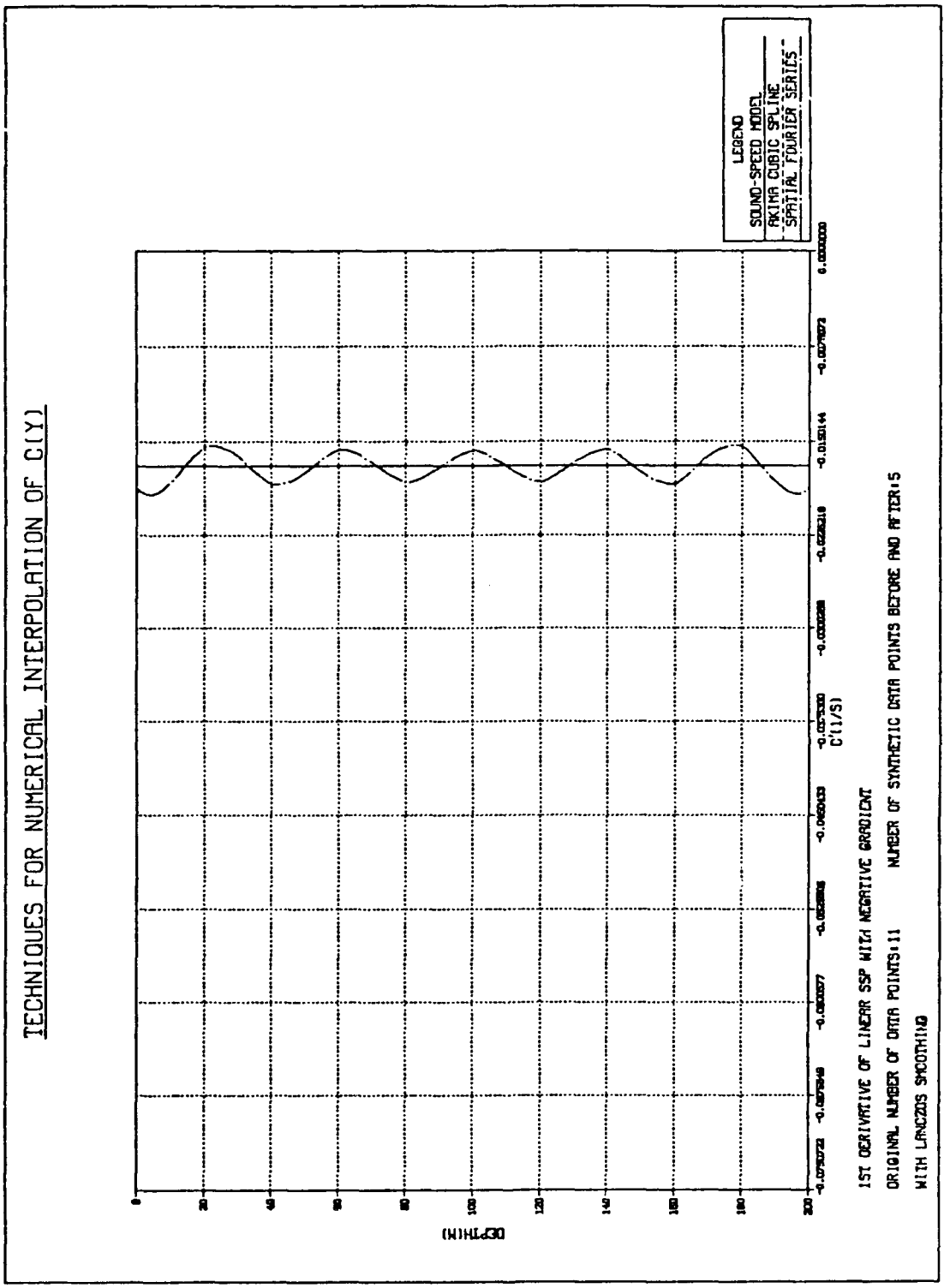

Figure 35. First-Order Derivative Fit - Linear SSP with a Negative Gradient and Synthetic Data.

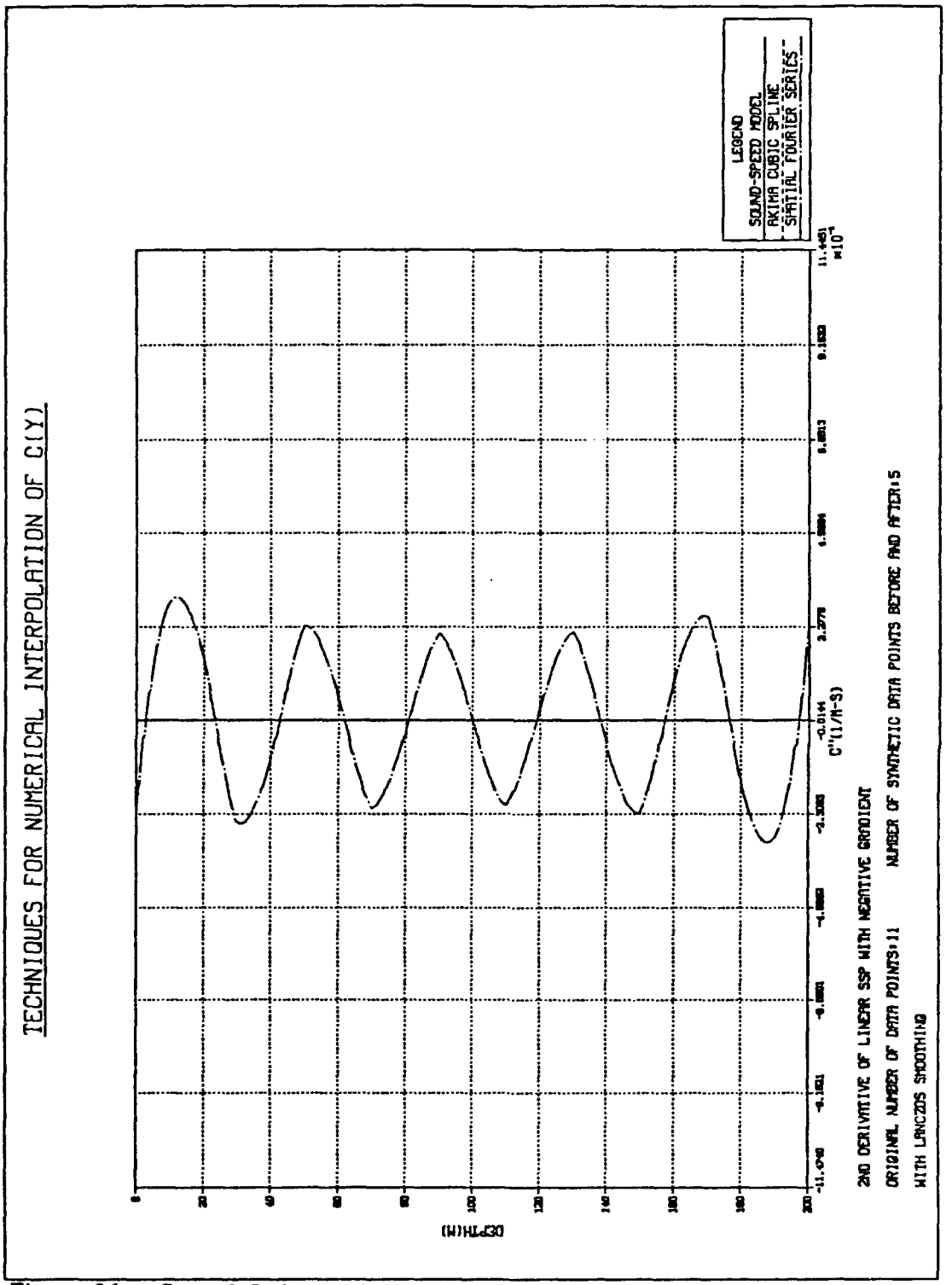

Figure 36. Second-Order Derivative Fit - Linear SSP with a Negative Gradient and Synthetic Data.

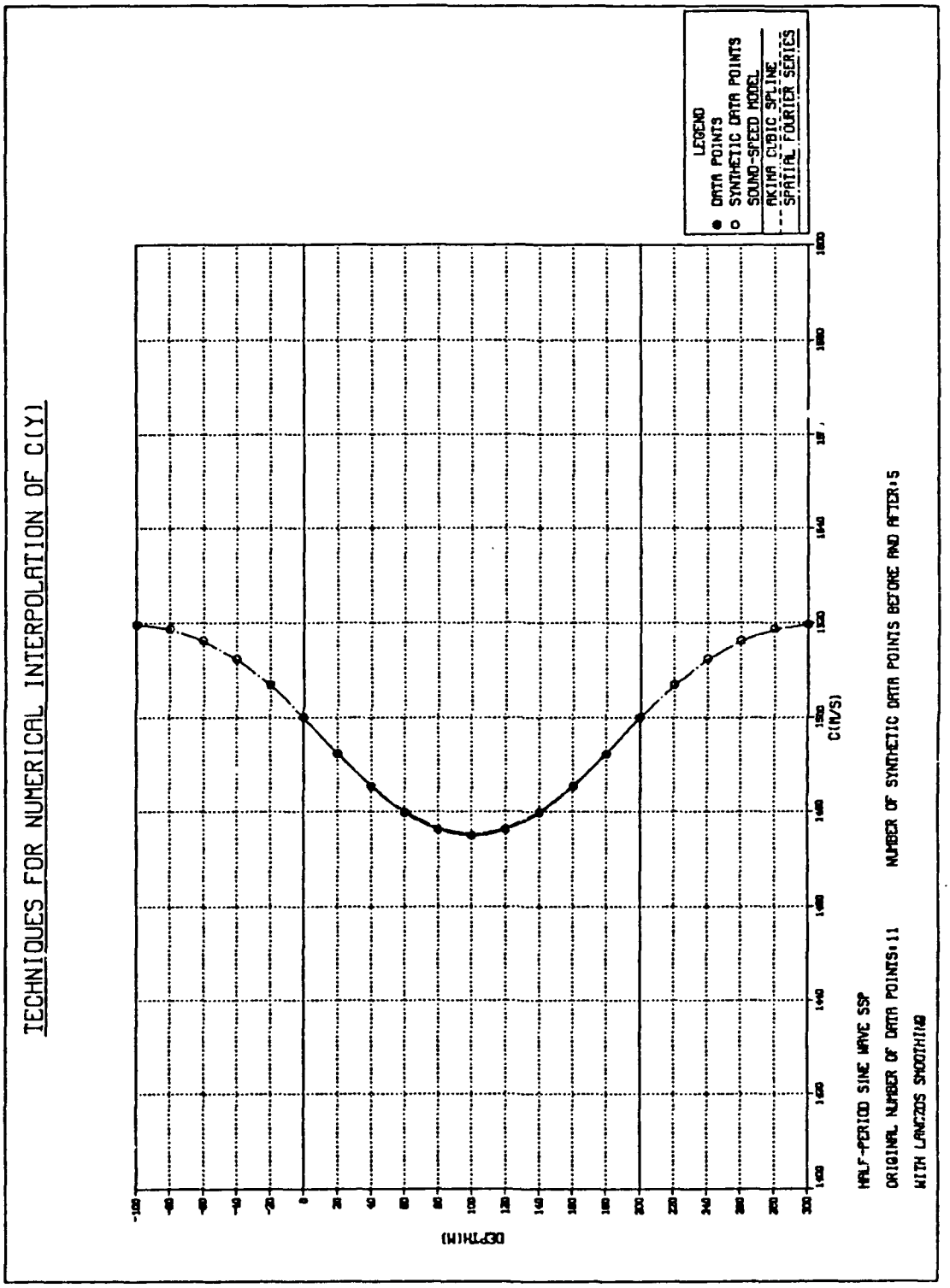

Figure 37. Sound-Speed Fit - Half-Period Sine Wave SSP with Synthetic Data.

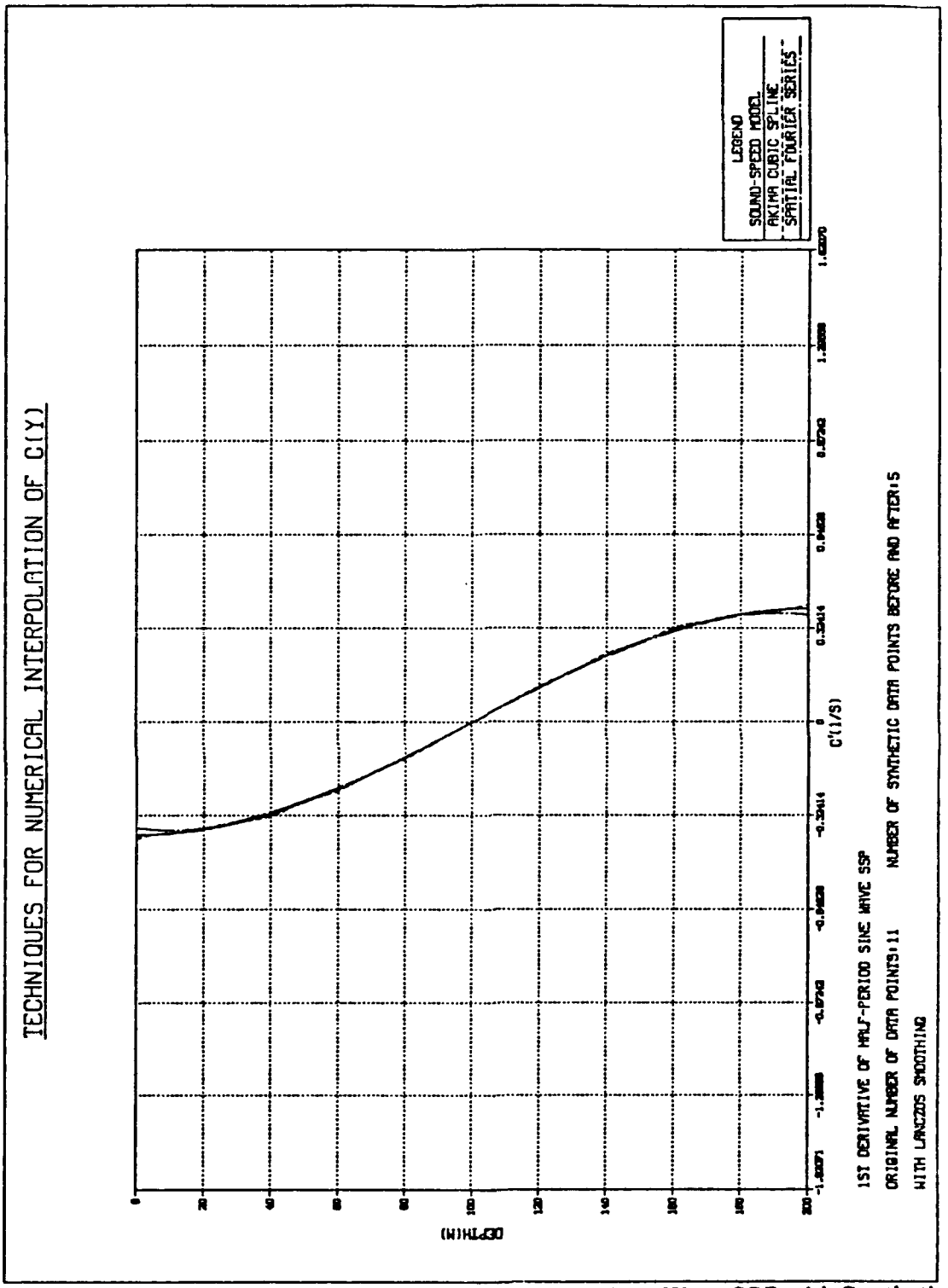

Figure 38. First-Order Derivative Fit - Half-Period Sine Wave SSP with Synthetic Data.

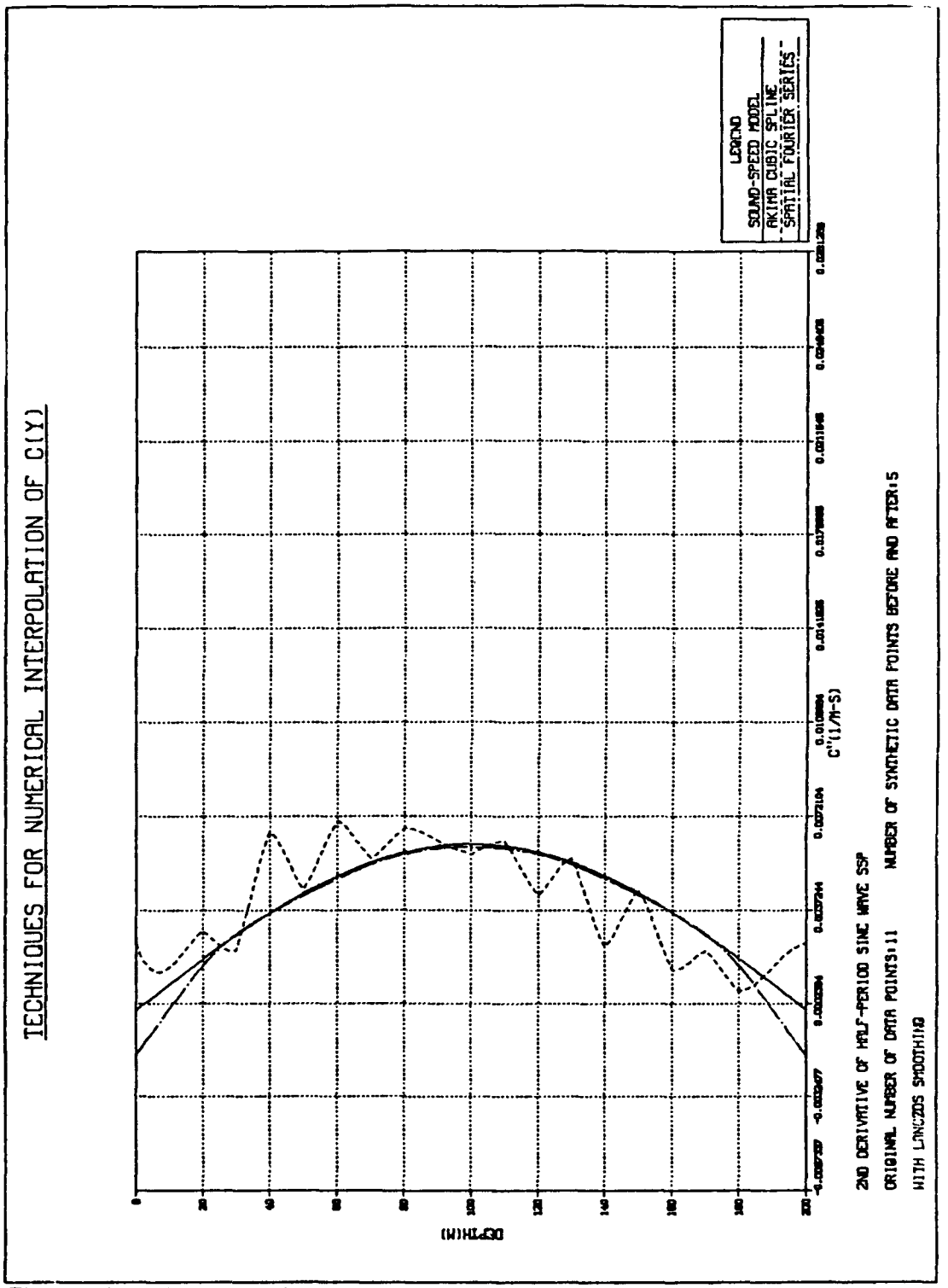

Figure 39. Second-Order Derivative Fit - Half-Period Sine Wave SSP with Synthetic Data.

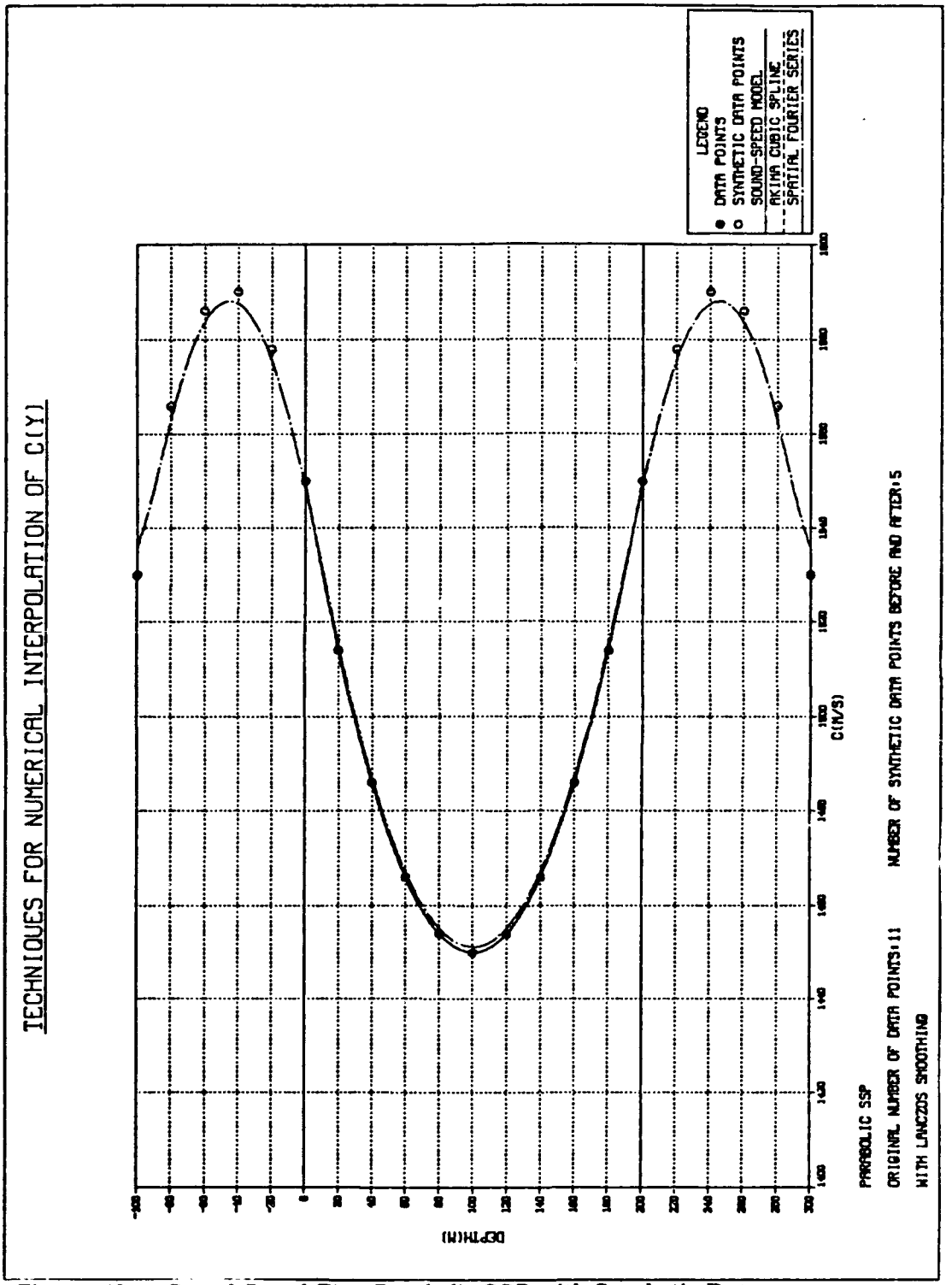

Figure 40. Sound-Speed Fit - Parabolic SSP with Synthetic Data.

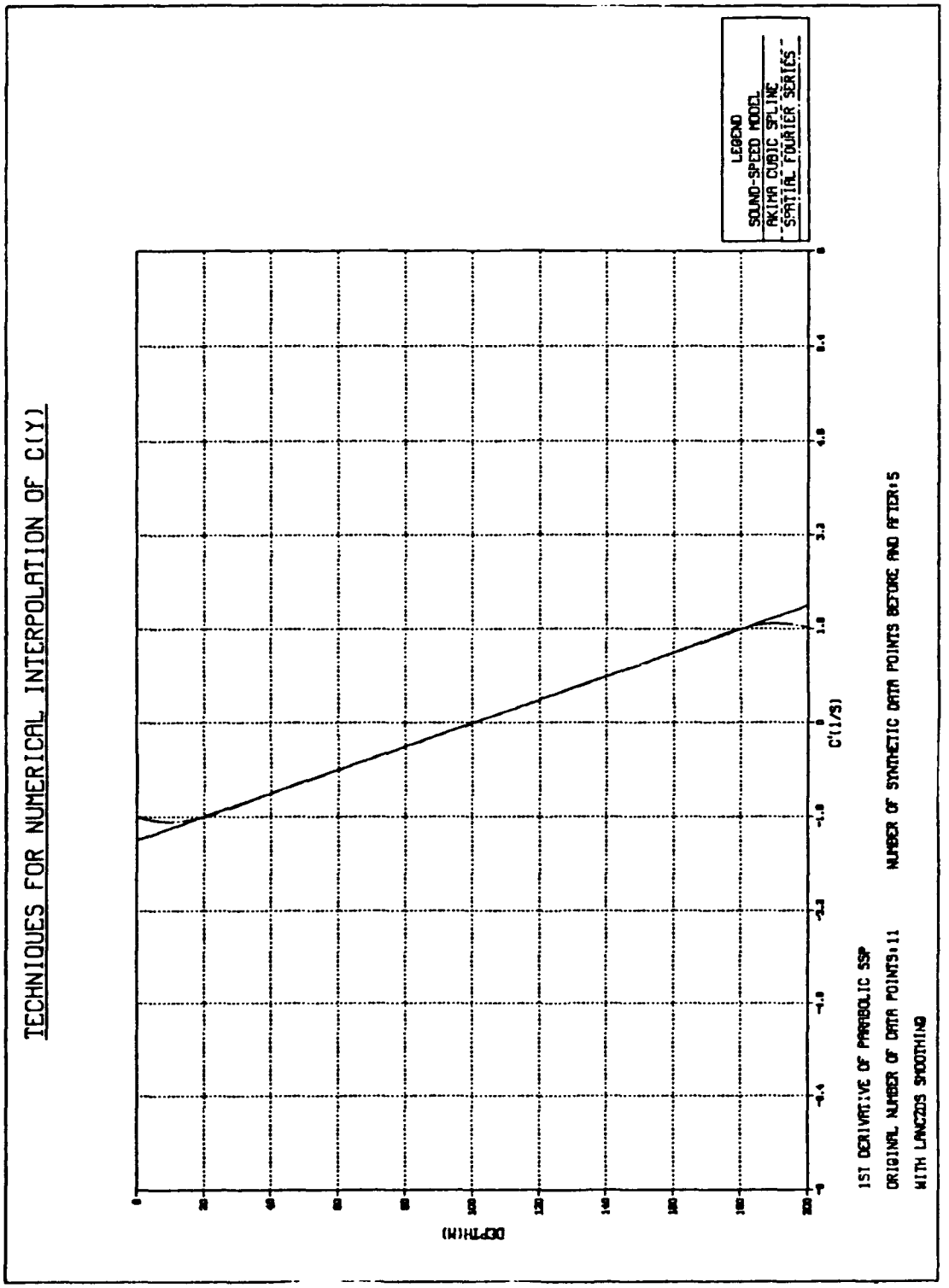

Figure 41. First-Order Derivative Fit - Parabolic SSP with Synthetic Data.

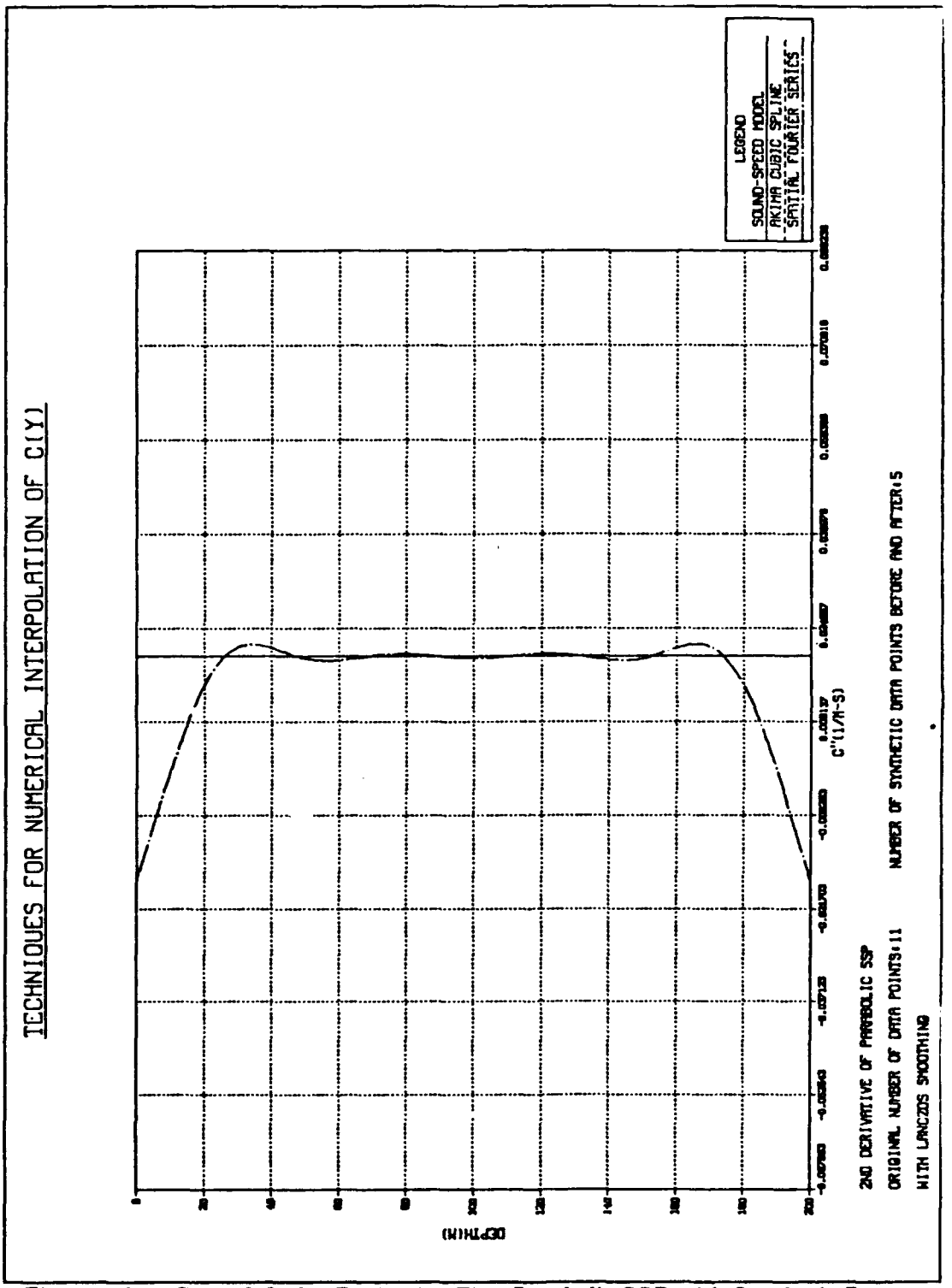

Figure 42. Second-Order Derivative Fit - Parabolic SSP with Synthetic Data.

Table 25. FOURIER SERIES RESULTS WITH LANCZOS SMOOTHING, SYNTHETIC DATA, AKIMA CUBIC SPLINE INPUT TO FOURIER METHOD - HALF-PERIOD SINE WAVE SSP

HALF-PERIOD SINE WAVE SOUND-SPEED PROFILE

NUMBER OF ORIGINAL DATA POINTS = 11
NUMBER OF SYNTHETIC DATA POINTS = 5
TECHNIQUE: SPATIAL FOURIER SERIES FIT WITH LANCZOS SMOOTHING

USING AKIMA CUBIC SPLINE FIT AS INPUT DATA

DEPTH (M)	C(EXACT) (M/S)	C(FIT) (M/S)	% ERROR	CDOT(EXACT) (1/S)	CDOT(FIT) (1/S)	% ERROR	CDOT2(EXACT) (1/M-S)	CDOT2(FIT) (1/M-S)	% ERROR
0.00	1500.0	1500.0	0.000	-0.3927E+00	-0.4005E+00	1.998	0.0000E+00	-0.1995E-02	********
10.00	1496.1	1496.1	-0.002	-0.3879E+00	-0.3849E+00	-0.771	0.9650E-03	0.1607E-02	66.529
20.00	1492.3	1492.3	0.000	-0.3735E+00	-0.3722E+00	-0.339	0.1906E-02	0.1840E-02	-3.451
30.00	1488.7	1488.7	0.002	-0.3499E+00	-0.3473E+00	-0.749	0.2800E-02	0.2233E-02	-20.255
40.00	1485.3	1485.3	0.000	-0.3177E+00	-0.3261E+00	2.655	0.3626E-02	0.4018E-02	10.808
50.00	1482.3	1482.3	0.000	-0.2777E+00	-0.2731E+00	-1.643	0.4362E-02	0.4479E-02	2.693
60.00	1479.8	1479.8	0.000	-0.2308E+00	-0.2365E+00	2.474	0.4990E-02	0.4723E-02	-5.351
70.00	1477.7	1477.7	0.000	-0.1783E+00	-0.1753E+00	-1.650	0.5496E-02	0.5663E-02	3.028
80.00	1476.2	1476.2	0.000	-0.1214E+00	-0.1243E+00	2.468	0.5867E-02	0.5576E-02	-4.955
90.00	1475.3	1475.3	0.000	-0.6143E-01	-0.6041E-01	-1.659	0.6093E-02	0.6278E-02	3.048
100.00	1475.0	1475.0	0.000	-0.1112E-15	-0.1186E-04	********	0.6169E-02	0.5832E-02	-5.462
110.00	1475.3	1475.3	0.000	0.6143E-01	0.6044E-01	-1.620	0.6093E-02	0.6275E-02	3.000
120.00	1476.2	1476.2	0.000	0.1214E+00	0.1243E+00	2.448	0.5867E-02	0.5582E-02	-4.855
130.00	1477.7	1477.7	0.000	0.1783E+00	0.1754E+00	-1.636	0.5496E-02	0.5653E-02	2.862
140.00	1479.8	1479.8	0.000	0.2308E+00	0.2365E+00	2.463	0.4990E-02	0.4736E-02	-5.099
150.00	1482.3	1482.3	0.000	0.2777E+00	0.2731E+00	-1.634	0.4362E-02	0.4463E-02	2.314
160.00	1485.3	1485.3	0.000	0.3177E+00	0.3261E+00	2.646	0.3626E-02	0.4039E-02	11.388
170.00	1488.7	1488.7	0.002	0.3499E+00	0.3473E+00	-0.741	0.2800E-02	0.2207E-02	-21.196
180.00	1492.3	1492.3	0.000	0.3735E+00	0.3722E+00	-0.347	0.1906E-02	0.1873E-02	-1.730
190.00	1496.1	1496.1	-0.002	0.3879E+00	0.3849E+00	-0.763	0.9650E-03	0.1567E-02	62.365
200.00	1500.0	1500.0	0.000	0.3927E+00	0.4004E+00	1.974	0.2125E-17	-0.1894E-02	********

Table 26. FOURIER SERIES RESULTS WITH LANCZOS SMOOTHING, SYNTHETIC DATA, AKIMA CUBIC SPLINE INPUT TO FOURIER METHOD - PARABOLIC SSP

PARABOLIC SOUND-SPEED PROFILE

NUMBER OF ORIGINAL DATA POINTS = 11
NUMBER OF SYNTHETIC DATA POINTS = 5
TECHNIQUE: SPATIAL FOURIER SERIES FIT WITH LANCZOS SMOOTHING

USING AKIMA CUBIC SPLINE FIT AS INPUT DATA

DEPTH (M)	C(EXACT) (M/S)	C(FIT) (M/S)	% ERROR	CDOT(EXACT) (1/S)	CDOT(FIT) (1/S)	% ERROR	CDOT2(EXACT) (1/M-S)	CDOT2(FIT) (1/M-S)	% ERROR
0.00	1550.0	1550.0	-0.001	-0.2000E+01	-0.1960E+01	-1.991	0.2000E-01	-0.1707E-01	-185.362
10.00	1531.0	1531.0	0.001	-0.1800E+01	-0.1800E+01	-0.001	0.2000E-01	0.1985E-01	-0.749
20.00	1514.0	1514.0	0.001	-0.1600E+01	-0.1600E+01	0.003	0.2000E-01	0.1997E-01	-0.133
30.00	1499.0	1499.0	0.001	-0.1400E+01	-0.1400E+01	-0.004	0.2000E-01	0.1996E-01	-0.187
40.00	1486.0	1486.0	0.001	-0.1200E+01	-0.1200E+01	0.002	0.2000E-01	0.1997E-01	-0.134
50.00	1475.0	1475.0	0.001	-0.1000E+01	-0.1000E+01	-0.001	0.2000E-01	0.1997E-01	-0.164
60.00	1466.0	1466.0	0.001	-0.8000E+00	-0.8000E+00	0.000	0.2000E-01	0.1997E-01	-0.130
70.00	1459.0	1459.0	0.001	-0.6000E+00	-0.6000E+00	0.004	0.2000E-01	0.1996E-01	-0.182
80.00	1454.0	1454.0	0.001	-0.4000E+00	-0.4000E+00	-0.006	0.2000E-01	0.1996E-01	-0.204
90.00	1451.0	1451.0	0.001	-0.2000E+00	-0.2000E+00	0.000	0.2000E-01	0.1998E-01	-0.111
100.00	1450.0	1450.0	0.001	0.0000E+00	-0.1206E-04	********	0.2000E-01	0.1997E-01	-0.170
110.00	1451.0	1451.0	0.001	0.2000E+00	0.2000E+00	0.012	0.2000E-01	0.2004E-01	0.185
120.00	1454.0	1454.0	0.001	0.4000E+00	0.4000E+00	-0.012	0.2000E-01	0.1997E-01	-0.151
130.00	1459.0	1459.0	0.001	0.6000E+00	0.6000E+00	0.008	0.2000E-01	0.2002E-01	0.079
140.00	1466.0	1466.0	0.001	0.8000E+00	0.8000E+00	-0.003	0.2000E-01	0.1999E-01	-0.052
150.00	1475.0	1475.0	0.001	0.1000E+01	0.1000E+01	0.001	0.2000E-01	0.1995E-01	-0.254
160.00	1486.0	1486.0	0.001	0.1200E+01	0.1200E+01	0.000	0.2000E-01	0.2000E-01	-0.013
170.00	1499.0	1499.0	0.001	0.1400E+01	0.1400E+01	-0.002	0.2000E-01	0.2000E-01	-0.013
180.00	1514.0	1514.0	0.001	0.1600E+01	0.1600E+01	0.001	0.2000E-01	0.2001E-01	0.057
190.00	1531.0	1531.0	0.001	0.1800E+01	0.1800E+01	0.000	0.2000E-01	0.1987E-01	-0.644
200.00	1550.0	1550.0	-0.001	0.2000E+01	0.1960E+01	-1.996	0.2000E-01	-0.1697E-01	-184.842

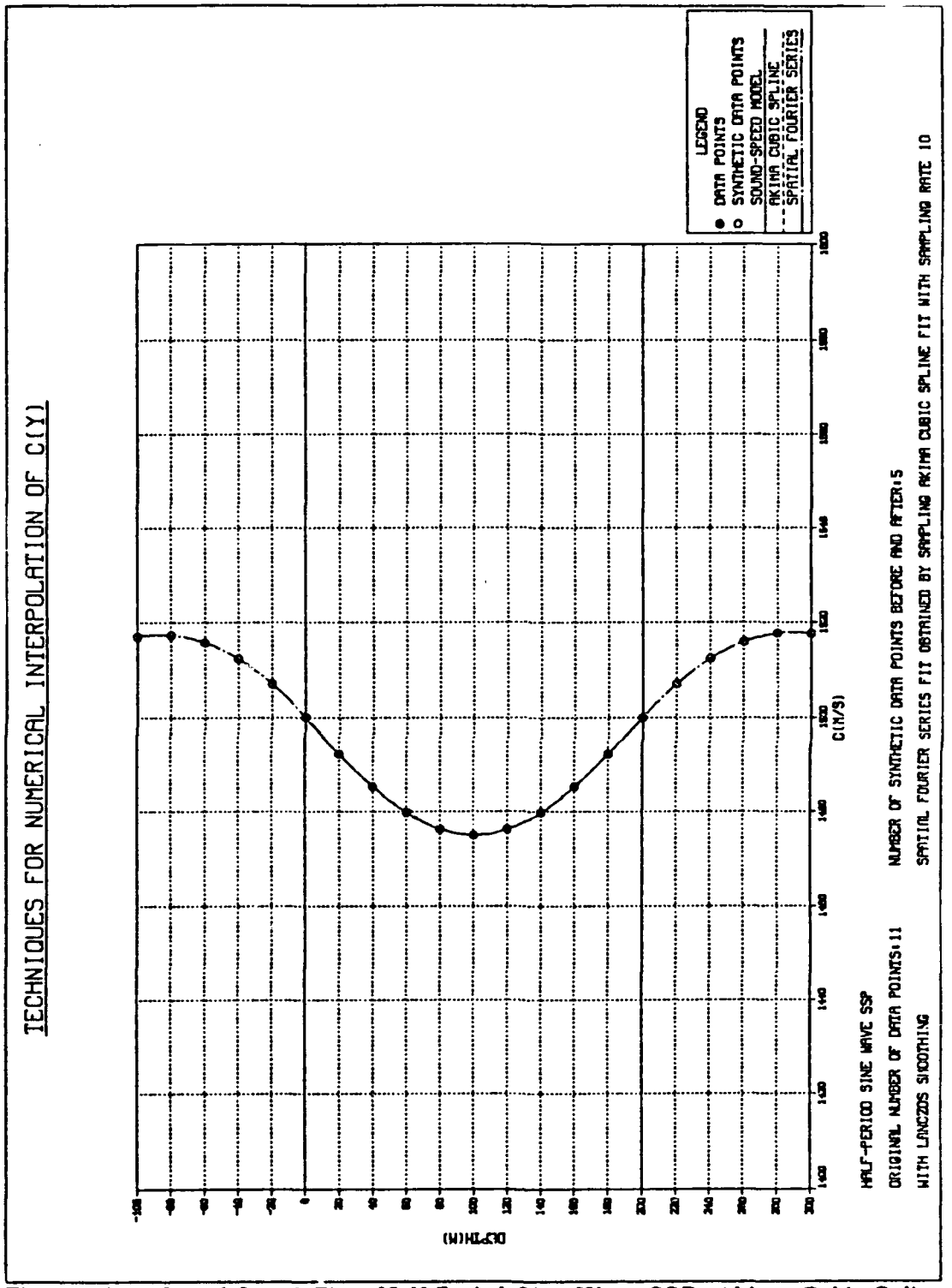

Figure 43. Sound-Speed Fit - Half-Period Sine Wave SSP, Akima Cubic Spline Input to Fourier Method.

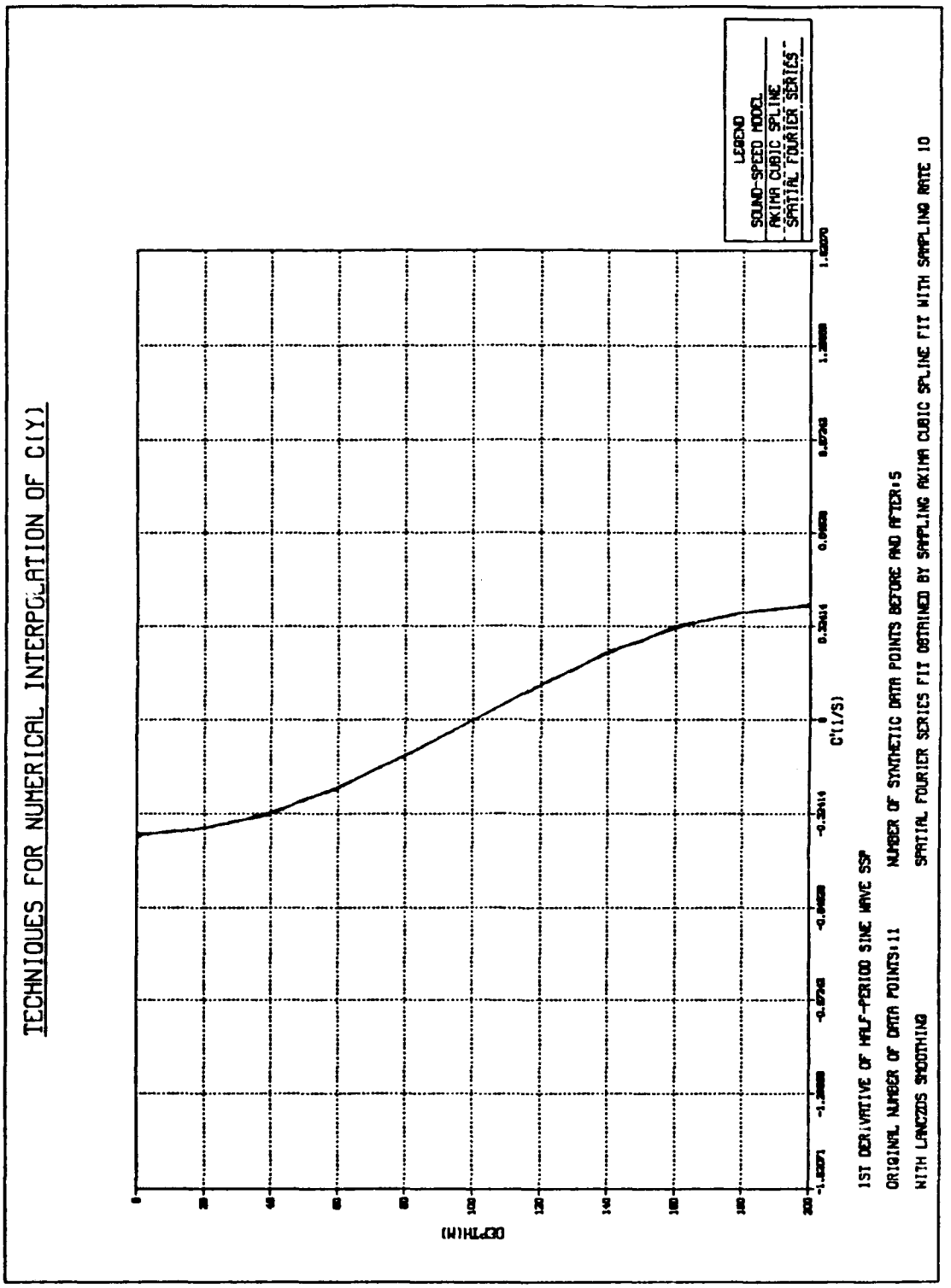

Figure 44. First-Order Derivative Fit - Half-Period Sine Wave SSP, Akima Cubic Spline Input to Fourier Method.

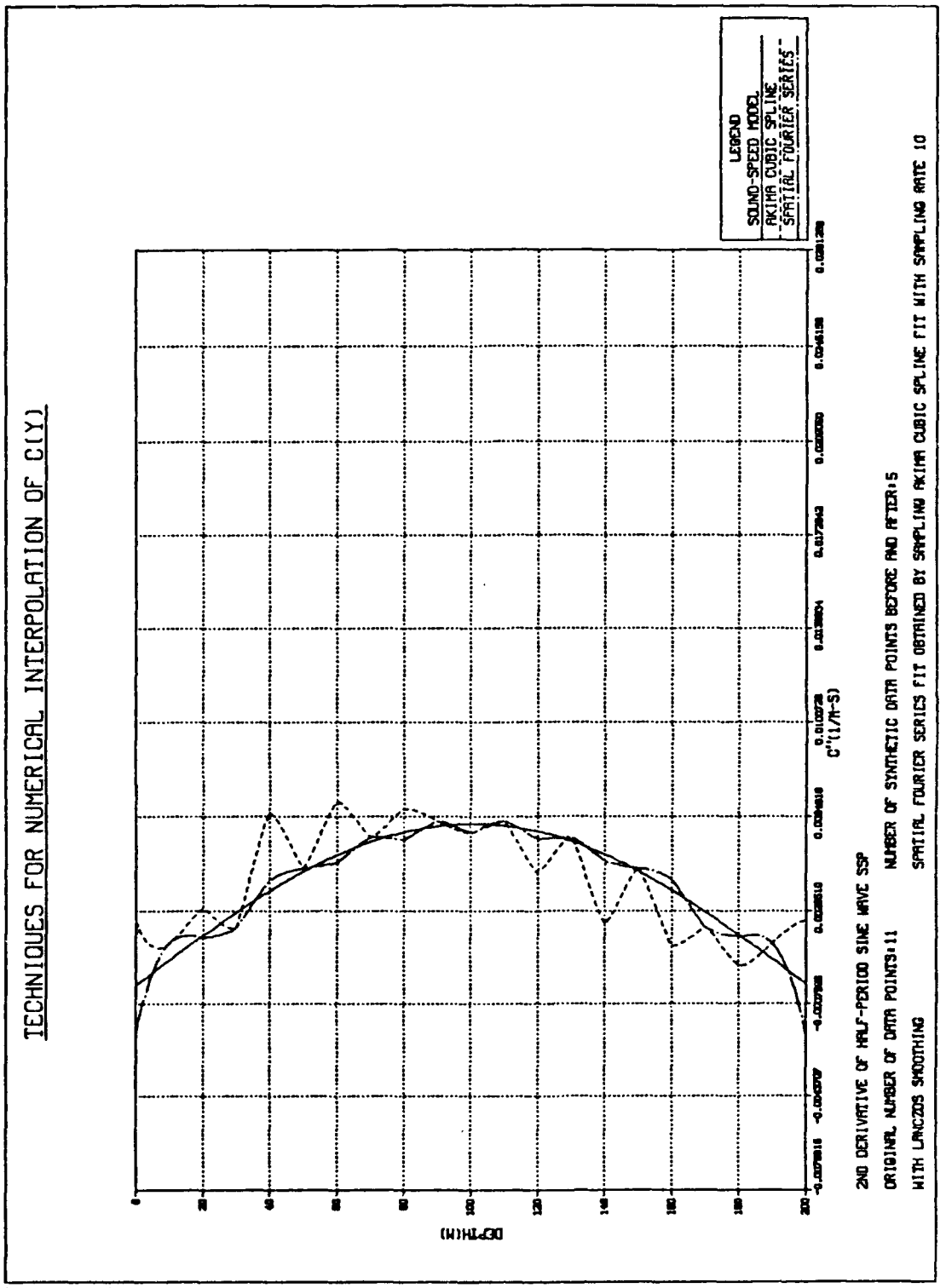

Figure 45. Second-Order Derivative Fit - Half-Period Sine Wave SSP, Akima Cubic Spline Input to Fourier Method.

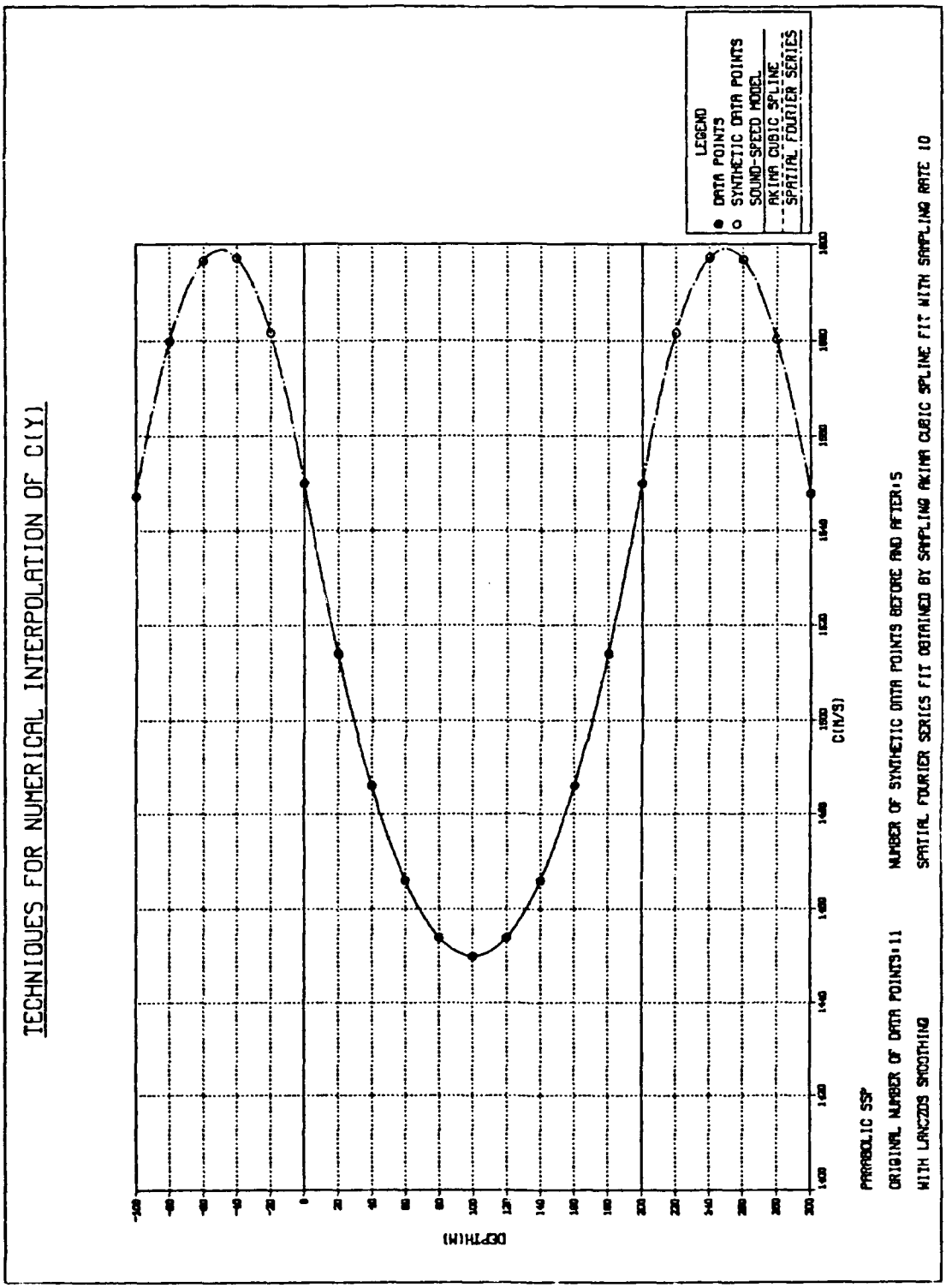

Figure 46. Sound-Speed Fit - Parabolic SSP, Akima Cubic Spline Input to Fourier Method.

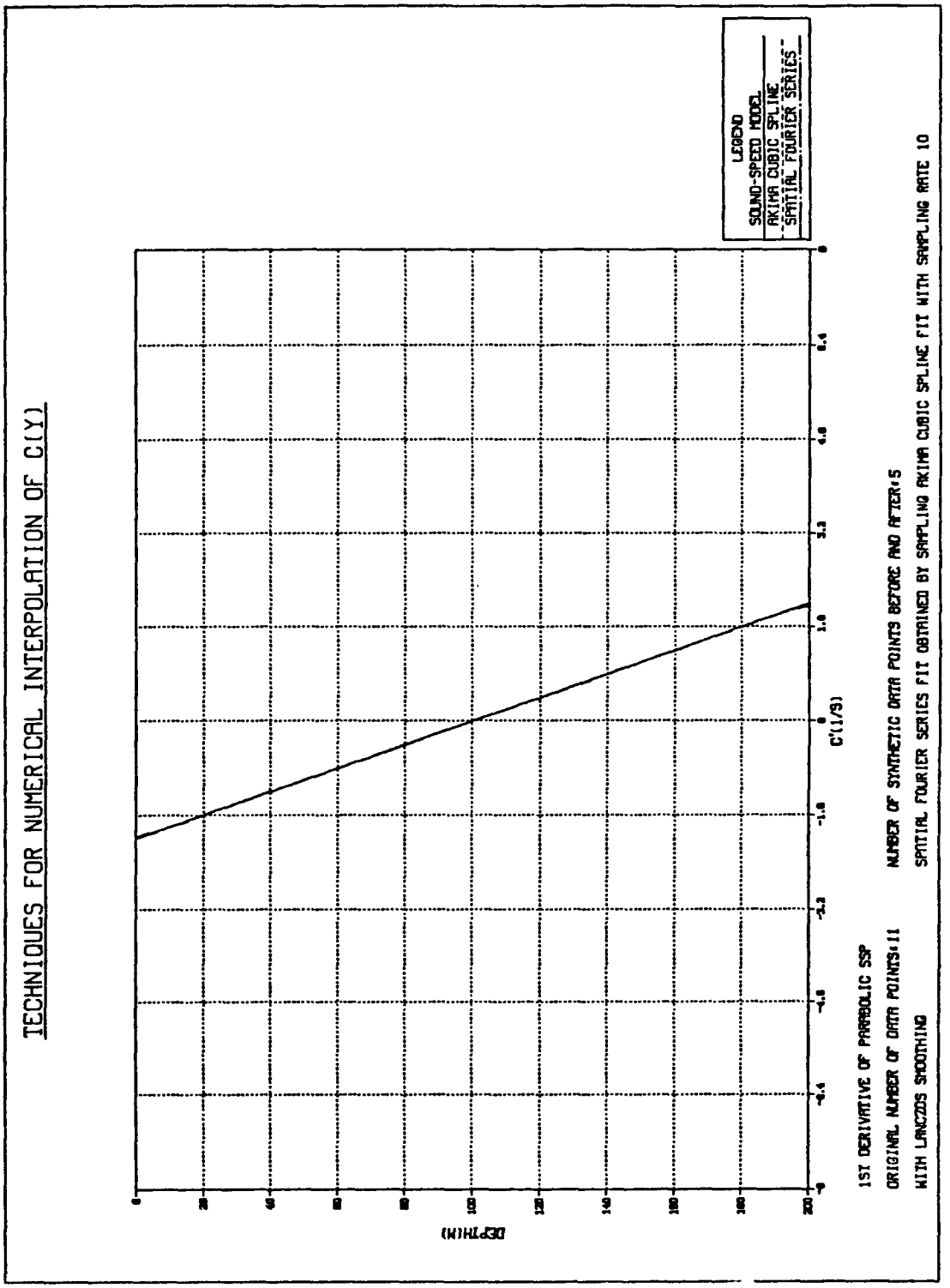

Figure 47. First-Order Derivative Fit - Parabolic SSP, Akima Cubic Spline Input to Fourier Method.

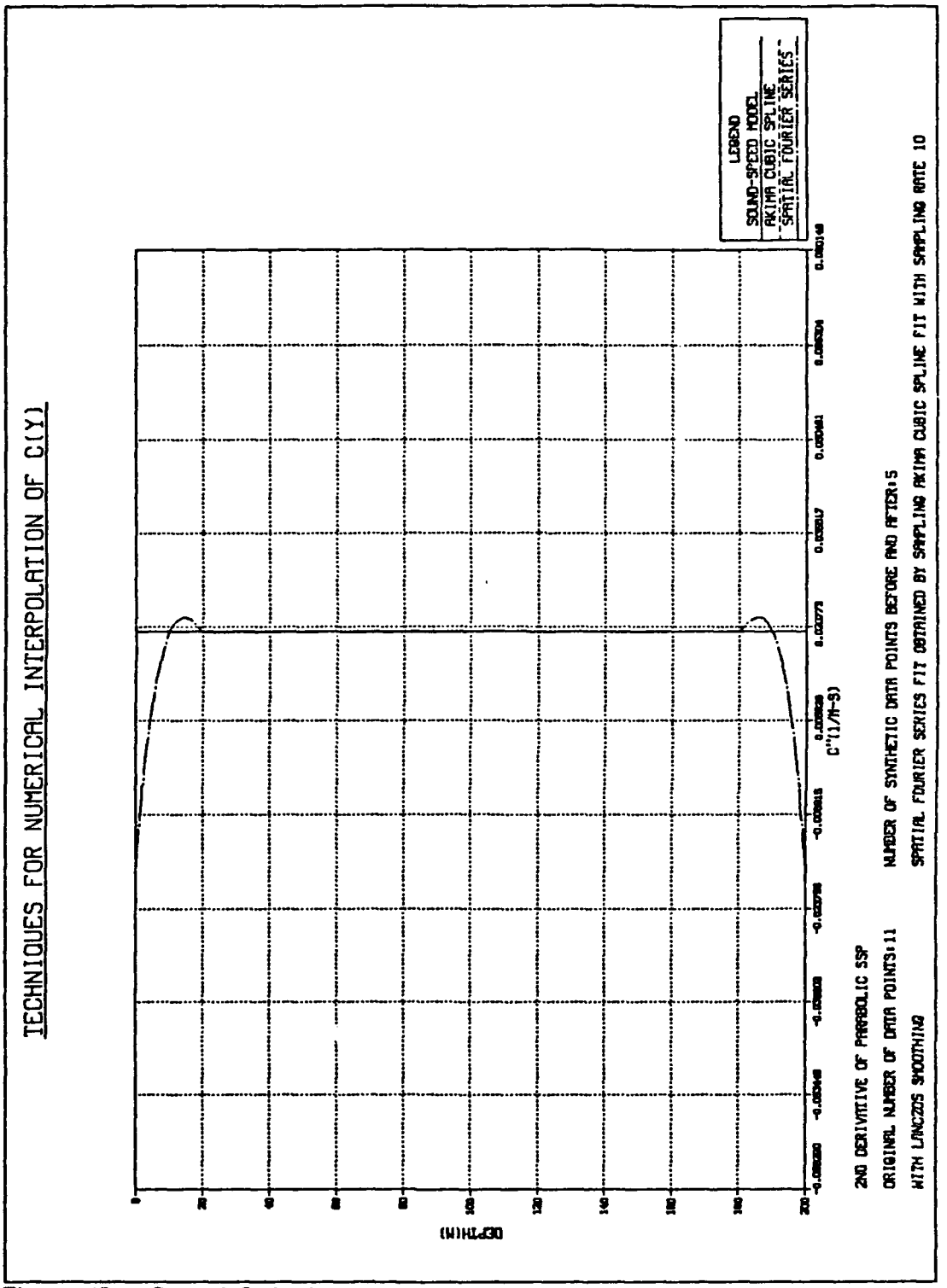

Figure 48. Second-Order Derivative Fit - Parabolic SSP, Akima Cubic Spline Input to Fourier Method.

B. RAY TRACE RESULTS USING SPATIAL FOURIER SERIES REPRESENTATION OF SOUND-SPEED DATA WITH THE RRA ALGORITHM

1. Sound Speed Including Deterministic Component Only

The RRA algorithm using the simple Fourier series sound-speed representation including Lanczos smoothing but without synthetic data or Akima cubic spline input to the Fourier method was tested using the same source locations, SSPs, and rays as in Chapter III, Section A. That is, the SSPs were once again defined as follows:

- SSP 1: Constant speed of sound ($c = 1500 m/s$)
- SSP 2: Linear SSP with a positive gradient ($c(y) = c(0) + g\,y$ m/s, where the speed of sound at the surface $c(0) = c(y = 0) = 1500$ m/s and $g = +0.017$ 1/s)
- SSP 3: Linear SSP with a negative gradient ($c(y) = c(0) + g\,y$ m/s, where the speed of sound at the surface $c(0) = c(y = 0) = 1500$ m/s and $g = -0.017$ 1/s)
- SSP 4: Parabolic SSP with vertex at y_0 where $c(y_0) = 1490$ m/s and the speed of sound at both the ocean surface and bottom is equal to 1500 m/s ($c(y) = c(y_0) + a(y - 100)^2$ m/s with $a = 0.001 \frac{1}{\text{m s}}$ for an ocean depth of 200 m).

The sound source spatial location was established at $x_0 = 0$ m and $z_0 = 0$ m. A source depth of $y_0 = 100$ m was established for an ocean depth of 200 m, unless otherwise noted. Launch angles β_0 were 45°, 85° and 135° for SSPs 1, 2 and 3; and 85°, 95°, and 135° for SSP 4, which again was designed to simulate a SOFAR channel.

The ODE algorithm using the Akima cubic spline fit to sound-speed data remained as the benchmark for comparison purposes, as detailed in Chapter III, Section A. For ease of reference, the results of the ODE algorithm are reproduced in the tables of this sub-section. The ODE's range step size was left at 2.0 m and the arc length step size in the RRA algorithm was left at 2.0 m as well, except where otherwise noted.

The results of the various computer simulation runs are presented in Tables 27 to 33 below.

Table 27. RAY ACOUSTICS RESULTS FOR SSP 1, RAYS 1 THROUGH 3, FOURIER SOUND-SPEED FIT

Method	y_0 (m)	β_0 (deg)	r (km)	y (m)	β (deg)	τ (sec)	s (km)
ODE	100.0	45.0	10.0	100.00	45.000	9.428090	14.1421
RRA	100.0	45.0	10.0	99.94	45.000	9.428088	14.1421
ODE	100.0	85.0	10.0	174.89	85.000	6.692132	10.0382
RRA	100.0	85.0	10.0	174.88	85.000	6.692132	10.0382
ODE	100.0	135.0	10.0	100.00	135.000	9.428090	14.1421
RRA	100.0	135.0	10.0	100.06	135.000	9.428088	14.1421

For SSP 1 (constant speed of sound), Table 27 shows that at a horizontal range of $r = 10$ km, the differences between the benchmark ODE algorithm and the RRA algorithm using the Fourier series sound-speed fit are as follows:

- between 0.01 and 0.06 m in depth y and
- 2 μ sec in travel time τ.

Note the significant degradation of the RRA results relative to those obtained using the Akima cubic spline fit as in Table 1 of Chapter III, Section A. This comparative degradation of consistency between the ODE and RRA algorithms will be evident throughout this subsection.

Table 28. RAY ACOUSTICS RESULTS FOR SSP 2, RAYS 1 THROUGH 3, FOURIER SOUND-SPEED FIT

Method	y_0 (m)	β_0 (deg)	r (km)	y (m)	β (deg)	τ (sec)	s (km)
ODE	100.0	45.0	10.0	99.99	45.000	9.417413	14.1421
RRA	100.0	45.0	10.0	99.97	45.000	9.417429	14.1421
ODE	100.0	85.0	10.0	162.5(	85.487	6.683492	10.0374
RRA	100.0	85.0	10.0	163.31	85.482	6.683550	10.0374
ODE	100.0	135.0	10.0	100.01	135.000	9.417413	14.1421
RRA	100.0	85.0	10.0	100.03	135.000	9.417430	14.1422

For SSP 2 (linear SSP with a positive gradient), Table 28 shows that at a horizontal range $r = 10$ km, the differences between the benchmark ODE algorithm and the RRA algorithm using the Fourier series sound-speed fit are as follows:

- between 0.02 and 0.19 m in depth y,
- 0.005 deg in angle of arrival β,
- between 16 and 58 μ sec in travel time τ, and
- 0.1 m in path length s.

Table 29. RAY ACOUSTICS RESULTS FOR SSP 3, RAYS 1 THROUGH 3, FOURIER SOUND-SPEED FIT

Method	y_0 (m)	β_0 (deg)	r (km)	y (m)	β (deg)	τ (sec)	s (km)
ODE	100.0	45.0	10.0	99.99	45.000	9.438784	14.1421
RRA	100.0	45.0	10.0	99.96	45.000	9.438799	14.1422
ODE	100.0	85.0	10.0	168.89	84.512	6.699404	10.0380
RRA	100.0	85.0	10.0	169.76	84.492	6.699471	10.0380
ODE	100.0	135.0	10.0	100.01	135.000	9.438784	14.1421
RRA	100.0	85.0	10.0	100.04	135.000	9.438798	14.1421

For SSP 3 (linear SSP with a negative gradient), Table 29 shows that at a horizontal range $r = 10$ km, the difference between the benchmark ODE algorithm and the RRA algorithm using the Fourier sound-speed fit are as follows:

- between 0.03 and 0.13 m in final depth y,
- 0.020 deg in angle of arrival β,
- between 14 and 67 μ sec in travel time τ, and
- 0.1 m in path length s.

The results contained in the above tables, while poorer than those detailed in Chapter III, Section A, nevertheless produce travel times which are consistent in the millisecond region. However, this is not the case for the SSPs examined next.

Table 30. RAY ACOUSTICS RESULTS FOR SSP 4, RAYS 1 THROUGH 3, FOURIER SOUND-SPEED FIT

Method	y_0 (m)	β_0 (deg)	r (km)	y (m)	β (deg)	τ (sec)	s (km)
ODE	100.0	45.0	10.0	37.06	87.244	6.710387	10.0183
RRA	100.0	45.0	10.0	42.86	86.674	6.709733	10.0185
ODE	100.0	85.0	10.0	162.94	92.756	6.710387	10.0183
RRA	100.0	85.0	10.0	157.14	93.326	6.709733	10.0185
ODE	100.0	135.0	10.0	144.97	134.922	9.448852	14.1104
RRA	100.0	85.0	10.0	143.98	134.930	9.448515	14.1112

For SSP 4 (parabolic SSP), Table 30 shows that at a horizontal range of $r = 10$ km, the differences between the benchmark ODE algorithm and the RRA algorithm using the Fourier series sound-speed fit are as follows:

- between 0.99 and 5.8 m in final depth y,
- between 0.008 and 0.570 deg in angle of arrival β,
- between 337 and 654 μ sec in travel time τ, and
- 0.2 m in path length s.

As in Chapter III, Section A, SSP 4 shows significantly less consistency between the two algorithms than the previous SSPs examined. Again, two approaches were taken to attempt to reduce this discrepancy. First, the arc length step size was reduced from 2.0 to 1.0 m (see Tables 12 and 13) and second, the steepness of the gradient was reduced from 0.1 to 0.02 1/sec (see Table 14).

Table 31. RAY ACOUSTICS RESULTS FOR SSP 4, RAYS 1 THROUGH 3, 2.0 M ARC LENGTH STEP SIZE, FOURIER SOUND-SPEED FIT

Method	y_0 (m)	β_0 (deg)	r (km)	y (m)	β (deg)	τ (sec)	s (km)
ODE	100.0	45.0	5.0	64.25	85.597	3.354779	5.0088
RRA	100.0	45.0	5.0	68.79	85.435	3.354591	5.0090
ODE	100.0	85.0	5.0	135.75	94.403	3.354779	5.0088
RRA	100.0	85.0	5.0	131.21	94.565	3.354591	5.0090
ODE	100.0	135.0	5.0	77.50	45.019	4.724411	7.0552
RRA	100.0	85.0	5.0	77.82	45.017	4.724162	7.0554

For SSP 4 (parabolic sound speed), Table 31 shows that at a horizontal range of r = 5 km, using an arc length step size of 2.0 m, the differences between the benchmark ODE algorithm and the RRA algorithm using the Fourier series sound-speed fit are as follows:

- between 0.32 and 4.54 m in final depth y,
- between 0.002 and 0.162 deg in angle of arrival β,
- between 188 and 249 μ sec in travel time τ, and
- 0.2 m in path length s.

The data in Table 31 above was generated in order to enable a direct comparison with the arc length step size set to 1.0 m, as shown in Table 32 below. The reduction in final range from 10 to 5 km was necessitated by the structure of the RRA computer code, which required large quantities of computer storage space to be allocated, particularly as arc length step size was reduced.

Table 32. RAY ACOUSTICS RESULTS FOR SSP 4, RAYS 1 THROUGH 3, 1.0 M ARC LENGTH STEP SIZE

Method	y_0 (m)	β_0 (deg)	r (km)	y (m)	β (deg)	τ (sec)	s (km)
ODE	100.0	45.0	5.0	64.25	85.597	3.354779	5.0088
RRA	100.0	45.0	5.0	68.86	85.442	3.354604	5.0090
ODE	100.0	85.0	5.0	135.75	94.403	3.354779	5.0088
RRA	100.0	85.0	5.0	131.14	94.558	3.354604	5.0090
ODE	100.0	135.0	5.0	77.50	45.019	4.724411	7.0552
RRA	100.0	85.0	5.0	77.74	45.019	4.724126	7.0554

For SSP 4 (parabolic SSP), Table 32 shows that at a horizontal range of $r = 5$ km, and with the RRA arc length step size set to 1.0 m, the differences between the benchmark ODE algorithm and the RRA algorithm using the Fourier series sound-speed fit are as follows:

- between 0.24 and 4.61 m in final depth y,
- 0.155 deg in angle of arrival β,
- between 175 and 285 μ sec in travel time τ, and
- 0.2 m in path length s.

Table 33. RAY ACOUSTICS RESULTS FOR SSP 4, RAYS 1 THROUGH 3, 2.0 M ARC LENGTH STEP SIZE, BOTTOM DEPTH 1000 M, FOURIER SOUND SPEED FIT

Method	y_0 (m)	β_0 (deg)	r (km)	y (m)	β (deg)	τ (sec)	s (km)
ODE	100.0	45.0	10.0	777.41	93.388	6.705898	10.0150
RRA	100.0	45.0	10.0	768.46	93.522	6.705420	10.0152
ODE	100.0	85.0	10.0	222.59	86.612	6.705898	10.0150
RRA	100.0	85.0	10.0	231.54	86.478	6.705420	10.0152
ODE	100.0	135.0	10.0	545.01	134.997	9.448829	14.1104
RRA	100.0	85.0	10.0	544.58	134.997	9.448180	14.1107

For SSP 4 (parabolic speed of sound), with vertex c(500) = 1490 m/s and speed of sound at the ocean surface c(0) = 1500 m/s and speed of sound at the ocean bottom c(1000) = 1500 m/s, i.e., an ocean depth of 1000 m; at a horizontal range of $r = 10$ km, the differences between the benchmark ODE algorithm and the RRA algorithm using the Fourier series sound-speed fit are as follows:

- between 0.43 and 8.95 m in final depth y,
- 0.134 deg in angle of arrival β,
- between 478 and 649 μ sec in travel time τ, and
- between 0.2 and 0.3 m in path length s.

Table 33 shows no significant improvement over Table 30 for SSP 4 with the original extreme gradient. The errors associated with the Fourier sound speed representation have resulted in this lack of improvement, whereas substantial improvement was observed between these two cases for the Akima cubic spline fit with the RRA algorithm (see Tables 4 and 7 in Chapter III, Section A).

2. Sound Speed Including Deterministic and Random Components

In order to investigate the effects of randomness in the SSP, a model of the power spectral density of the random component of the speed of sound $c_R(y)$ had to be proposed. The most straightforward model of band-limited white noise was used, as given by

$$S_{c_R}(f_y) = \begin{cases} S_0, & |f_y| \leq BW \\ 0, & |f_y| > BW \end{cases} \tag{4.10}$$

where BW is the bandwidth, and S_0 is the constant magnitude of the power spectrum at all spatial frequencies f_y.

As a consequence of the assumption of zero mean white noise, the variance of $c_R(y)$ is given by

$$\sigma^2_{c_R} = 2\, S_0\, BW \tag{4.11}$$

and, as a result,

$$S_0 = \frac{\sigma^2_{c_R}}{2\, BW} . \tag{4.10}$$

A value for the variance of $c_R(y)$ in shallow water of 2.5×10^{-7} was obtained from Brekhovskikh and Lysanov [Ref. 8: p. 208]. The simulation program was run with randomness incorporated as above and for SSP 1 (constant speed of sound). When the results were compared with those from the RRA algorithm previously run using the Fourier series representation of sound-speed data, differences of a maximum of 0.1 m in final depth y, 0.002 deg in angle of arrival β, and 2 μ sec in travel time τ were observed. The RRA algorithm was then run with SSP 4 (parabolic SSP in a 200 m deep ocean) incorporating randomness and differences of a maximum of 0.22 m in final depth y, 0.018 deg in angle of arrival β, and 16 μ sec in travel time τ were observed.

The variance was then increased to determine at what magnitude it caused the randomness to become significant. Further simulation runs revealed that for SSP 1, differences in travel times of greater than 10 μ sec needed $\sigma^2_{c_R}$ to be at least of the order of 10^{-3}, four orders of magnitude greater than the estimate given in Brekhovskikh and Lysanov [Ref. 8: p. 208].

V. CONCLUSIONS AND RECOMMENDATIONS

The recursive ray acoustics (RRA) algorithm was shown to be an accurate ray acoustics algorithm when used in conjunction with an Akima cubic spline fit to sound-speed data. The RRA algorithm can be made as accurate as desired by reducing the arc length step size. Although the ODE algorithm computes amplitudes which the RRA algorithm does not, the RRA algorithm was observed to be significantly faster in terms of computer execution time.

The ability of the RRA algorithm to handle sound speed as a function of all three spatial coordinates enables its application to real world problems wherein a horizontal gradient of sound speed exists, either in the cross-range or down-range direction. This could conceivably be the case for either long range ray propagation or for propagation in estuaries or across current boundaries where significant horizontal gradients can exist.

A spatial Fourier series (SFS) representation of sound-speed data, while attractive for reasons of its spectral content and the ease of incorporation of randomness at specific harmonics, encountered difficulty with regard to providing accurate fits to sound-speed data. Several techniques were used to attempt to rectify this, including the use of Lanczos smoothing , addition of synthetic data above the ocean surface and below the ocean bottom, and sampling of the Akima cubic spline fit to provide data points for input to the SFS method. These techniques resulted in some substantial success in the reduction of the inaccuracies of the SFS method. However, although the SFS method eventually provided accurate fits to the sound-speed data, it still provided inaccurate first and second-order derivatives when compared against the results obtained from the Akima cubic spline method.

A comparison was made between the ODE algorithm using an Akima cubic spline sound-speed representation and the RRA algorithm using a SFS sound-speed representation, with the SFS representation in its most basic form, that is, with none of the techniques referred to in the above paragraph incorporated. The RRA/SFS combination was found to be wanting in accuracy.

As was mentioned previously, the RRA algorithm using the Akima cubic spline fit to sound-speed data was proven fast and accurate, and can be made as accurate as desired by reducing the arc length step size. However, investigation is warranted to de-

termine if the RRA algorithm can be generalized to include amplitude calculations, especially at focal points and, hence, caustics.

Throughout the simulations undertaken in this thesis, a zero-slope, flat ocean surface and bottom was assumed. In order to apply the RRA algorithm to realistic ocean boundaries, the ability to accommodate arbitrarily shaped surfaces should be included.

LIST OF REFERENCES

1. Klein, M. V., *Optics*,Wiley, New York, 1970, pp. 29-31.

2. Moler, C. B. and Solomon, L. P., *Use of Splines and Numerical Integration in Geometrical Acoustics*, Journal of the Acoustical Society of America 48, pp. 739-744 (1970).

3. Kee-Lim, Chwee, *Acoustic Ray Tracing*, Master's Thesis, Naval Postgraduate School, Monterey, 1990.

4. Ziomek, Lawrence J., *Underwater Acoustics - A Linear Systems Theory Approach*, Academic Press, Inc., San Diego, 1985.

5. Lanczos, C., *Applied Analysis* , Prentice Hall, Inc., 1956, pp. 219-220.

6. Hamming, R. W., *Digital Filters*, 3rd edition, Prentice Hall, Inc., 1989.

7. Thomas, John B., *Statistical Communication Theory*, John Wiley and Sons, New York, 1969, pp. 148-153.

8. Brekhovskikh, L. and Lysanov, Y. *Fundamentals of Ocean Acoustics*, Springer-Verlag, Berlin, 1982.

INITIAL DISTRIBUTION LIST

		No. Copies
1.	Defense Technical Information Center Cameron Station Alexandria, VA 22304-6145	2
2.	Library, Code 52 Naval Postgraduate School Monterey, CA 93943-5002	2
3.	Professor L. J. Ziomek, Code EC/Zm Department of Electrical and Computer Engineering Naval Postgraduate School Monterey, CA 93943-5000	2
4.	Professor Hung-Mou Lee, Code EC/Lh Department of Electrical and Computer Engineering Naval Postgraduate School Monterey, CA 93943-5000	1
5.	Professor A. L. Schoenstadt, Code MA/Zh Department of Mathematics Naval Postgraduate School Monterey, CA 93943-5000	1
6.	Mr. Thomas Martin Undersea Warfare Program Office PRC, Inc. 1555 Wilson Blvd. Arlington, VA 22209	1
7.	Lieutenant F. W. Polnicky c/o Director, Naval Requirements Major-General George R. Pearkes Building Ottawa, Canada K1A 0K2	2